Application of a semi-distributed hydrological model based on the REW approach to the Collie River Basin, Western Australia

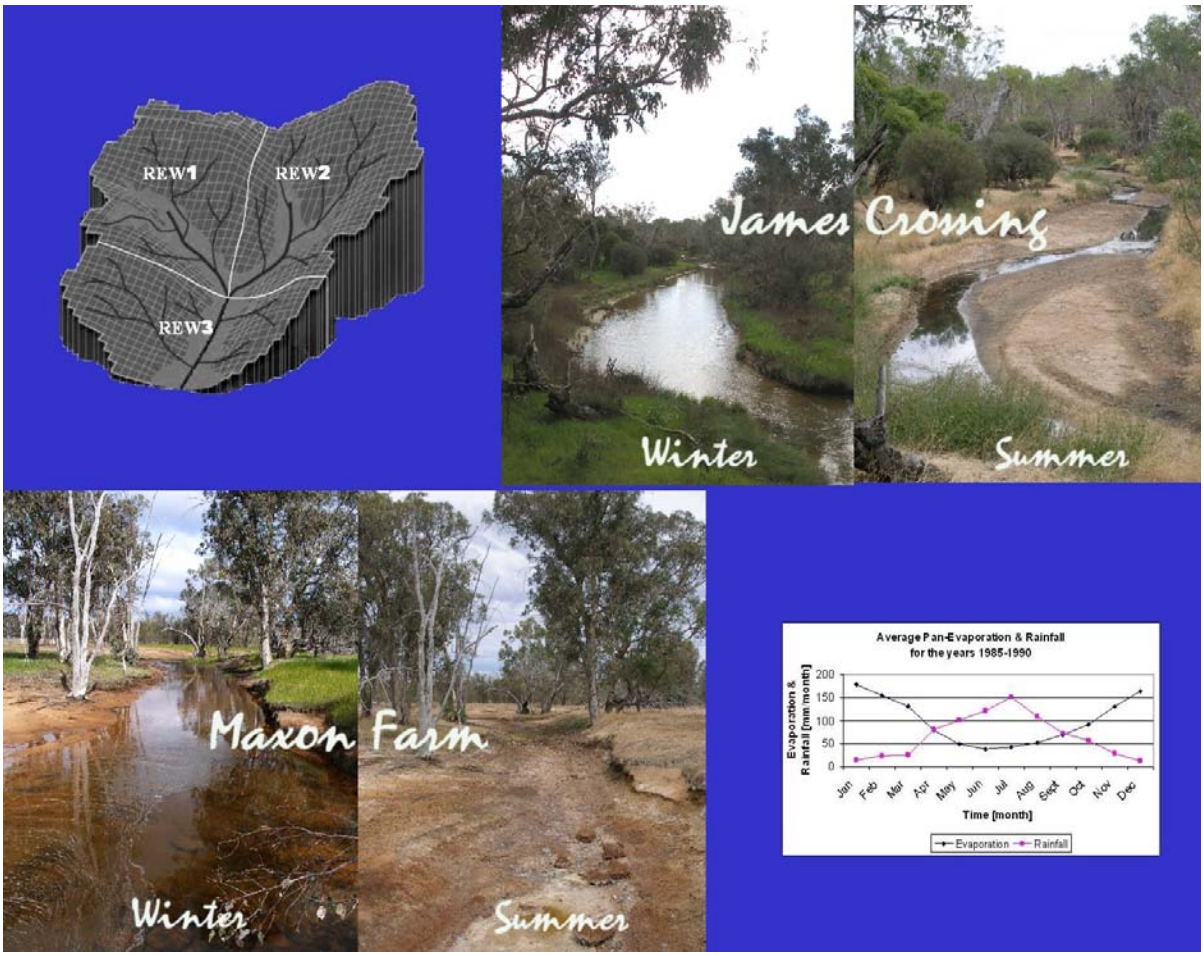

Ellen Tromp
Perth, October 2005

TU Delft

Delft University of Technology

Faculty of Civil Engineering and Applied Geosciences,
Department of Water Management,
Section Water Resources

In cooperation with:

The University of Western Australia

Centre for Water Research
a School in the Faculty of Engineering, Computing and Mathematics

Application of a semi-distributed hydrological model based on the REW approach to the Collie River Basin, Western Australia

M.Sc. Thesis by:
E. Tromp

Perth, October 2005

Thesis Committee:

Prof. dr. ir. H.H.G. Savenije
Prof. M. Sivapalan
Ir. W.M.J. Luxemburg
Prof.ir. J.C. van Dijk

Preface

This report is the result of the M.Sc. Thesis of Ellen Tromp (C1041290). This thesis is part of the study Civil Engineering at the Delft University of Technology (TU Delft).

Many students go abroad during their study. This is a great opportunity to learn about different cultures and other approaches to work. Ever since I started my study at the TU Delft I wanted to come to Australia and the combination of doing my final research and going to Perth sounded ideal. As CWR has people from all over the world, I have come in contact with many different habits and cultures. Not only have I learned a lot about hydrology and conducting research, also I have learnt to stand on my own two feet as well as dealing with different cultures and religions. As Australia is a completely different country (other climate, flora and fauna, geology, etc.) which is at the moment dealing with drought, the possibilities to learn all new phenomena were endless.

It was ir. W.M.J. Luxemburg who mentioned that there were contacts in Australia and he told me I should contact prof.dr.ir. H.H.G. Savenije.
I want to thank ir W.M.J. Luxemburg for all the advice, help and time he gave me when I was working on my thesis. I also wish to express my gratitude towards prof.dr.ir. H.H.G. Savenije for being the welcoming party in Perth and for all the advice, help, time and discussions we had during our mutual stay in Perth and via email.

While I was in Perth for nine months, there were a lot of people that helped me with my research or made me feel at home in Perth.
First of all I want to thank all the people of the Centre for Water Research, University of Western Australia, especially prof. M. Sivapalan, who made it possible for me to work in Perth and Mr. Haksu Lee for helping with the REW-model and their knowledge regarding the hydrology.
Also I would like to thank Mary-Ann Coppolina and Renee Dixon of the Department of Environment, Water and Rivers Commission for their help providing the DEM to me and organising a fieldtrip to the Collie River Basin and David Rowlands and Mohammed Bari for accompanying professor Savenije and myself on the fieldtrip (8th March 2005).

Furthermore, Mr. G.P. Zhang was a great help in helping me understand the theory behind the REW approach. Also I owe a great deal to Hessel Winsemius, who provided the scripts and knowledge for PCRaster. Without him I was not able to make a heterogeneous rainfall field, as presented in this thesis.

I had not been able to stay in Perth without the help of Wendy Nadebaum, Yanti Sri Adiyanti and Beatriz Villegas (the last two as my housemates). The girls from my office, Patricia (Trish) Okely and Claire Spillman made working there much fun and I will miss the coffee breaks and the horoscope in the West Australian. And finally everybody who participated in the weekly soccer games, especially Katie, Ed, Mike and Rocio!

Finally I want to thank my parents, Jochem (brother) and Vincent (boyfriend) for their overall support during my thesis work in a country which lies on the other side of the world. It was sometimes difficult to be so far apart from each other, but it was all worth it, especially the holidays!

Ellen Tromp
Perth, 20 October 2005

Summary

The current generations of hydrological models have their advantages and disadvantages. One of the major shortcomings of the existing models (physically-based distributed models) is that they require detailed information about soil properties and geometry and suffer from immense demands on data, and time consuming.
In order to overcome these problems, a new approach has been developed, which is called the Representative Elementary Watershed (REW) approach. This approach has equations which have been derived at the scale of REW. This is the scale at which predictions are usually required. A catchment is divided into several REW's. Each REW includes an ensemble of five zero-dimensional sub-regions in which water fluxes are simulated, based on the coupling of mass conservation and momentum balance equations. In order to close this set of equations, the exchange flux terms must be parameterized using expressions in terms of other resolved variables. In other words, closure relations involving landscape and climate and soil properties have to be sought out.

In the last couple of years much improvement has been made on these closure relations by e.g. Lee and Zhang. This led to two different models. REWASH, developed by Zhang *et al.*, and is mainly tested in a temperate climate, while CREW (Lee) has been tested in both a temperate and an arid climate. These models were investigated during this research. Both models have the same theoretical background although the outcome is different. Differences have been recognised e.g. in the way hydraulic conductivities for the unsaturated and saturated zone have been defined, the definition of groundwater flow, mass exchange across mantle segment and the description of the variable source area.
It depends on the climate, soil and physiography which of the closure relations are most suitable. In the near future, the developed closure relations can be used for a REW model in a way that for that specific climate, soil and physiography the most optimum closure relation can be used.
For this research CREW has been applied to the Collie River Basin, Western Australia, in order to see how the model represents the real world and what sort of modifications ought to be made to improve the applicability of the model. The Collie River Basin is characterised by strong spatial gradients in precipitation, potential evaporation, vegetation cover and its large size.

A top-down approach has been applied to analysing the available data of the catchment. Starting with annual data, it was shown that the precipitation in the Collie River Basin varies from 1200mm in the west till 600mm in the east. Evaporation is in the range of 1400-1600mm per year.
From the monthly analysis it was shown with the formula of Kagan that the correlation between stations was 0.88. With a simple multiple linear regression model the interception rate was found, around 60 mm/month. The model also showed that the precipitation has a residence time of four months in the subsurface.
Through daily analysis a conclusion can be drawn that the precipitation concentrates in just a few days. The interception analysis has shown strong correlation with the Budyko curve, as the formulae have strong similarities.

During the implementation of CREW to the Collie River Basin a few issues were encountered, for which a solution has been found. As there was no program available to derive the REW's based on a specified Strahler order a script suitable for PCRaster, a free GIS software package, was written. So all the REW's have just one stream and only two REW's connecting to the upstream inlet as required by the theory.
Due to the high spatial variability precipitation (ranging from 1200 (west) till 600 mm (east)) in the catchment, a heterogeneous precipitation field was applied in the model. The differences

of the results using a homogeneous and a heterogeneous precipitation field have been illustrated, and it has been proven that using the heterogeneous precipitation field produced better simulations for stream flows. For the heterogeneous precipitation field, inverse distance was used as an interpolation technique. With scripts written for PCRaster, all the gauge stations were taken into account to develop a precipitation field for the entire catchment. In the future only two or three nearby gauge stations should be taken into account. Otherwise spatial variability in precipitation is neglected.

In this research there are three cases where the entire catchment is discretized into 1, 5 and 27 REW's respectively. The results for the latter two with a heterogeneous precipitation field show the most promising results. In these cases, the peaks were better simulated by the model. Up till now the importance of the temporal and spatial variability of the vegetation as well as the routing has not been investigated. The results show that there is a time delay of several days between simulated and observed runoff.
The routing can be optimized by fine-tuning state variables such as cross-sectional area and the depth of the river. In the catchment land clearing has taken place, which resulted in higher groundwater level and Hortonian overland flow in the cleared area. In order to account for these effects, deforestation and reforestation as well as differences in vegetation species should be defined in the model in the future.

The first year is always poorly simulated due to the initial conditions. Up till now the results for 5 and 27 REW's are similar, but it is expected that when the parameters with distributed values are assigned to each REW, not only geometrical information, the model should give better overall results.
As was found in literature for the Collie River Basin, the saturated excess overland flow and the lateral flow through the upper soil profile are important streamflow generation mechanisms. The first one was predicted by the model.

Depending on the purpose of the model, try to reduce the physics and first learn from patterns in a catchment. Let the model help to identify the important hydrological processes. With the top-down analysis for the available data and the bottom-up analysis (= REW approach) it can be seen that both give similar results. With the information that was found with the top-down analysis the results of the CREW model could be checked. By using both, better understanding about the system and occurring hydrological processes is established. Moreover it helps to see patterns and thresholds in a system, without complex modelling.

Table of Contents

List of Figures

List of Tables

1. Introduction

The behaviour of the catchment as a closed hydrological system, its response to atmospheric inputs and the descriptions of the hydrological processes over spatial and time scales have been and will continue to be research topics. Hydrological models are important and necessary tools for water and environmental resources management. Demands from society with respect to the predictive capabilities of such models are becoming higher and higher, leading to the need of enhancing existing models and even developing new theories.

Among the current generation of hydrological models two major categories can be distinguished, which are called, physically-based and conceptual models. Freeze was the first one who introduced a physically-based watershed model. This model was founded on a rigorous numerical solution of partial differential equations (PDE) governing flow through porous media, overland flow and channel flow.
Following the blueprint proposed by Freeze and Harlan (1969), a number of distributed and physically based models have been developed, among which the well known SHE (Abbott *et al.*, 1986a, 1986b), MIKE SHE (Refsgaard and Storm, 1995) and IHDM (Beven *et al.*, 1987) models. Although these models are supposed to offer a great potential and utility in predicting the effects of land-use change and the hydrological response of ungauged basins, considerable debate on both the advantages and disadvantages of such models (e.g. Beven 1989, 1996a, 1996b, 2002; Grayson *et al.*, 1992b) has arisen along with the research and application of those models, but there are several advantages and disadvantages to this kind of approach. The main advantage of these models is that they explicitly consider conservation of both mass and momentum. However, this is expressed on point scale.
Their main shortcomings are the following: the models require detailed information about soil properties and geometry, which is often not available for most watersheds. Secondly these models suffer from immense demands on data. They are time-consuming and parameter identification is extremely difficult, viz. the equifinality problem (Beven 1993; Savenije 2001)

Conceptual models are by far the largest group of hydrological models that have been developed in the hydrological community. They are most applied in operational practice, (e.g. LASCAM (Sivapalan *et al.* 1996b), TOPMODEL (Beven,1995). Most existing conceptual models are spatially lumped. These models do not take into account the detailed geometry of the system and small-scale variability's. The disadvantages of a lumped conceptual model are that they are only based on the mass balance and they lack physical meaning.

Now there has been developed another approach, which is called Representative Elementary Watershed approach. This approach has equations which have been derived at the scale of REW. This is namely the scale at which predictions are usually required; the resulting models are not complex in terms of data input requirements.
In this thesis a model, developed at the Centre for Water Research, Perth, Australia will be applied on the Collie River Basin, Western Australia.
The complexity in this catchment, apart from its size (2845 km^2) is that it has strong spatial gradients of precipitation, potential evaporation and vegetation. More over, in the past part of the catchment has been cleared for agriculture and mining, leading to an increase of groundwater level and salinization. Normally the roots of the trees keep the groundwater level low, but as they are removed groundwater level can rise.

The aim of this research is to analysis the available data, to get a first impression of how in this basin the hydrological processes react and what the timescales are. Secondly to learn about the REW approach and to test a new developed model to this catchment to see in what way the model may lack to capture the hydrological processes in this specific basin.

At first an analysis of the problems and objectives of this thesis are presented in chapter 2. Hereafter all the hydrological processes that might occur in the Collie River Basin are presented and specified in chapter 3. An introduction of the REW approach with the differences between three models is presented in chapter 4. The description of the study catchment: Collie River Basin (chapter 5) is followed by the top down approach of the data analysis of the catchment in chapter 6. Chapter 7 describes the computer model in more detail and shows the code. The implementation of the model to the Collie River Basin and the issues that have to be dealt with are discussed in chapter 8. Subsequently the results for calibration and validation for 1, 5 and 27 REW's are presented. In chapter 10 an overview is given of the closure relations for the three models based on several criterions. Finally, in chapter 11, the conclusions and recommendations of this research are presented.

2. Problem analysis

2.1. Problem statement

1. The blue print of physically based models (Freeze and Harlan, 1978) has run into serious 69problems, such as complexity due to data-intensive equations equifinality and dimensionality. Still the models have the advantages that they explicitly consider conservation of mass and momentum and can compute internal states of the system. Parallel to these models, the conceptual models were developed. However these models lack physical basis. As a consequence of this, a new hydrologic modelling framework has been developed which combines the good sides of both the approaches.

2. During the last few years a new hydrologic modelling framework has been developed, which is called the REW approach. However, before the REW scale governing equations can be used as the basis of a new blueprint, considerable progress must be made in a number of areas, such as closure relations and application of model to real catchments. It is important to know in what way the model represents the real world and what kind of faults the model still contains.

3. The model will be applied to a large catchment, the Collie River Basin. The model has never been applied to such a catchment with the semi-arid environment. The complexity of this basin, apart from its size, is that it has strong spatial gradients of rainfall, potential evaporation and vegetation cover, but parts of the catchment have been cleared for agriculture and mining (in the past).

2.2. Objectives

1. The first objective of this thesis is to evaluate the latest model development within the framework of the REW approach. At this moment there are three models which are based on the previously mentioned approach.

2. The second objective of this thesis is to apply one of the models to the Collie River Basin. In this way the model simulated the runoff generation of the Collie River Basin catchment with observed rainfall and potential evaporation time series. Also the accuracy of water balance computation by the model will be reviewed. The model results will be compared with the observed results and the runoff generations mechanisms are reviewed on their behaviour. Recommendations will be made to improve the model and the analysis.

3. The third objective is to present an overview of the closure relations that are adequate for a certain catchment with its particular climate, geology, and topography and data availability.

3. Hydrological processes involving the rainfall-runoff relation

3.1. Introduction

The origin of water resources is precipitation. Therefore the source of the water in a stream is precipitation. However, before a raindrop becomes part of the discharge of a stream the water particles have been transported to and stored in several surface and/or subsurface storage systems. Often this is referred to as the rainfall- runoff process, which is a process of stocks and fluxes. In this chapter the hydrologic processes that take place in a catchment are described in order to schematise and define the involved processes and storages. In Figure 1 the different water resources are schematised. This chapter is not yet focussed on the Collie River Basin. As the REW approach is suitable for any kind of catchment, all the processes are described here below.

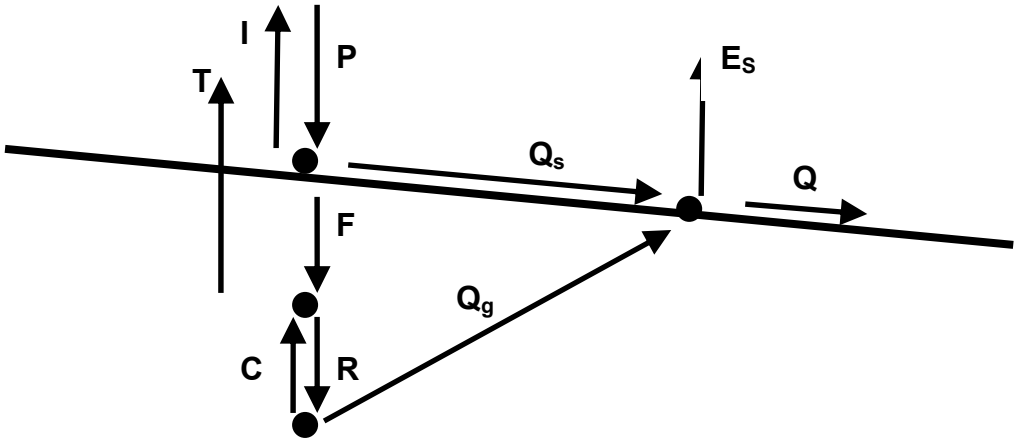

Figure 1 Water resources (P= Precipitation; I = Interception; T= Transpiration; F= Infiltration; R= Percolation; C= Capillary Rise; Q_g= Groundwater flow; Q_s=Surface runoff; E_s=Surface evaporation; Q= Total Runoff

3.2. Precipitation (P)

Precipitation comprises all the water that moves from the atmosphere to the earth surface. This is the source for the water in a catchment and it is the start of the rainfall- runoff process. Under the term precipitation the following water movements are meant: rainfall, snowfall, hail, dew and fog. In Western Australia, rainfall is the most common form of precipitation. In this region they never had snowfall. For the last three above-mentioned they only represent a small amount of precipitation water.
The intensity of the precipitation, the duration and the spatial scale of occurrence of the precipitation are the most determining factors for the quantity of discharge in the Collie River. These factors are different for different types of rainfall. The type of rainfall depends on the lifting mechanisms of the air.

The three common lifting mechanisms are convection, frontal lifting and orographic lifting (Savenije *et al.* 2003)

- *Convective storms* are the result of instability of the air and can occur during the summer period. The instability is the effect of the heating of the lower air layers by the hot earth surface and the cooling by outgoing radiation of the upper layers. This lifting mechanism causes rainfall events with a high intensity for a short time in a small area. Good examples for this type of rainfall are the thunderstorms at the end of a warm and sunny day.

- Rainfall caused by *frontal lifting* is the result of an area with low pressure, which causes the surrounding air to move into the depression. The low-pressure air is pushed upwards, which may then be cooled down to the dew point. If cold air is replaced by warm air, a warm front, the frontal zone is large and the rainfall is of low intensity, but with a long duration. If warm air is replaced by cold air, a cold front, the frontal zone is smaller and the rainfall has a higher intensity of shorter duration than with a warm front (see Figure 2). Normally these rainfall events have a lower intensity and a longer duration in a large area than the convective storms.

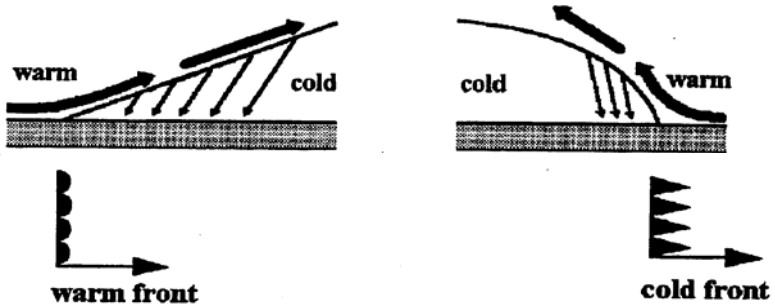

Figure 2: Frontal lifting for a warm and a cold front [Savenije H.H.G. et al., 2003]

- *Cyclones, tropical depressions and hurricanes*. These are active depressions which gain energy while moving over warm ocean water and which dissipate energy while moving over land or cold water. They may cause torrential rains and heavy storms. Typical characteristics of these tropical depressions are high intensity rainfall of long duration (several days). In 1982 a tropical depression reached the coast of Western Australia and caused flooding in most catchments, including the Collie River Basin. To remember this event, several signs were placed at the gauge stations.
- With the last mechanism, *orographic lifting*, the air is forced to rise by the topography, i.e. air passing a mountain. This mechanism can explain local variations, because on one side of a hill more rain can fall than on the other side, due to the most common wind direction.

The precipitation can be measured with a rain gauge. There are a lot of different types of rain gauges.

3.3. Interception (I)

Interception is the part of the precipitation that does not infiltrate into soil or becomes surface runoff. It is temporarily stored on natural or artificial ground cover, until it evaporates back to the atmosphere or is absorbed by vegetation.
In rural areas the interception consists of the precipitation that is stored on the leaves of trees, plants and on or in the mulch on the ground. As for urban areas, the interception consists of the precipitation stored on the roofs at part that do not drain to the gutter, and also the precipitation on areas that drain to the sewerage system.
In both cases, only a certain amount of water can be stored. When it has reached its maximum, the interception capacity, all extra precipitation will become part of the net precipitation. The water which is intercepted evaporates in time and the interception storage volume becomes available for the next rainfall event.
The degree of interception depends on the type of trees and mulch in the rural part and the type of roofs in the urban part.
The actual interception (I_{actual}) is the amount of water that is stored during a certain period.

3.4. Evaporation (E)

Evaporation is the amount of water that transfers from the liquid to the gaseous stage by physical processes. The water that has been intercepted becomes water vapour and returns to the atmosphere by evaporation. In semi-arid climates water will evaporate from the river as well as from the surface storage. There are three conditions which apply in case of evaporation (van den Akker C., Boomgaard M.E., 2001):

- The first condition is that there has to be a gradient between the vapour pressure at the surface (e_s) and the atmospheric vapour pressure (e). If e_s>e the surface has a water vapour demand and condensation can occur. If e_s<e there is an atmospheric demand for water vapour and evaporation can occur.
- Energy is needed for evaporation. The net input of energy by the sun to a water surface increases the water temperature. Therefore the kinetic energy of the water molecules increases. The energy from the sun also increases the maximum amount of water vapour that the air can contain. In this way the atmospheric demand is also influenced.
- The saturated air above the water surface needs to be replaced. By replacing the air above the surface the gradient between the vapour pressure at the surface and the atmospheric vapour pressure remains present. If the air is not removed the gradient will decrease and the evaporation will stop.

Evaporation is important for the interception. After all, water stored in trees or on a roof, needs to evaporate to make storage available for the next precipitation event.
Sometimes evaporation and transpiration are taken together as evapotranspiration. This is hydrologically speaking incorrect and will be further explained in the paragraph about transpiration.

Evaporation can be measured with i.e. a Class A or B pan. Also it can be calculated with the Penman formula.

3.5. Net precipitation (P')

The net precipitation is the part of precipitation which is not intercepted, i.e. the sum of through fall and stem flow. Through fall is water that has fallen through openings in the canopy. It is also possible that it came in contact with the canopy but splashed off. Stem flow is the transfer of water down leafs, stems and branches to the ground along the main stem or trunk of a plant/tree. Combined this is the part of the precipitation that reaches the ground. Still there is a part that is lost to interception in the mulch. The part that is not evaporated from the mulch is net precipitation.
The intensity of the net precipitation depends on the intensity of the precipitation and the actual interception. The actual interception is strongly related to the interception capacity, succession in time of rainfall events and evaporation. The spatial variation of the net precipitation is larger than the spatial variation of the precipitation, due to the interception and stem flow.

The net precipitation can be calculated with the following formula:

$$\mathbf{P'(t) = P(t) - I_{actual}(t)}$$

P' = net precipitation [mm/h]
P = precipitation [mm/h]
I_{actual} = actual interception [mm/h]

3.6. Surface storage ($S_{surface}$)

The net precipitation that has reached the ground becomes part of the surface storage. The water is stored in puddles, as a small film on the ground or as drops on trees and blades of grass. Most of the time, surface storage is empty and only during or just after precipitation events water is on the surface. The water of the surface storage can evaporate, infiltrate or flow to the river as surface runoff. Most of the time, infiltration will be dominant and only a small amount of water is stored on the surface.
It is not possible to measure the surface storage because of its large spatial variation. It is however possible to determine if there is surface storage, or not.

The water balance of the surface storage is as follows:

$$\frac{\Delta S_{surface}}{\Delta t} = (P' - E) \times A - F - Q_s$$

$\Delta S_{surface}$ =	difference in surface storage [l]
Δt =	time step [h]
P' =	net precipitation [mm/h]
E =	evaporation [mm/h]
F =	infiltration [l/h]
Q_s =	surface runoff [l/h]
A =	surface area [m²]

3.7. Infiltration (F)

The water that is stored on the ground in surface storage can infiltrate into the ground. The water flows through the soil-atmosphere interface, filling the pores in the ground and becomes part of the unsaturated zone. The process of entering the soil is driven by the gravity potential. The amount of water, that is infiltrated in a certain time space, is called the infiltration rate. The maximum infiltration rate is called the infiltration capacity. The infiltration rate has large spatial differences, which makes it difficult to determine the mean infiltration rate for a large area. The infiltration capacity depends on the type of soil, soil structure, the vegetation and porosity. Macro pores in the top soil have a big effect on the infiltration rate.

3.8. Surface runoff (Q_s)

When the surface storage capacity is reached, surface runoff can occur. Water that can not be stored flows over the surface. This will occur if net precipitation is larger than the evaporation (low during rainfall events) combined with the infiltration capacity.
There are two different types of surface runoff.

- *Hortonian overland flow*
  The intensity of the net precipitation is larger than the infiltration capacity. The surface storage is already filled and the amount of water reaching the ground surface by precipitation is larger than the water infiltrating in the ground (P>F+E). This phenomenon can occur everywhere in the catchment, even if the groundwater table is deep under the ground surface. The overland flow flows first in thin sheets over the land and then returns into small rills.
- *Saturated overland flow*
  The groundwater level reaches the ground surface. Infiltration is no longer possible due to the fact that the unsaturated zone is completely filled and has turned into groundwater storage. So the unsaturated and surface storage both have reached their capacity. The precipitation can no longer be stored or infiltrated, so it will flow over the surface to the stream or river.

The amount of surface runoff is difficult to measure in a catchment because of its spatial variation.

3.9. Unsaturated zone ($S_{unsaturated\ zone}$)

Water that infiltrates the ground enters the unsaturated zone. Water is here stored in the pores between the grains of the soil. The unsaturated zone is part of the soil where the pores still contain some air. The water particles are attracted to the solid grain surfaces (adhesion) and to each other (cohesion). This tension is called Matric potential and keeps the water in the unsaturated zone. The tension caused by gravity is called the gravity potential and pulls the particles down. By using a tensiometer one can measure the pressure in the unsaturated zone. Water from this storage is also removed by vegetation and transpiration. Capillary rise will deliver the water from the saturated zone to the unsaturated zone.
The water balance of the unsaturated zone:

$$\frac{\Delta S_{unsaturated\_zone}}{\Delta t} = F + C - T - R - M$$

$\Delta S_{unsaturated\ zone}$	=	in unsaturated zone storage [l]
Δt	=	time step [h]
F	=	infiltration rate [l/h]
C	=	capillary rise [l/h]
T	=	transpiration [l/h]
R	=	percolation to saturated zone [l/h]
M	=	Macro pore flow to surface [l/h]

3.10. Transpiration (T)

Transpiration is the withdrawal of water from the unsaturated zone by the roots of plants. The plants use the water to grow. The amount of water that is withdrawn by the plants depends on the availability of water in the unsaturated zone (soil moisture content in the unsaturated zone), the type of vegetation and meteorological factors like humidity, wind speed and radiation (sunshine). Transpiration can not be measured, but several formulas estimate the transpiration. Most of the time these formulas combine the transpiration, interception and evaporation, often called evapotranspiration, because they are depending on sunshine, wind speed, temperature and atmospheric vapour pressure. Theoretically it is incorrect to use the term evapotranspiration. Evaporation is a physical process and transpiration a biological process. However more important is that the source of water is different. Water from the surface storage evaporates and water from the unsaturated zone is usually removed by transpiration. Due to the fact that it is difficult to measure the evaporation or transpiration accurately, both terms are combined and calculated with empirical or physical models (Savenije, 2004).

3.11. Percolation (R)

When the Matric potential in the unsaturated zone is smaller than the gravity potential, the water will flow downwards to the saturated zone.
Percolation is referred to as the transport of soil moisture through the matrix of the unsaturated zone to the groundwater.
The difference between the unsaturated zone and the saturated is that in the unsaturated zone the pores are not completely filled, the water is present in small water films on the grains with air between them. In the saturated zone the pores are completely filled with water and no air is present in the pores.

3.12. Capillary Rise (C)

Capillary rise is the transport of water from the subsurface to the unsaturated zone. This process transports water in the opposite direction of the percolation. The amount of capillary rise depends on the water availability in the subsurface and the tension in the unsaturated zone.

3.13. Saturated zone ($S_{saturated}$)

The saturated zone is part of the soil where the pores are filled with water. The term groundwater storage is often used for the saturated zone. The residence time of the water in the saturated zone is the longest of all storages.

The water balance of the saturated zone storage is:

$$\frac{\Delta S_{saturated\_zone}}{\Delta t} = R - Q_g$$

$\Delta S_{saturated\ zone}$	=	difference in saturated zone storage [l]
Δt	=	time step [h]
R	=	percolation to saturated zone [l/h]
Q_g	=	groundwater flow [l/h]

3.14. Groundwater flow (Q_g)

The groundwater is discharged from the saturated zone by seepage through the pores to exfiltration points on hill slopes and the river bed of the streams. Part of the discharge that originates from groundwater flow is called base flow.
During dry times the discharge of the streams only exists of base flow. The time lag between precipitation inputs and groundwater outputs is the longest of all processes.

4. Representative Elementary Watershed (REW) Approach

In this chapter first the Representative Elementary Watershed approach will be discussed as initially proposed by Reggiani *et al.(1998,1999, 2000, 2001)* Secondly, the modifications made by G.P. Zhang and H. Lee will be presented. Also the main differences between the existing models will be discussed. Finally, an overview of the closure relations for each model will be presented.

4.1. Theory

Recently, Reggiani *et al*. (1998, 1999) has proposed a new unifying hydrologic modelling framework by deriving balance equations for mass, momentum, energy and entropy at a scale of a spatial domain, which is called the Representative Elementary Watershed (REW).
Reggiani *et al.* (1998) defined the Representative Elementary Watershed (REW), as the smallest and most elementary unit, into which one can discretize the watershed for a given time scale of interest, and also as the functional unit representative of other sub-entities of the entire watershed.
Each REW includes an ensemble of five zero-dimensional sub-regions in which water fluxes are simulated based on a coupling procedure of mass conservation and momentum balance equations.
The sub-regions are the following: the unsaturated zone flow (u-zone), saturated zone flow (s-zone), saturation overland flow (o-zone), concentrated overland flow, also known as Hortonian overland flow (c-zone) and channel zone (r-zone).
The sub regions are chosen on the strength of previous field evidence about different processes, which operate within catchments, their flow geometries and time scales.
For each of these sub regions all associated variables and properties are spatially lumped quantities, and can vary only in time.
The unsaturated and saturated zones form the subsurface regions of the REW, where the soil matrix coexists with water (and the gas phase in case of the unsaturated zone). The concentrated overland flow sub region includes: surface flow within rills, gullies and small channels, and the regions affected by Hortonian overland flow. The saturated overland flow sub region comprises the seepage faces, where the water table intersects the land surface and makes up the saturated portion of the REW land surface.

Since the equations have been derived from first principles, such as, Newton law's of motions, the second law of thermodynamics, they are general enough to be applicable in a wide range of conditions. Because they are derived at the scale of REW, which is namely the scale at which predictions are usually required, the resulting models are not complex in terms of data input requirements. For that reason, the REW framework, as defined by Reggiani *et al. (1998,1999, 2000, 2001),* has been suggested as the basis for a new generation of distributed, physically based models at the catchment's scale (Beven, 2002; Reggiani and Schellekens, 2003) as an alternative to the current generation of distributed models based on the REV-scale theories (REV = Representative Elementary Volume). These REV-scale theories have the disadvantage that it is not as flexible due to the fact that there are restrictive assumptions made at the outset. Therefore, the REW approach can benefit directly from further advances in process understanding. Also the REW approach is applicable directly at the catchment scale, while the REV-scale approach is a point-scale model.

The equations in the approach have been obtained by averaging micro-scale equations in space over the REW. The watershed-balance equations have been supplemented with constitutive relationships, governing mass fluxes and exchange of pressure forces between the unsaturated zone, the saturated zone and the overland flow areas. The most significant simplification in the equations has been that of evaporation & transpiration. The theoretical development has so far ignored explicit treatment of radiation exchange at the surface, the effect of plant roots and leaf canopies (interception), the atmospheric boundary layer, and the water vapour transport in soils.

Figure 3 presents the schematic of a typical watershed that is discretized into three REW's based on the geometry of channel network, whereas figure 3(b) illustrates the sub regions making up the REW, and the mass exchange fluxes between different sub regions of each REW and those between different REW's.

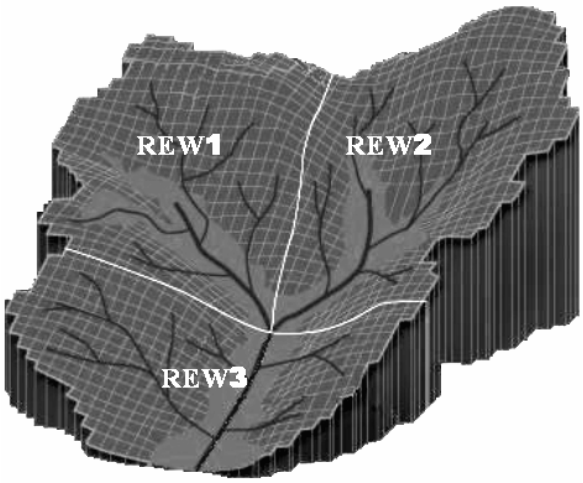

(a)

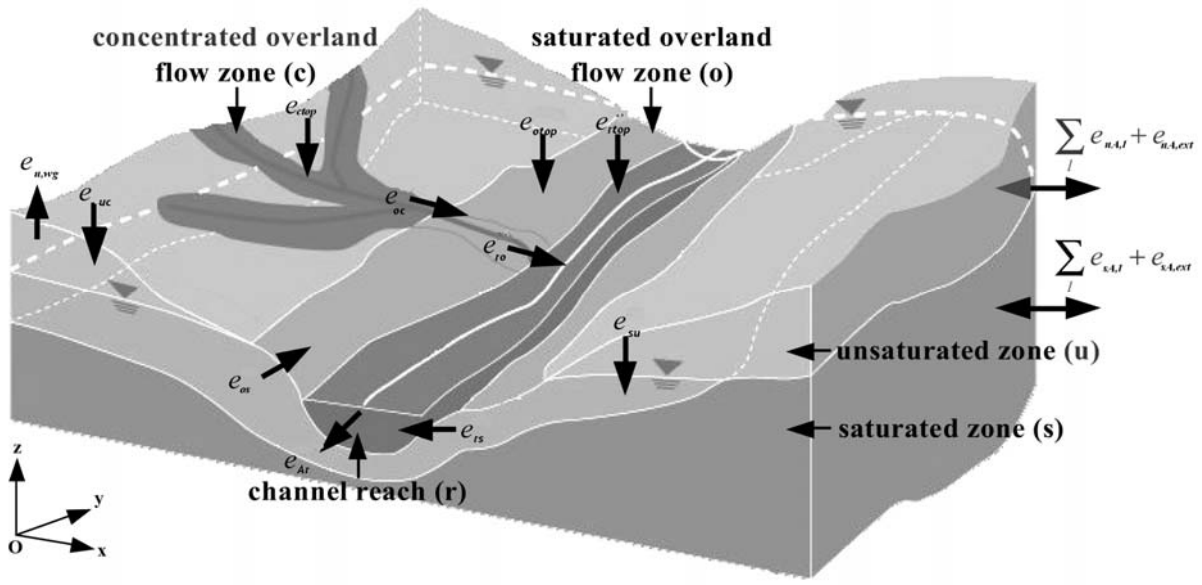

(b)

Figure 3 (a) Catchment discretization into 3 REW units (b) mass exchange fluxes and sub-regions making up the spatial domain of a REW (after Reggiani et al., 1999, 2000): e_{uc} denotes infiltration, $e_{u,wg}$ evapotranspiration from unsaturated zone, e_{su} recharge or capillary rise, e_{ctop}, e_{otop} and e_{rtop} rainfall or evaporation at c, o and r-zones respectively, e_{oc} concentrated overland flow, e_{ro} saturated overland flow, e_{os} seepage flow, e_{rs} flow from saturated zone to channel, e_{Ar} channel flow at outlet, and $\sum_l e_{uA,l} + e_{uA,ext}$ and $\sum_l e_{sA,l} + e_{sA,ext}$ are mass exchanges across mantle segment at u and s-zones respectively [Lee, 2005a]

The set of equations first derived by Reggiani are given below. For further details regarding their derivation and the meaning of the various variables, the reader is referred to Reggiani *et al.* (1998, 1999, 2000), and the nomenclature given in the end of this thesis.

Mass Balance:

$$\underbrace{\frac{\mathrm{d}}{\mathrm{d}t}(\varepsilon y_s \omega_s)}_{\text{storage}} = \underbrace{e_{so}}_{\text{seepage}} + \underbrace{e_{su}}_{\text{exchange with unsat. zone}} + \underbrace{e_{sr}}_{\text{sat. zone-river exchange}} + \underbrace{\sum_l e_{sA,l} + e_{sA,ext}}_{\text{exchange across mantle segments}} \quad \text{(s-zone)}$$

$$\underbrace{\frac{\mathrm{d}}{\mathrm{d}t}(\varepsilon y_u \omega_u s_u)}_{\text{storage}} = \underbrace{e_{uc}}_{\text{infiltration}} + \underbrace{e_{us}}_{\text{exchange with sat. zone}} + \underbrace{e_{u,wg}}_{\text{evaporation}} + \underbrace{\sum_l e_{uA,l} + e_{uA,ext}}_{\text{exchange across mantle segments}} \quad \text{(u-zone)}$$

$$\underbrace{\frac{\mathrm{d}}{\mathrm{d}t}(y_c \omega_c)}_{\text{storage}} = \underbrace{e_{cu}}_{\text{infiltration into unsat. zone}} + \underbrace{e_{co}}_{\text{flow to sat. overl. flow}} + \underbrace{e_{ctop}}_{\text{rainfall or evaporation}} \quad \text{(c-zone)}$$

$$\underbrace{\frac{\mathrm{d}}{\mathrm{d}t}(y_o \omega_o)}_{\text{storage}} = \underbrace{e_{or}}_{\text{lat. channel inflow}} + \underbrace{e_{os}}_{\text{seepage}} + \underbrace{e_{oc}}_{\text{inflow from conc. overl. flow}} + \underbrace{e_{otop}}_{\text{rainfall or evaporation}} \quad \text{(o-zone)}$$

$$\underbrace{\frac{\mathrm{d}}{\mathrm{d}t}(m_r \xi_r)}_{\text{storage}} = \underbrace{e_{ro}}_{\text{lateral inflow}} + \underbrace{e_{rs}}_{\text{channel- sat. zone exch.}} + \underbrace{\sum_l e_{rA,l} + er}_{\text{infow, outflow}} + \underbrace{e_{rtop}}_{\text{rainfall or evaporation}} \quad \text{(r-zone)}$$

Momentum Balance:

$$\underbrace{\pm\sum_l A_{sA,l,\lambda}[-p_s + \rho(\phi_{sA,l} - \phi_s)]}_{\text{inter- REW driving force}} + \underbrace{\pm A_{s,A,ext,\lambda}[-p_s + \rho(\phi_{s,A,ext} - \phi_s)]}_{\text{force acting on the external boundary}} + \underbrace{\pm A_{s,bot,\lambda}[-p_s + \rho(\phi_{s,bot} - \phi_s)]}_{\text{force at the bottom boundary}}$$

$$= \underbrace{-R_s v_{s,\lambda}}_{\text{resistance to flow}} \quad ; \lambda\text{=x,y} \quad \text{(s-zone)}$$

$$\underbrace{\pm\sum_l A_{uA,l,\lambda}[-p_u + \rho(\phi_{uA,l} - \phi_u)]}_{\text{inter- REW driving force}} + \underbrace{\pm A_{uA,ext,\lambda}[-p_u + \rho(\phi_{uA,ext} - \phi_s)]}_{\text{force acting on the external boundary}} = \underbrace{-R_u v_{u,\lambda}}_{\text{resistance to flow}} \quad ; \lambda\text{=x,y} \quad \text{(u-zone, hor.)}$$

$$\underbrace{[-p_u + \rho(\phi_{uc} - \phi_u)]\varepsilon\omega_u}_{\text{force top}} - \underbrace{\rho\varepsilon s_u y_u \omega_u g}_{\text{gravity}} = \underbrace{-R_u v_{u,z}}_{\text{resistance force}} \quad \text{(u-zone, ver.)}$$

$$\underbrace{\rho y_c \omega_c \frac{\mathrm{d}v_c}{\mathrm{d}t}}_{\text{inertial term}} - \underbrace{\rho y_c \omega_c g \sin\gamma_c}_{\text{gravity}} = \underbrace{-U_c v_c |v_c|}_{\text{resistance to flow}} \quad \text{(c-zone)}$$

$$\underbrace{\rho y_o \omega_o \frac{\mathrm{d}v_o}{\mathrm{d}t}}_{\text{inertial term}} - \underbrace{\rho y_o \omega_o g \sin\gamma_o}_{\text{gravity}} = \underbrace{-U_o v_o |v_o|}_{\text{resistance to flow}} \quad \text{(o-zone)}$$

$$\underbrace{\rho m_r \xi_r \frac{\mathrm{d}v_r}{\mathrm{d}t}}_{\text{inertial term}} = \underbrace{\rho g m_r \xi_r \sin\gamma_r}_{\text{gravitational force}} \underbrace{-U_r v_r |v_r|}_{\text{Chezy resistance}}$$

$$+ \underbrace{\pm\sum_l \mathrm{A}_{\mathrm{rA,l}} \cos\delta_l [-p_r + \rho(\phi_{rA,l} - \phi_r)]}_{\text{pressure forces exchanged among REW's}} + \underbrace{\mathrm{A}_{\mathrm{rA,ext}}[-p_r + \rho(\phi_{rA,ext} - \phi_r)]}_{\text{pressure force at watershed outlet}} \quad \text{(r-zone)}$$

In order to close the set of equations, i.e. to make the number of equations equal to the number of unknowns, the exchange fluxes must be expressed in terms of other resolved variables. These are the state variables relating to the sub-regions between which the mass fluxes are being exchanged. These so-called closure relations are the best mechanisms to ground the REW theory to reality, through physically realistic descriptions of actual hydrological processes and their underlying physical mechanisms. The relations are expressed in terms of parameterizations involving landscape and climatic properties.
Before the REW-scale balance equations of Reggiani *et al.* (1998, 1999) can be used as the basis of a new model blueprint, progress had to be achieved among other things in closure

relations, methods for parameter estimation and application of a model to real catchments. Since Reggiani, Zhang *et al.* (2005) and Lee *et al.* (2005a) further defined the closure relations and the numerical schemes to accurately solve the resulting coupled differential equations. In following the REW approach and the differences between two different models will be discussed in more detail.

4.2. REW models

4.2.1. CREW Model

Starting from the original work of Reggiani, the governing equations for mass balances are improved with new physically reasonable closure relations for mass exchange fluxes that incorporate the effects of sub-REW scale heterogeneities. To assist in the numerical simulations, as a first step the mass balances are converted into univariate derivative form with the aid of a number of geometric relationships. The resulting coupled system of equations is then solved, along with a simplified momentum balance equations, using the 4^{th} order Runge- Kutta integration method.

There are several methods available for the development of closure relations that effectively parameterize the effects of sub-grid or sub-REW heterogeneities on the various mass exchange fluxes. Four methods were discussed by Lee *et al.*(2005a) for the development of the closure relations, namely use of detailed field experiments, theoretical/analytical derivations, detailed numerical simulations, and hybrid approaches which may be a combination of any of the above. The closure relations for rainfall, infiltration, exfiltration, groundwater recharge and capillary rise were derived analytically using assumptions regarding sub-grid heterogeneity. Closure relations for concentrated overland flow, saturated excess overland flow were derived by a combination of the analytical approach assisted with limited numerical models, i.e. hybrid approach. Finally the closure relation for seepage flow was derived by application of the numerical simulation approach, with the use of the CATFLOW model, a physically based, distributed model.
In previous research,(Lee *et al.* 2005b), sensitivity analysis showed that the derived closure relations could indeed describe the dynamics of the different hydrological processes in a physical reasonable way under different combinations of climate, soil, vegetation and topography.

4.2.2. REWASH model

An integrated watershed-scale hydrological simulator, REWASH (*Re*presentative *E*lementary *WA*ter*S*hed *H*ydrology) has been developed (Zhang and Savenije *et al.*, 2005). The simulator has been applied in the Geer river basin (Belgium). REWASH is a deterministic, semi-distributed and physically based model. When applying REWASH, a river basin is to be divided into a number of sub-watersheds, so called REW's, according to Strahler order of the river network. REWASH describes the most of the dominant hydrological processes, i.e. subsurface flows in the unsaturated and the saturated domains, overland flow on the surface by either the saturation-excess or the infiltration-excess mechanism, and stream flow in the river channels. By allowing water flux exchanges among the different spatial domains within a REW, the dynamic interactions between surface and subsurface are fully connected.
REWASH is a parsimonious tool, which can be revised to include more components to represent specific processes when applied to a specific river basin when such processes are observed or envisaged to be dominant. Until now, REWASH has been used to model hydrological responses in humid temperate catchments. In these catchments the groundwater and rapid subsurface flow were important for good representation of the reality.
At this moment interception is addressed in REWASH by using a simple parametric approach. The interception process plays an important role in the water balance of a watershed and is often disregarded in modelling practice. In addition, a refinement for the transpiration in the

unsaturated zone has been made. Finally, an improved approach for simulating the saturation overland flow, by relating the variable source area to both the topography and the groundwater level, has been made.
In the model a distinction has been made, between vertical and horizontal saturated hydraulic conductivity, as well as for soil porosity in the upper and lower layer of the soil column respectively. Due to the new subsurface parameterizations, closure relations for the various flow processes have been derived. Compared with Reggiani *et al*. (1999, 2000, and 2005) some modifications to the closure relations are made.

4.3. Overall conclusion regarding the approach and models

In this paragraph several differences between the existing models are described and discussed.

Different Hydraulic conductivities for saturated and unsaturated regions
In *REWASH*, Zhang *et al.*(2005), the soil bottom elevation of each REW is redefined with respect to the REW's own surface elevation so that the bottom boundary of the entire catchment is no longer horizontal. So, the sloping of the hydrological base of a basin is implicitly introduced. The soil column is divided into two layers of which the upper layer is of greater porosity and saturated hydraulic conductivity than the lower one. This model approach is originated from the evidence of an exponential decay in hydraulic conductivity with depth (Beven, 1984) and the form of porosity decay (Kirkby, 1997). In this model is assumed that both soil properties are spatially constant in their respective domain. The effective saturated hydraulic conductivity for the unsaturated (vertical) and saturated (horizontal) zone, and the effective soil porosity of these two zones are updated by a depth-weighted averaging method. Due to this, better depictions of processes with different time scale in the two subsurface regions are expected. In practice a more responsive groundwater table is possible.
The CREW-model did not incorporate this. Therefore one hydraulic conductivity (K_s) for the unsaturated and saturated zone has been taken into account. In this way the different timescales for both zones are neglected. From literature it was found that the saturated zone is more compact and is less porous as the unsaturated zone. Therefore it is recommended to separate them.

Interception vs. Evapotranspiration
From the three existing models only the REWASH brings interception in account. The need to implement this in every existing hydrological model will be shown by the comparison of the results of Zhang and Savenije *et al.* (2005) and Reggiani and Rientjes (2005). Both their models have been applied to the Geer river basin in Belgium.
From Zhang (2005) it can be concluded that a model without interception does not cover the full range of the low flows, suggesting erroneous simulation of the water balance. This is because more water, which would have been intercepted, is added to the subsurface stores, participating in the surface and subsurface flux exchanges, and subsequently contributes to stream flow. Especially during the smaller rainfall events, the part of the rainfall flux that would have been intercepted leads to a higher antecedent soil moisture state, which either initiates a quicker surface runoff or gives rise to higher stream flow during the low flow regime.
If the results of both models are compared it can clearly be seen that REWASH captures, even during low flow regime, the runoff quite nicely, the other model does not give satisfying results for this kind of regime.

Groundwater flow

In REWASH it is assumed that there is variation in the flux exchange between the saturated zone and the river channel. This depends on the hydraulic conductivity for the river bed transition zone, the length of the channel wetted perimeter of the river cross section, as well as on the total hydraulic heads in the river channel, and the saturated zone. In CREW-model this is assumed to be constant, and therefore ignoring the dynamic variability between those zones. The assumption can be valid in case of a long term dry season. In this situation a steady state has been reached. A difficult aspect remains to be, what kind of value q_s should be.

Mass exchange across mantle segment

As proposed by Reggiani, mass can be exchanged across the mantle segments from one REW to another. This can be contradictory in the REW's upstream in the river. All things considered, it is common to say that the catchment is discretized into REW's in such a way that the watershed divide has been taken into account. If this is the case, the REW's lie on the same level with respect to a datum and no water can flow from one REW to another. However, it is possible that water can flow between REW's that lie downstream of each other. In that case it can be verified that groundwater will flow from one REW to another.

The REWASH model still has a closure relation to describe this process, while the CREW model assumes that it is a zero flux boundary. Both assumptions contain some part of the actual hydrological process. It will depend on the catchment probably which closure relation is best suited to simulate the hydrological processes. However it is permanently incorrect to say that all REW's exchange mass across the mantle segments. In some special cases this can occur, but more likely it is to say that this does not occur.

Variable Source Area (VSA) fraction

Reggiani (2000) proposed the following relations to model the VSA:

$$\begin{cases} \omega_o = \dfrac{y_s + z_s - z_r}{z_{surf} - z_r} & (\text{if } y_s + z_s \geq z_r) \\ \omega_o = 0 & (\text{if } y_s + z_s < z_r) \end{cases}$$

(Reggiani *et al.* 2000)

From this formula can be stated that ω_o is a linear function of the groundwater table. Zhang *et al.* (2005) however found that this relation is inadequate to simulate the storm hydrographs accurately. Their model, REWASH, which is suitable for humid and vegetated regions, ignores the concentrated overland flow. This, because in these regions, the infiltration capacities are high and Hortonian overland flow hardly occurs (Dunne, 1978). In this model only saturated overland flow is a mechanism that produces storm runoff. It can be expected that the larger the gradient of the hill slope, the slower the expansion or retreating of the saturated area will be. Zhang *et al.* therefore, proposed a power function between ω_o and the groundwater table to address this effect. The relation between variable source area (VSA) and groundwater table has been defined as:

$$\begin{cases} \omega_o = \alpha_{sf} \left(\dfrac{y_s + z_s - z_r}{z_{surf} - z_r} \right)^{\text{tg}\gamma_o} & (\text{if } y_s + z_s \geq z_r) \\ \omega_o = 0 & (\text{if } y_s + z_s < z_r) \end{cases}$$

(Zhang *et al.,* 2005)

For γ_o, which may vary spatially over the hill slope, the hill slope angle derived from DEM analysis can be used. For a first estimation of α_{sf} , the runoff coefficient can be used as long as the average groundwater level is considered.

In the CREW model a possible functional relationship between the saturation zone depth and saturated surface area by means of a topographic index of TOPMODEL has been investigated. The TOPMODEL theory has been applied to a certain catchment in Germany which leads to the following formula:

$$\begin{cases} \omega_o = 0 & (\text{if } y_s \le z_r - z_s) \\ \omega_o = \dfrac{1}{\beta_{1,\omega_o} + \beta_{2,\omega_o} \exp\{-\beta_{3,\omega_o}(y_s - Z + |\Psi_b|)\}} & \\ \quad - \dfrac{1}{\beta_{1,\omega_o} + \beta_{2,\omega_o} \exp\{-\beta_{3,\omega_o}(z_r - z_s - Z + |\Psi_b|)\}} & (\text{if } y_s \le z_r - z_s) \\ \omega_o = 1 & (\text{if } y_s = Z) \end{cases}$$

(Lee et al., 2005a)

The $\beta_{1,\omega_o}, \beta_{2,\omega_o}$ en β_{3,ω_o} are parameters to be estimated. These parameters should be estimated for each catchment, they are not universally applicable.
Until now the REWASH model is only tested in catchments where hardly Hortonian overland flow occurs, this does not mean that it is only applicable in these catchments. Further testing should tell whether that is the only application for the model. The same thing applies for CREW. The question that arises is wheter TOPMODEL is applicable for each catchment and in case the answer is no, can TOPMODEL-bases relations be applicable to every catchment? What is known is that the relation has been derived with the TOPMODEL while applying it to a catchment in Germany, where also hardly Hortonian overflow occurs. TOPMODEL has been applied to a Mediterranean climate, which successfully simulated the discharges. However other studies showed that TOPMODEL will only provide satisfactory simulations once the catchment has wetted up (Beven, 1995). For more information regarding TOPMODEL, see (Lee,2005)

Here below the existing closure relations, developed by Reggiani, Lee and Zhang are presented to give a full overview of the differences in formulae. Also the equations for the variable source area fractions are given.

Table 1 Closure relations for exchanging mass flux

Flux term	Closure relations (Reggiani *et al.* 1999, 2000, 2005)	Closure relations Lee *et al.* 2004)	Closure relations (Zhang *et al.* 2004)
Infiltration (e_{uc})	$\min\left[i\omega_u, \frac{\overline{K_s}\omega_u}{s_u y_u}\left(-\lvert\Psi_b\rvert(s_u)^{-1/\mu}+\frac{1}{2}y_u\right)\right]$	$\min\left[i\omega_u, \omega_u\overline{K_s}\left(1+\alpha_{uc}\frac{\lvert\Psi\rvert(1-s_u)\varepsilon}{s_u y_u}\right)\right]$	$\min\left[(i-i_{dc}), \frac{K_{su}}{\Lambda_u}\left(\frac{1}{2}y_u+h_c\right)\right]\rho\mathrm{A}\omega_u$
Evaporation/ Transpiration ($e_{u,wg}$)	$\omega_u s_u e_p$	$\min\left[\omega_u\left(e_p+Mk_v\overline{e_p}\right), \alpha_{u,wg}\frac{\omega_u\overline{K}_s}{(1-s_u)y_u}\frac{(s_u)^{2+d}\varepsilon\lvert\Psi_b\rvert}{m}\right]$	$\rho\omega_u\ \min\left[1, 2\frac{\theta_u}{\xi_u}\right](\mathrm{e_p}\text{-}\mathrm{i_{dc}})$ (2005) $e_{ca}=\min(i,i_{dc})\rho\mathrm{A}\omega_c$ (interception, 2005)
Recharge or Capillary rise (e_{us})	$\varepsilon\omega_u v_{u,z}$	$\alpha_{us}\varepsilon\omega_u v_{u,z}$	$\pm\alpha_{us}\rho\omega_u\mathrm{A}\frac{K_u}{y_u}\left[\left(\frac{1}{2}-\frac{\theta_u}{\varepsilon_u}\right)y_u+h_c\right]$
Saturated overland flow (e_{ro})	$2l_r v_o$ (2005)	$\alpha_{ro}\xi_r y_o v_o$	$2y_o l_r v_o$
Concentrated overland flow (e_{oc})	$\frac{B_{co}\Lambda_{co}(y_o+y_c)(v_o+v_c)}{4\rho}$ (1999)	$\alpha_{oc}\xi_r y_c v_c$	$2y_c l_r v_c$ (Not yet implemented)
Seepage flow (e_{os})	$\frac{\overline{K_s}\omega_o}{\cos(\gamma_o)\Lambda_s}(h_o-h_s)$	$\omega_o\alpha_{os,1}\overline{K_s}^{\alpha_{os,2}}\left[\frac{y_u s_u\omega_u+y_s}{Z\lvert\Psi\rvert}\right]^{\alpha_{os,3}}$	$\pm\frac{\rho K_{ss}\omega_o\mathrm{A}}{\Lambda_s\cos\gamma_o}(h_s-h_o)$
Inflow and outflow at channel reach ($\sum_l e_{rA,l}+e_{rA,ext}$)	$\pm\sum_l\frac{B_{rA,l}\mathbf{A}_{rA,l}(v_r+v_r\lvert_l)}{2\rho}+e_{rA,ext}$ (1999)	$\sum_l\frac{m_{r,l}v_{r.l}}{\Sigma}-\frac{m_r v_r}{\Sigma}$	$e_{rin}=\rho\sum_i\frac{1}{2}m_{ri}\left(v_r+v_{ri}\right)$ $e_{rout}=\rho\frac{1}{2}m_r\left(v_r+v_{rj}\right)$
Rainfall or evaporation at C -zone (e_{ctop})	$\omega_c J$ (1999)	$\omega_c J$	$e_{ca}=\rho A\omega_u*\min\left(i,i_{dc}\right)$ (2005) $e_{ctop}=\rho iA\omega_c$ (2005)
Rainfall or evaporation at O -zone (e_{otop})	$\min[e_{so}, \omega_o e_p\Sigma]$	$\omega_o J$	$-e_p\rho\omega_o\mathrm{A}$ Rainfall $e_{otop}=\rho i\mathrm{A}\omega_o$
Rainfall or evaporation at R -zone (e_{rtop})	$\xi_r\omega_r J$ (1999)	$\omega_r J$	$-e_p\rho l_r\omega_r$ $e_{rtop}=\rho i l_r\omega_r$
Ground flow to channel (e_{rs})	$\frac{K_{r,bot}l_r P_r}{\Lambda_r}(h_r-h_s)$	q_s	$\pm\frac{\rho K_{sr}l_r P_r}{\Lambda_r}(h_r-h_s)$
Mass exchange across mantle segment at U-zone ($\sum_l e_{uA,l}+e_{uA,ext}$)	$\sum_l B_{uA,l}\frac{1}{2\rho}[\pm\mathbf{A}_{uA,l,x}(v_{u,x}+v_{u,x}\lvert_l) +\pm\mathbf{A}_{uA,l,y}(v_{u,y}+v_{u,y}\lvert_l)]+e_{uA,ext}$ (1999)	Zero flux boundary condition	Zero flux boundary
Mass exchange across mantle segment at S-zone ($\sum_l e_{sA,l}+e_{sA,ext}$)	$\sum_l B_{sA,l}\frac{1}{2\rho}[\pm\mathbf{A}_{sA,l,x}(v_{s,x}+v_{s,x}\lvert_l) +\pm\mathbf{A}_{sA,l,y}(v_{s,y}+v_{s,y}\lvert_l)]+e_{sA,ext}$ (1999)	Zero flux boundary condition	$\pm\alpha_{si}\rho(h_s-h_{si})$

Geometric Relationship

$$\begin{cases} \omega_o = \dfrac{y_s + z_s - z_r}{z_{surf} - z_r} & (\text{if } y_s + z_s \geq z_r) \\ \omega_o = 0 & (\text{if } y_s + z_s < z_r) \end{cases}$$

(Reggiani, 2000)

$$\begin{cases} \omega_o = 0 & (\text{if } y_s \leq z_r - z_s) \\ \omega_o = \dfrac{1}{\beta_{1,\omega_o} + \beta_{2,\omega_o} \exp\{-\beta_{3,\omega_o}(y_s - Z + |\Psi_b|)\}} & \\ \quad - \dfrac{1}{\beta_{1,\omega_o} + \beta_{2,\omega_o} \exp\{-\beta_{3,\omega_o}(z_r - z_s - Z + |\Psi_b|)\}} & (\text{if } y_s \leq z_r - z_s) \\ \omega_o = 1 & (\text{if } y_s = Z) \end{cases}$$

(Lee, 2004)

$$\begin{cases} \omega_o = \alpha_{sf} \left(\dfrac{y_s + z_s - z_r}{z_{surf} - z_r} \right)^{\text{tg}\gamma_o} & (\text{if } y_s + z_s \geq z_r) \\ \omega_o = 0 & (\text{if } y_s + z_s < z_r) \end{cases}$$

(Zhang *et al.* , 2005)

These were all the major differences between the existing models. Of course this is subject to changes, as a new model will keep developing and might get new features.

5. Study Catchment: Collie River Basin, WA

5.1. Introduction

The total Collie River Basin covers an area of 3,580 km^2 in the south-west of Western Australia., approximately 200 kilometres south west of Perth. (Figure 4) The Collie River is the dominant river system extending nearly 100 km inland. A number of major tributaries branch from the Collie River including the Wellesley, Brunswick, Harris and Bingham rivers (see Figure 5). Their headwaters start on the Darling Range and the edge of the Yilgarn Plateau where annual rainfall is about 600 mm. In the eastern part of the basin most reaches of the river drain catchments with varied land uses, including agriculture, mining and forests. The catchment includes rural centre and coal mining town Collie. Collie has a population of 8.000.

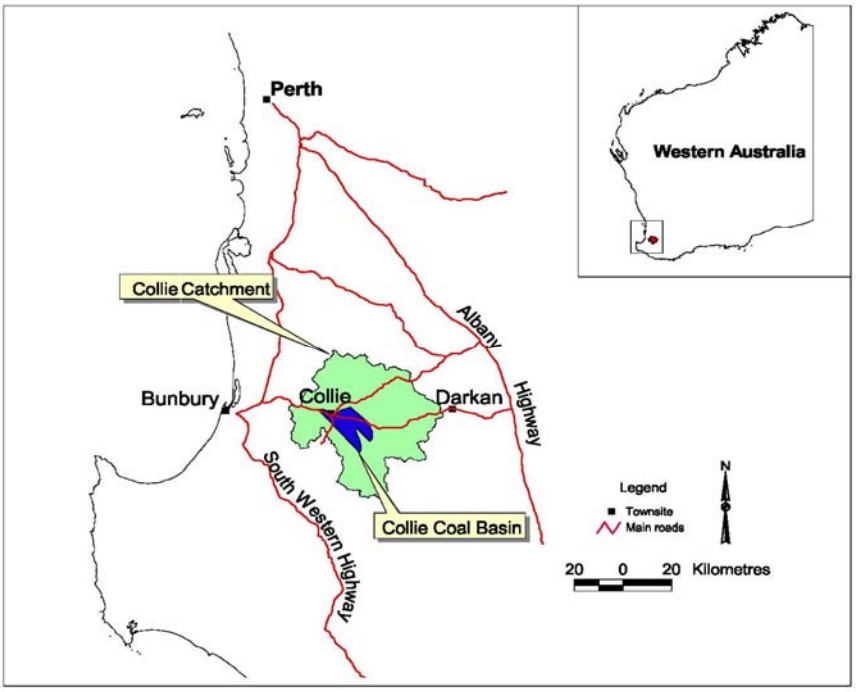

Figure 4 Location map of the Collie River Basin

The study catchment has an area of about 2545 km^2, comprising most of the Collie River Basin. It covers most of the sub catchments shown in Figure 5, only the Wellington Reservoir sub catchment is not taken into account in this research. From the Wellington Reservoir the Collie River discharges the water to the ocean, near Bunbury. See appendix 2 for catchment boundaries.

Hydrological data consist of over 25 stream gauges (including 16 major sub catchment areas) and there are over 20, well distributed, rain gauges. Details about vegetation, climate, soils, geology and land formation are described by Rutherford *et al.* (2000) and Mauger *et al*.(2001) and are summarised below.

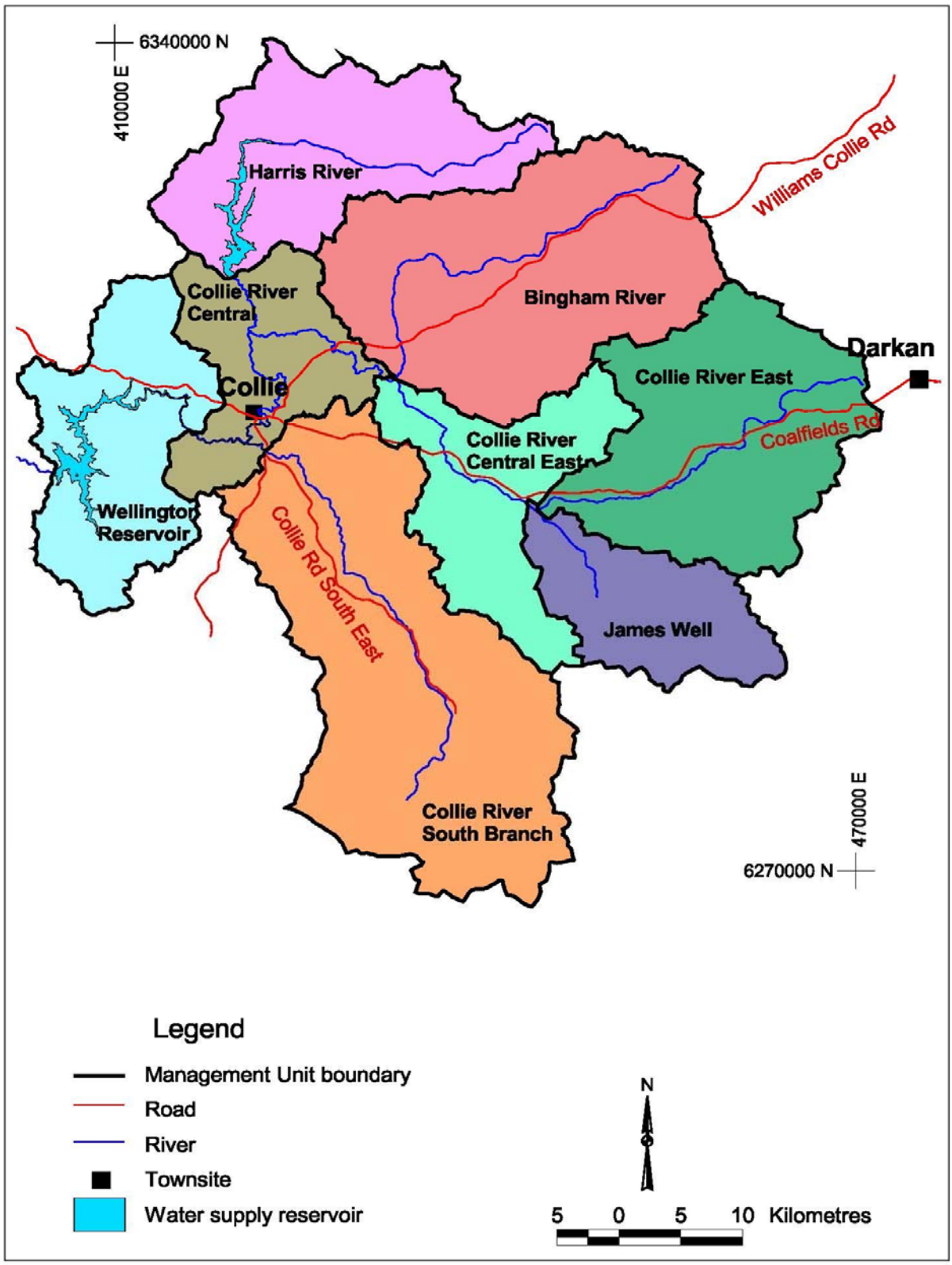

Figure 5 Sub catchments of the Collie River Basin [Mauger et al. , 2001]

5.2. Climate

The region has a Mediterranean climate with cool, wet winters (June-August) and warm to hot, dry summers (December-February). The temperatures for the town of Collie range from 5°C to 16°C during winter months and from 13 to 30°C during summer months.
The average rainfall decreases from west to east and is in the range 1350-550 mm/year. There is a substantial decrease in rainfall from the western, coastal and escarpment areas towards the gently undulating areas 100 km inland. About 80% of the yearly total is received in the May to October period. The wettest month is June; the driest month is January.
The Class A pan evaporation rate is in the range 1300-2000 mm/year. Daily pan evaporation rates range from as high as 10 mm/day in January to less than 2 mm/day in July. Mean annual pan evaporation increases from the southwest to the northeast across the Collie River Catchment.
Rainfall intensities are generally low to moderate. Looking at the 1 and 100 year recurrence interval the intensities are estimated to be, respectively, 56 and 115 mm/ hour at the two high rainfall catchments. At these sites, 50% of the rainfall occurs at less than 5.5 mm/hour.

5.3. Physiography

There are three main physiographic areas on Collie: the Darling Plateau, Blackwood Plateau and the Swan Coastal plain. The Darling Plateau is the major physiographic feature on the Collie. The plateau has an undulating surface, with elevation ranging between 250 and 370 m AHD (Australian Height Datum). This plateau covers the entire study catchment. Perennial and seasonal drainage systems on the Darling Plateau exhibit towards the Indian Ocean. However, in the eastern section of the plateau, gradients decrease and depressions are common features.

5.4. Vegetation

In this catchment four major vegetation systems can be distinguished, namely the Darling, Beaufort, Williams and Bannister systems. The variation in vegetation corresponds to changes in soils, climate and physiography.
The Darling system occupies the western margin of the Darling Plateau, where major areas of native vegetation are constrained to State Forests. In these areas jarrah (*Eucalyptus marginata*) is prevalent on areas of laterite whilst sandy areas comprise mixed jarrah-marri (*Corymbia calophylla*) open forest and blackbutt (*E. patens*).
The Beaufort system, located on the drier, eastern section, is dominated by jarrah and wandoo (*E. redunca*) in the remnant woodland, and swamp yate (*E. occidentalis*) with an understorey of *Melaleuca spp.* in and around small lakes and swamps. Open heath (*Myrteaceae*) and high, closed forests frequently vegetated drainage lines.
At the valley floors the *Eucalyptus wandoo* and *Eucalyptus rudis* are situated.
The cleared areas are typically sown with annual pastures. The presence of cleared and uncleared areas is assessed from Landsat TM images (visible bands). The interpretation of these satellite images shows that about 30% of the catchment area has been cleared of native vegetation and replaced by annual pasture.
In appendix 3 more precise information can be found regarding the vegetation.

5.5. Hydrogeology

In the study catchment several hydrogeological units can be divided. They will be discussed here below. In appendix 4 a map with the geology of the Collie River Basin can be found.

5.5.1. Groundwater occurrence

There are two major hydrogeological units, namely sediments and crystalline basement. The most substantial supplies of groundwater occur in sedimentary rocks within the Collie Basin

(geological term). The weathered profile of the basement rocks in the Yilgarn-Southwest-Province predominantly exhibits low porosities and low hydraulic conductivities and contains only localised groundwater. Groundwater occurs in surficial aquifers in the Yilgarn-Southwest Province, and particularly within Quaternary alluvium in modern drainage lines, in Cainozoic sediments where thick sequences of sands are preserved, and in Early Tertiary (Eocene) alluvial sands and clays which commonly occupy palaeochannels and topographical depressions. Groundwater in Archaean granitoid and gneissic basement exists in faults, fractures and joints in the unweathered rocks, and in the pore spaces of the overlying weathered profile. In granitoid basement, aquifers possessing higher hydraulic conductivities commonly developed at the contact between the unweathered rock and the overlying saprolite.

5.5.2. Collie basin

The largest of the Permian basins, is the Collie Basin. This sedimentary basin covers a surface area of approximately 225 km^2. The basin is structurally controlled and has an elongate bilobate shape. Groundwater exists in the Shotts Formation (*Ps*) and the Collie group (*Pcm*). The Collie Group is the major aquifer in the basin. The Shotts formation can be either an aquitard or a minor aquifer where groundwater is generally confined. Groundwater recharge to the Collie basin is mainly derived from the direct infiltration of rainfall. Recharge may occur in the south-eastern part (of catchment) through the downward leakage of surface water from the Collie River South Branch, where the river elevation exceeds that of the water table.
Groundwater flow, deeper in the Collie basin, is complex and not well understood. The hydraulic connection of these aquifers is complex, controlled by a number of factors including coal seams, basin structure, faults and the heterogeneity of the aquifer.

5.5.3. Yilgarn-Southwest Province

In the Yilgarn-Southwest Province the tectonic evolution of the landscape in conjunction with the chemical and physical properties of the basement rocks, has shaped the contemporary topography. Surficial sediments accumulate where lessening topographic gradients have decreased the ability of the river systems to remove weathered and transported material. Groundwater may reside in these surficial sediments where they are preserved in topographic lows above the weathered granitic basement rocks.
The hydrogeology of the granitic rocks of the Yilgarn-Southwest Province is complex. A significant quantity of groundwater discharges into the river systems. Locally however, the topography of the basement, and the presence of geological barriers such as faults, and aquitards within the regolith affect groundwater flow, which results in groundwater discharging at seeps in valley flanks.

Surficial aquifer
The surficial aquifer consists of Late Tertiary to Quaternary sediments of varying character and extent. Predominantly this aquifer is unconfined and comprised heterogeneous fluvial sediments. Recharge takes either place through the direct infiltration of rainfall or indirectly through surface runoff (derived upstream or from granitic outcrop, or from localised aquicludes formed by clay layers). Groundwater flow is largely topographically controlled with discharge occurring mainly through evaporation, interception and transpiration and direct flow into streams, lakes and swamps.
Extensive Cainozoic alluvial deposits (*Czg*) are identified in three main locations. The major deposit is located in the Collie plains, a topographically low-lying area located approximately five kilometres north of the Collie Basin. Further deposits include a locality which straddles the divide of the Collie River and Blackwood River catchments. These sediments consist of alluvial silt, clay, sand and gravel, and form minor unconfined aquifers with variable intergranular porosities and hydraulic conductivities.
Archaean gneiss and granitoids (*An, Ag*)
These rocks are the largest part of the Collie River catchment. They comprise the fine- to medium grained layered gneiss of the Balingup Metamorphic Belt (*An*) and the variably textured

granodiorite-adamellite granites (*Ag*) of the Darling Range Batholith. Granitic outcrops represent areas of high surface runoff and retains little to no groundwater in joints and fractures. However, outcrop covers only 20% of the Yilgarn-Southwest Province, the remaining is deeply weathered and contains groundwater in pore spaces within the weathered profile and the fractures and joints in the bedrock.
The weathering profile shows marked variations in thickness. These variations are unrelated to landscape position, and thicknesses may exceed 40 m. The profile is often typified by a complex vertical zonnation with fractured material termed grus developing at the weathering front of granitoid rocks.
Groundwater recharge is through direct infiltration of rainfall, surface runoff from outcrop and throughflow derived form upslope sections of the weathering profile. Topography of the basement exerts the dominant control of groundwater flow and major discharge takes place in drainage lines and in areas where the water table intersects the land surface.

5.6. Soil properties

The jarrah forest soils consist of a 2-5 meter thick A horizon, with predominantly gravely and sandy laterites, with some yellow podzolics, overlying less permeable sandy loams and kaolinitic clays (B horizon). The regolith averages 30 meter in depth to a granitic basement. A schematic diagram of a typical hill slope flow strip in the steeper, higher rainfall areas in the Collie River is presented in figure 5. Sharma *et al.* found saturated hydraulic conductivities in the surface soils to be in the range 5.7- 39.5 m/day. The saturated hydraulic conductivities of the subsurface clays are about two orders of magnitude smaller. Carbon *et al*. found most root material to be in the 1-2 meter deep sandy, gravely surface soils. The density of roots is decreased by 10 to 100 times in the underlying sandy loams and clays (see appendix 5).

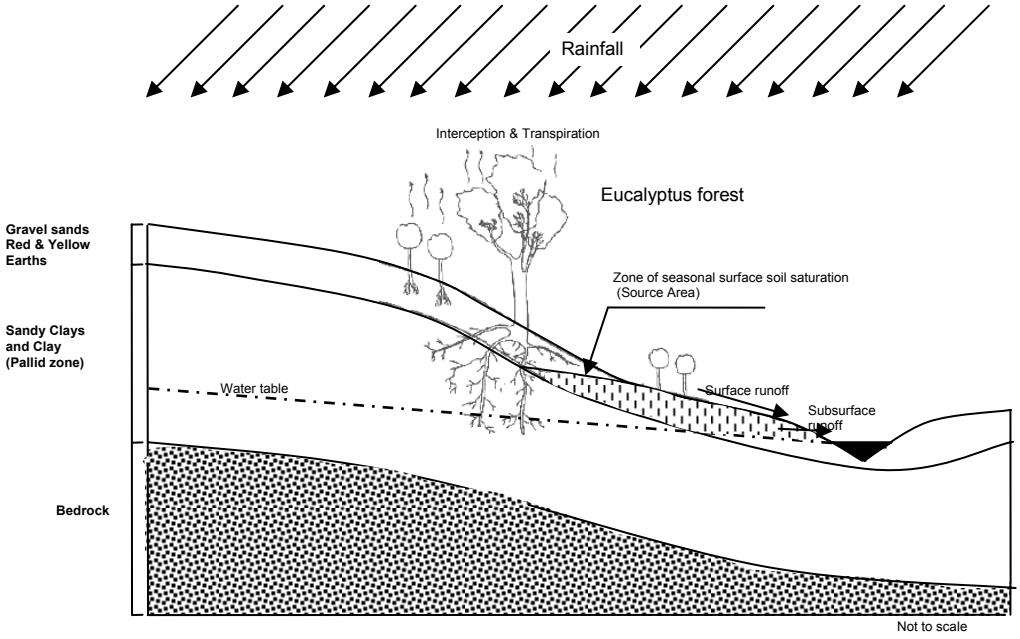

Figure 6 Typical hill slope flow strip in Collie River Basin (adapted from Sharma, 1984)

5.7. Runoff Generation

The infiltration capacities of the sandy and gravely surface soils in the jarrah forests are much higher than the peak rainfall intensities of most flood-producing events. Infiltration excess runoff is thus considered to be almost insignificant in forested catchments. Low land areas, where finer material has accumulated, lower infiltration capacities do give rise to the possibility of overland flow during high rainfall intensity events. However, widespread overland flow and soil erosion have been observed on many catchments after the clearing of native vegetation, and on locations where soil structure has been destroyed (e.g. along vehicle tracks) leading to soil compaction and crust formation. Sharma *et al.* (1987) suggested that forest clearing had induced an order of magnitude reduction in saturated hydraulic conductivity for at least one soil type.
The lateral flow of water through the upper soil horizon is considered to be the major source of stream flow in jarrah forest catchments (Stokes, 1985). Saturation excess overland flow, generated from variable source areas, is also considered to be an important streamflow generation mechanism in jarrah forest catchments, particularly for peak flows (Stokes, 1985). The variable source areas are caused by the intersection of either the perched groundwater table, or the deep groundwater table with the ground surface.

5.8. Transpiration and Interception

Average interception loss for the eucalypt stand in the jarrah forest has been estimated to be about 15% of the mean annual rainfall (Stokes, 1985; Williamson *et al.,* 1987). Transpiration of water is the major loss component in the hydrological cycle of the jarrah forest. Williamson *et al.* (1987) estimated transpiration to be about 75-80% of annual rainfall. Sharma (1984) estimated that evapotranspiration typically accounted for about 90% of rainfall and was greater during winter (2.9 mm/day) than during summer (2.2 mm/day), despite the much greater summer evaporative demand. Sharma postulated that this was due to high interception losses in the winter.
It was also found that the deep-rooted, evergreen, eucalypt vegetation effectively exploits a large soil volume, transpiring water from deep into the profile and often into the deeper groundwater table. As a result, the major overstorey species, jarrah (*E. marginata*), is able to maintain a substantial rate of transpiration throughout the arid summer in spite of considerable soil moisture deficit in the upper soil profile. Sharma *et al.* (1987) found that a substantial amount of water extraction by the forests occurs up to and beyond 6 m depth. They found that about 20% of the total summer evapotranspiration could be derived from depths below 6 m.

6. Measuring Results

6.1. Introduction

The data used for the application of the model based on the REW approach has been collected from the Water and Rivers Commission (WA) and the Bureau of Meteorology. In this chapter analyses will be done to gain knowledge about the hydrologic behaviour of the catchment and to check the data on errors.

Hydrological data consists of over 25 stream gauges (including 16 major subcatchment areas) and there are over 20, well-distributed, rain gauges. See Table 2 for the important gauge stations. We selected a 6 year sequence of daily rainfall and runoff time series (1985-1990) during which most of the rain gauges were operational, unless stated otherwise. In total there are 16 stream gauges and 17 rain gauges used in this analysis. In this analysis most attention is paid to the gauge station located at Collie River South, James Crossing and Harris River. (See appendix 6 and Figure 7 for the location of the gauge stations).

In general there are two kinds of approaches towards the development of theories and models of hydrological response at catchment scale, namely the top-down and bottom-up approach. The bottom-up attempts to combine, by mathematical synthesis, the empirical facts and theoretical knowledge available at a lower level scale into theories capable of predicting the responses at a higher level. The most recent example of this approach is the REW approach, which is applied further on in this thesis. On the other hand, the top-down approach strives to find a concept directly at the level or scale of interest and then looks for the steps that could have led to it from a lower level or scale. For the data-analysis the top-down approach is used.
First the annual data is analysed, where after respectively the monthly and daily data is explored, leading to good understanding of the important processes in this basin.

Table 2 Overview of gauge station with available data (for locations of the stations, see also Figure 7)

station #		Name
612001	rv	**Coolangatta Farm**
	rn	
612002	rv	**Mungalup Tower**
	rn	
612034	rv	**Collie River South**
509376	rn	
612017	rv	**Harris River**
509392	rn	
612014	rv	**Palmer**
509309	rn	
612021	rv	**Stenwood**
509374	rn	
612009	rv	**Lemon**
	rn	
612008	rv	**Ernies**
509249	rn	
612007	rv	**Dons**
509248	rn	
612016	rv	**Maxon Farm**
509321	rn	
612230	rv	**James Crossing**
509108	rn	
612026	rv	**Maringee Farms**
509409	rn	
612025	rv	**James Well**
509408	rn	

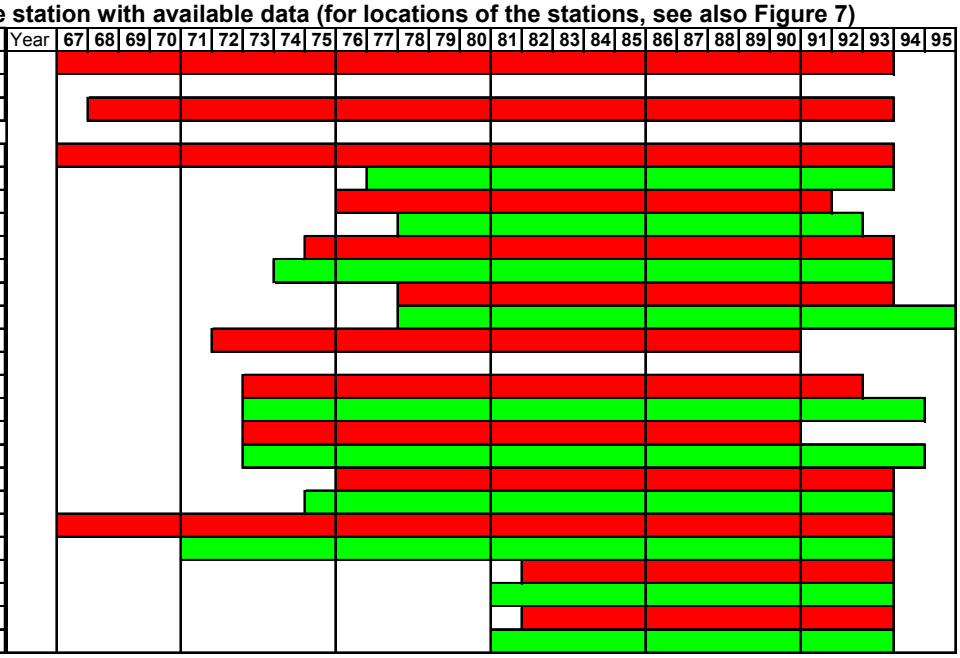

Legend		
	rv	river
	rn	rainfall

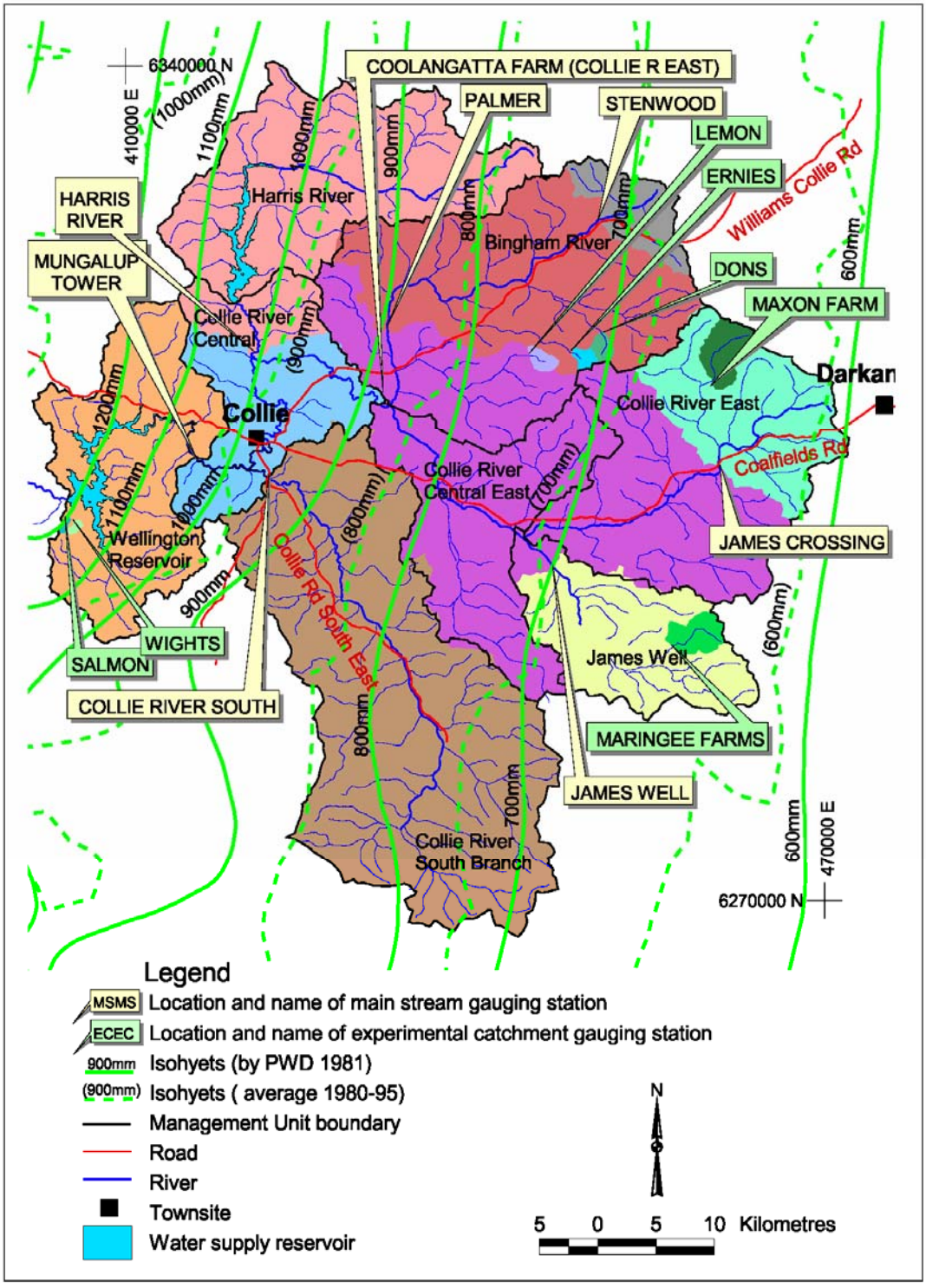

Figure 7 Gauged catchments, rivers and isohyets

6.2. Annual analysis

6.2.1. Precipitation

The precipitation is measured at 17 different locations. There is only daily data available at the moment. In Figure 8 the spatial variability of the precipitation in the catchment is shown. As mentioned before the annual average rainfall decreases from 1100 to 550 mm from west to east, with about 80% of annual rainfall occurring in the May-October period. There is also a spatial variability due to the vegetation cover and the potential evaporation in the catchment (Figure 9) This can also been seen from the precipitation data shown in Appendix 7: Precipitation and Appendix 8: Cumulative Precipitation, obvious errors are already removed from the data.

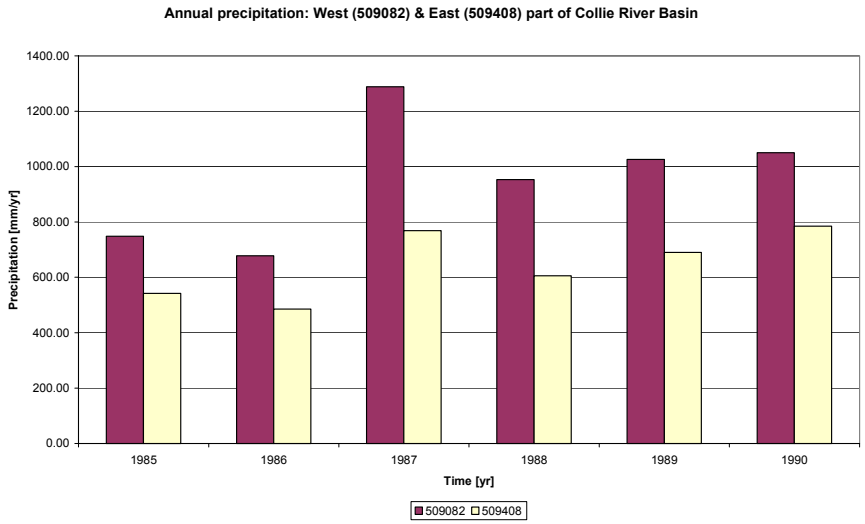

Figure 8 Annual Precipitation for West (509321) and East (509392) part of the Collie River Basin for the period 1985- 1990

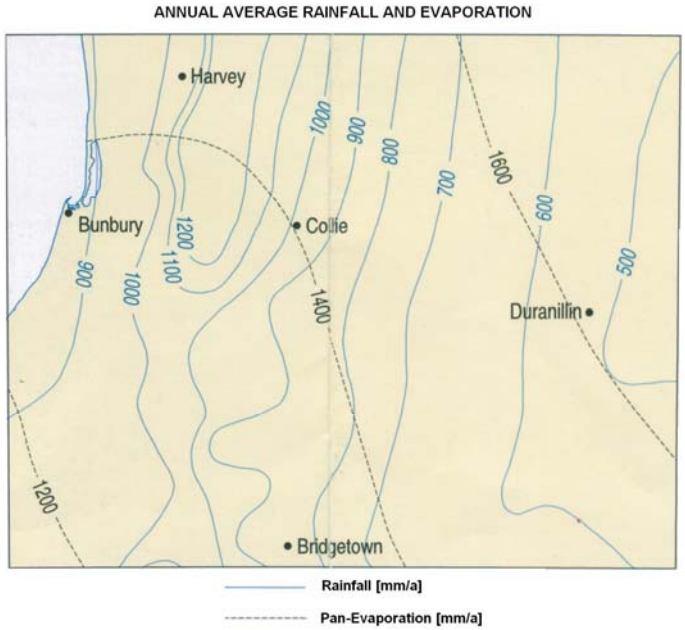

Figure 9 Annual average rainfall and evaporation (Rutherford, 2000)

The precipitation data of the rain gauges have the same shape. Figure 10 shows the correlation between the different rain gauges with a double mass analysis. The average value of the cumulative precipitation is used as reference station. Through a double mass curve inhomogeneities in the time series (in particular jumps) can be investigated, i.e. originating from

change in observer, rain-gauge type, etc. This is indicated in the curve of a double mass plot, showing an inflection point in the straight line.

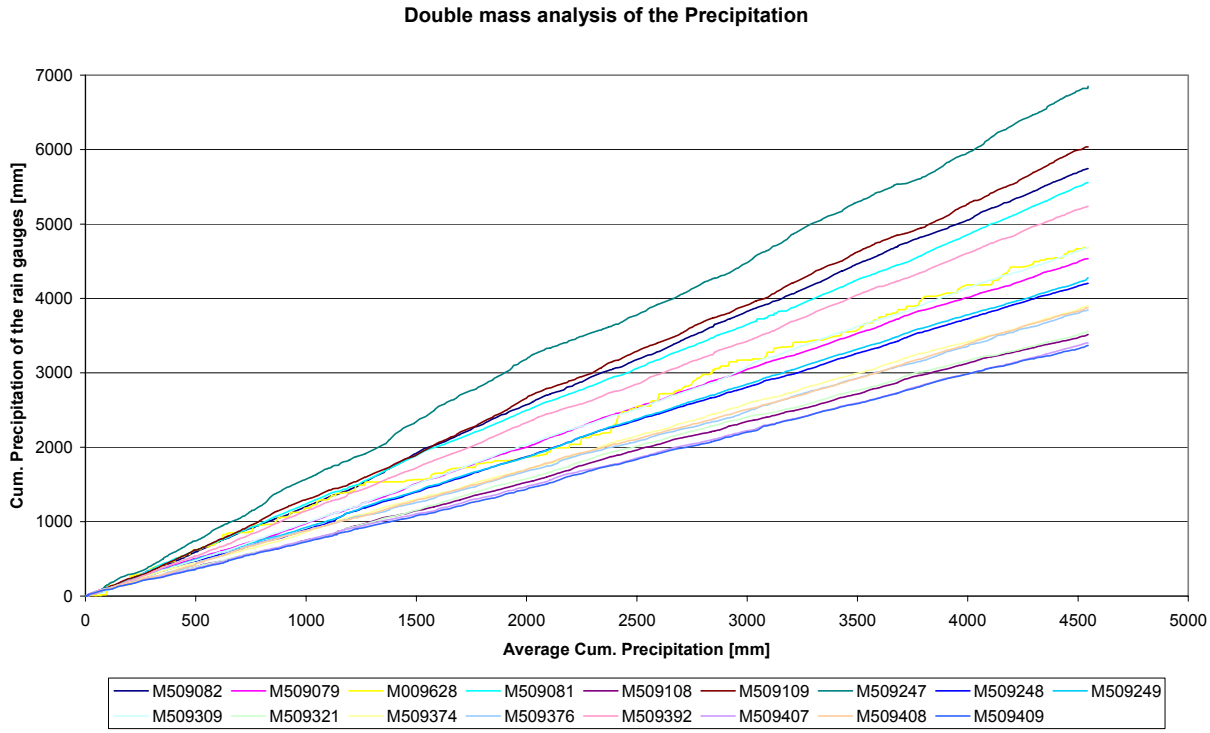

Figure 10 Double Mass Analysis of the Precipitation, with the average of the cum. Precipitation as reference station

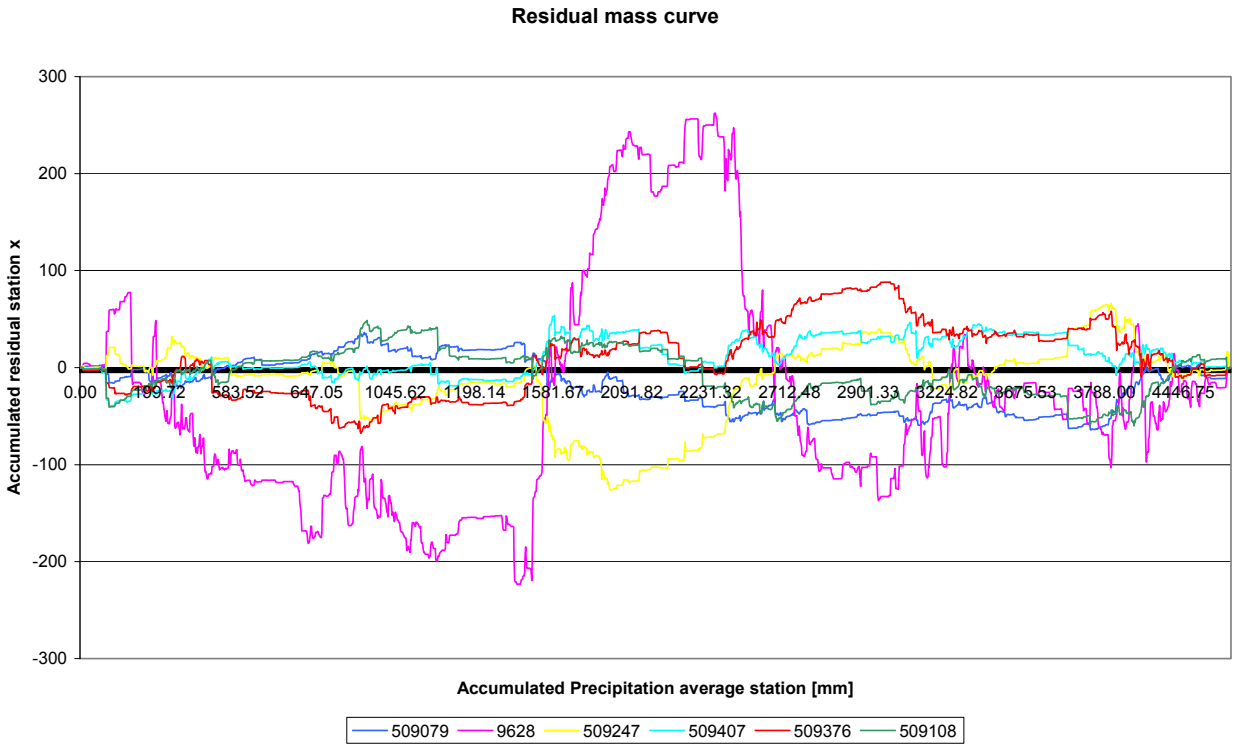

Figure 11 Residual mass curve, with the average of the cum. Precipitation as reference station

From Figure 10 can be seen that station 009628 and 509247 do not have a linear relation with the average station. Especially station 009628 shows a capricious path. This can be caused by the altitude of the station. From Figure 11 can be seen that there are clear deviations between

the average station and the others. An upward curve indicates relative high values of a certain station and downward curve relative low values.

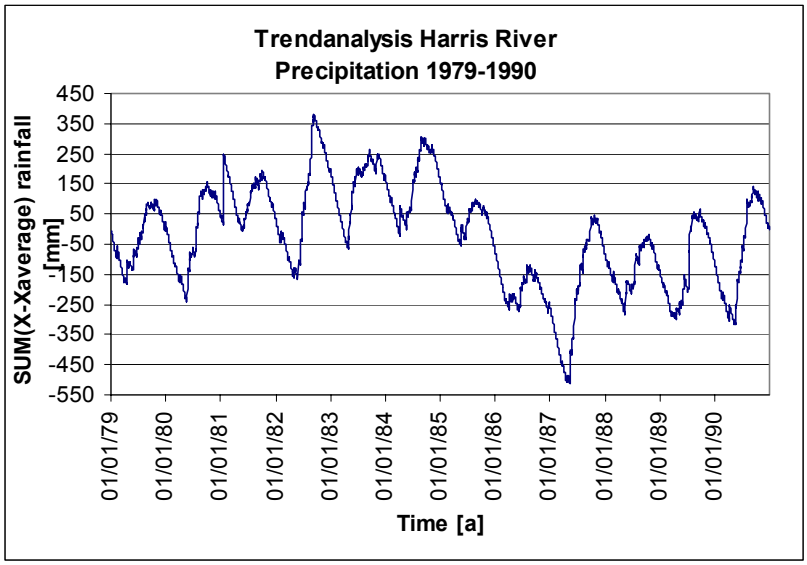

Figure 12 Trend analysis for Harris River precipitation for the period 1979-1990

From Figure 12 can be seen that the years prior to 1986 had high precipitation quantities. With a trend analysis trends in a basin can be identified, as this give the opportunity to look over the years, e.g. comparing two years it can be become clear that a subsequent year has less rainfall than could be expected from the former year.

6.2.2. Discharge

For the three gauge stations, the yearly discharge-precipitation curves are presented in Figure 13. Due to the differences in catchment size the discharge can differ in the order of 5.

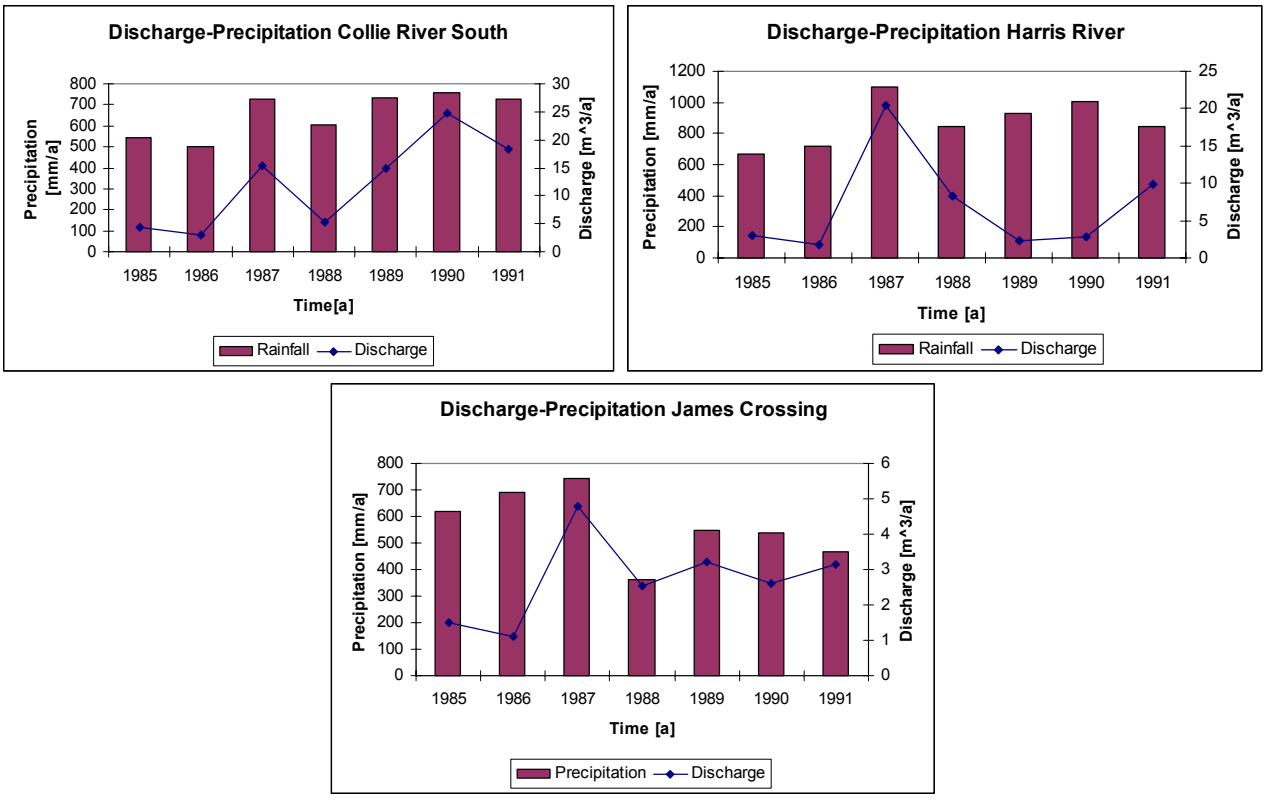

Figure 13 Yearly Discharge- Precipitation for Collie River South, Harris River and James Crossing

The inter-annual water yield graph (Figure 14) shows that there is a small probability of occurrence.

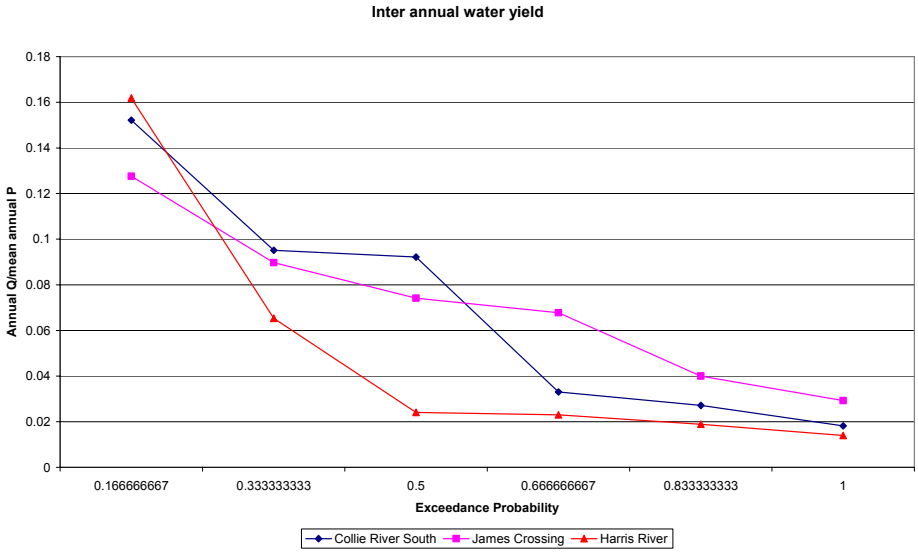

Figure 14 Inter annual yield Collie River South, James Crossing and Harris River

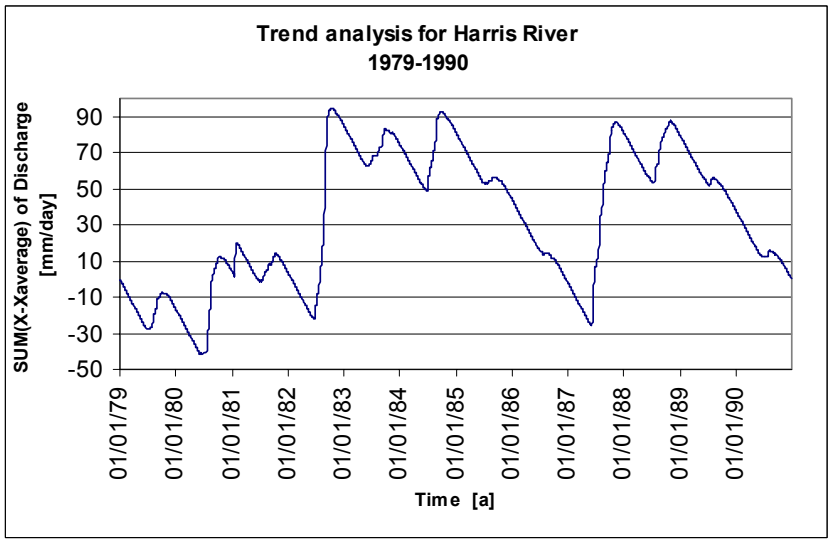

Figure 15 Trend analysis for Harris River discharge for the period 1979-1990

From Figure 15 and Figure 12 the conclusion can be drawn that starting from the year 1985 the precipitation and discharge have the same decrease. In 1987 more precipitation fell which led to more runoff.

6.2.3. Runoff analysis

For the three sub catchments the annual runoff coefficient has been derived. In Table 3 and Figure 16 the differences for the catchments can be found. The runoff is different for each subcatchment. This can be caused by the spatial gradients which influence the precipitation, discharge and evaporation.

Table 3 Runoff coefficients for three sub catchments

	Collie River South	James Crossing	Harris River
1985	0,032	0,050	0,032
1986	0,023	0,039	0,017
1987	0,084	0,106	0,129
1988	0,035	0,065	0,068
1989	0,081	0,069	0,018
1990	0,130	0,081	0,020
Mean	0.064	0,068	0,047

Figure 16 shows that in the case of years with high precipitation the runoff is non-linearly increased. This non-linear relationship is due to the fact that when the storages are filled, all the water will immediately become runoff. When analyzing the monthly runoff this non-linear relationship will be shown to be caused by the interception and fast transpiration

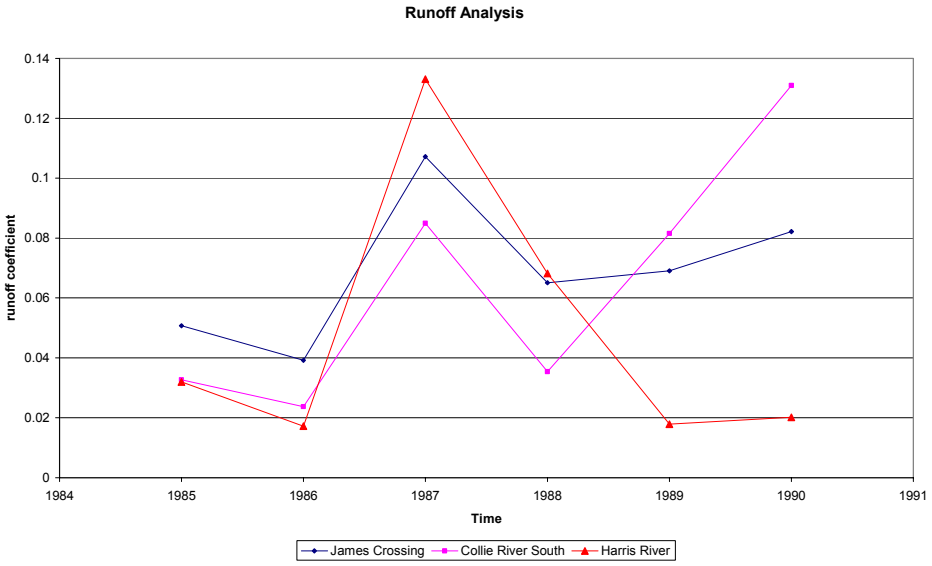

Figure 16 Runoff Analysis for three sub catchments

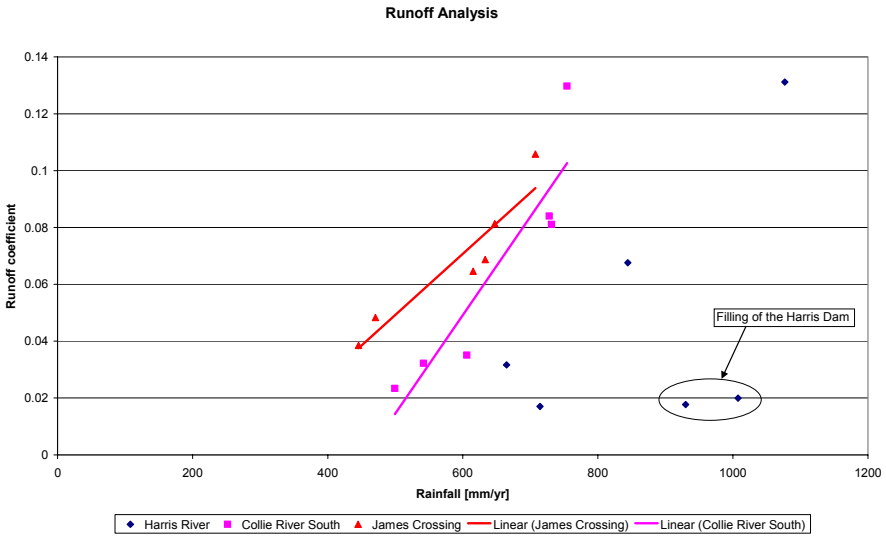

Figure 17 Runoff analysis for the runoff coefficient to the precipitation (1985-1990)

From Figure 17 can be seen that for a certain threshold no runoff takes place. This threshold differs from one station to another. It depends on the quantity of precipitation, interception and evaporation. It was observed that for the gauge station located at the Harris River the last two runoff coefficients for the years 1989 and 1990 have a relative great influence on the linear rainfall- runoff. In the years 1989 and 1990 a dam was built in the Harris River, resulting in a considerable change of the runoff coefficient for the river basin. In Figure 18, the runoff coefficient of the Harris River Basin for the year 1989 and 1990 was excluded. The linear relationship between rainfall and runoff for the Harris River becomes obvious. For data-analysis after 1990 it should be noted that the runoff coefficient has changed while comparing with the years before 1990.

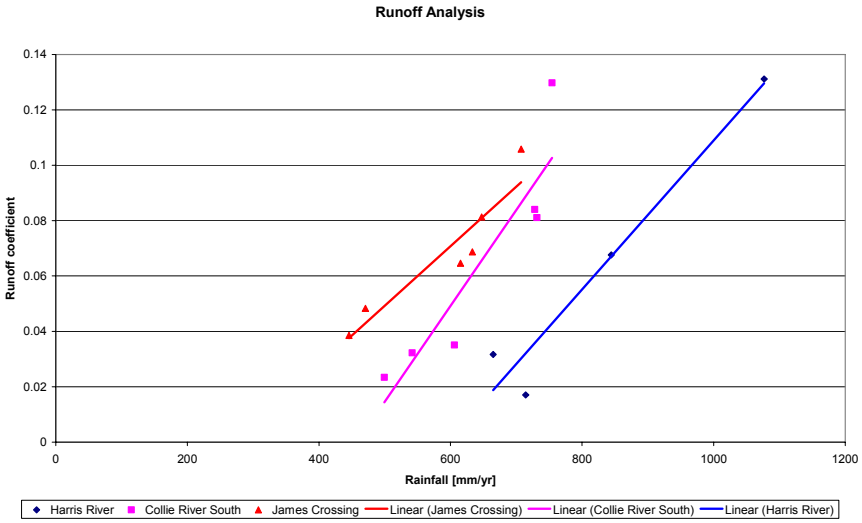

Figure 18 Runoff Analysis with neglecting the years 1989-1990 for the Harris River (period 1985-1990)

6.2.4. Evaporation

For the Collie River Catchment two stations are available that measure the evaporation, namely Roelands and Wakelup. They both are situated in the western part of the catchment. Just as the precipitation, the evaporation also decreases from west to east, namely from 1600 to 1400 mm. For the calculation further on in this thesis the long-term averaged annual potential evaporation (1500 mm) will be used. That this is justified shows Figure 19. Naturally more water evaporates during summer. The monthly variance of evaporation is shown in Figure 41.

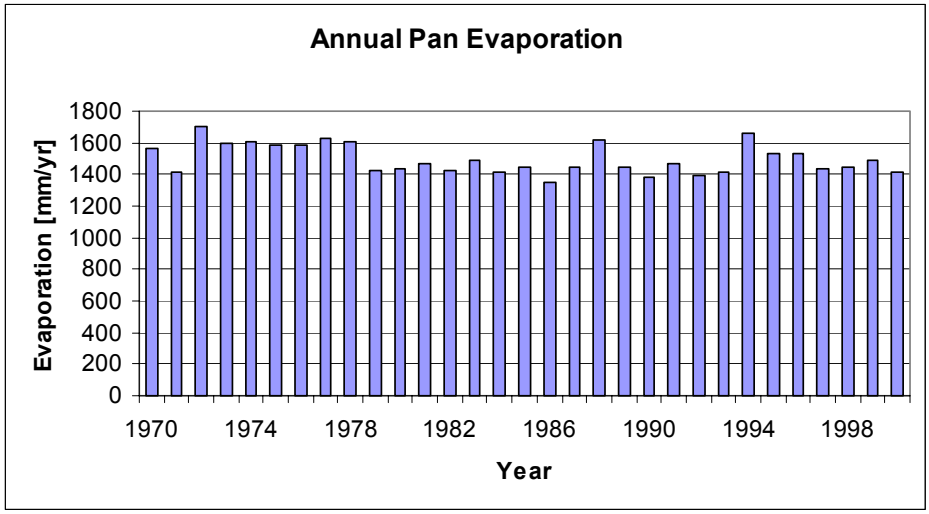

Figure 19 Annual pan evaporation in Collie River Basin

Budyko curve

The Budyko curve is an important tool to first characterize the area of study from a hydrological point of view. It permits to distinguish between energy limited and water limited environments, by means of the aridity index or dryness, to identify which proportion of annual precipitation is converted in evaporation, transpiration and which one in runoff and finally to identify anomalous years. In the study catchment, the obtained Budyko curve is reported in Figure 20. To calculate the actual evaporation, the following formula was used (Brutsaert, 1934)

$$E_a = P(1 - \exp(\frac{-E_p}{P})$$

Where

P Annual Precipitation [mm/a]

E_p Pan Evaporation [mm/a]

In order to find the values for the different years, the assumption can be made that the storage during a hydrological year is zero. In this case the following formula applies:

$$\frac{\mathrm{d}s}{\mathrm{d}t} = 0 = P - E_a - \frac{Q}{\mathrm{A}} \quad \rightarrow \quad E_a = P - \frac{Q}{\mathrm{A}}$$

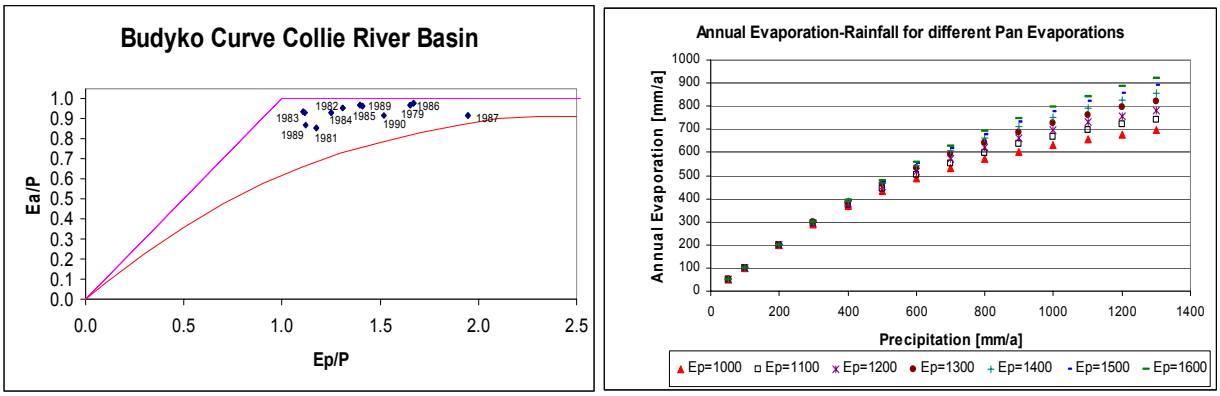

Figure 20 The Budyko curve and Annual Evaporation- Rainfall for different Pan Evaporations (in Collie River Basin the Pan Evaporation varies between 1400-1600 mm/a)

6.3. Monthly analysis

6.3.1. Precipitation

As was seen from the annual data none of the rain gauges has a correlation of 1 with the average of the cumulative precipitation, but most of the lines are more or less a straight line, which indicate a constant correlation. Normally the correlation between rain gauges decreases with increasing distance between the rain gauges. This is for example used in the formula developed by Kagan:

$$\rho = \rho_0 \times e^{-r/r_0}$$

ρ = correlation at distance r [-]
ρ_0 = correlation at distance r_0 [-]
r = distance between rain gauges [m]
r_0= reference distance [m]

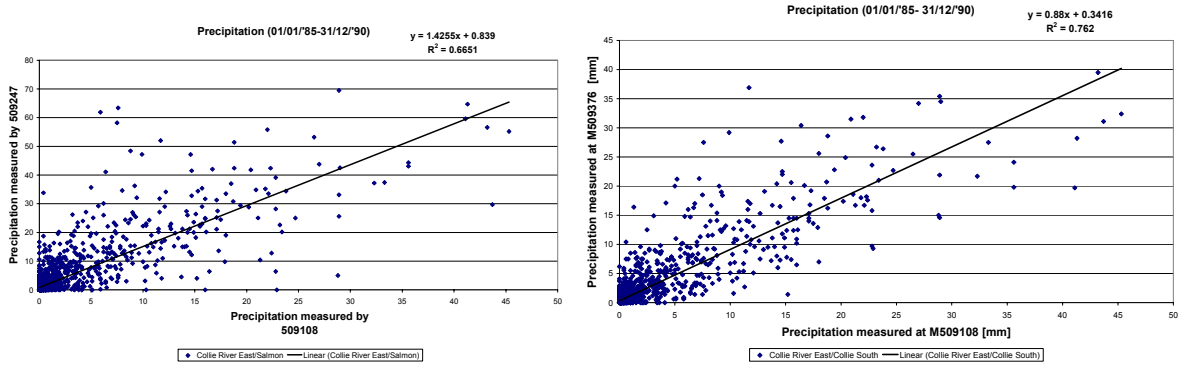

Figure 21 The extremities of the correlation

The correlation between stations that lie close by should be the highest, which is the case. The coefficient a of the linear regression line (Y=aX+b) between the stations varies between 0.88 and 1.43 (see Figure 21).The stations which lie close by show a correlation of nearly 1 with the reference station (see Figure 22). That this is true is shown by Figure 23.

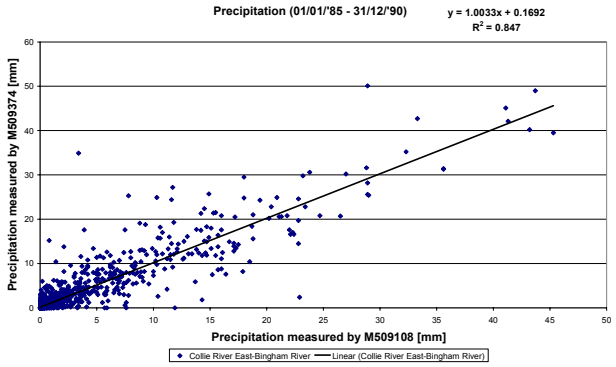

Figure 22 Almost a perfect correlation between stations M509108 - M509374

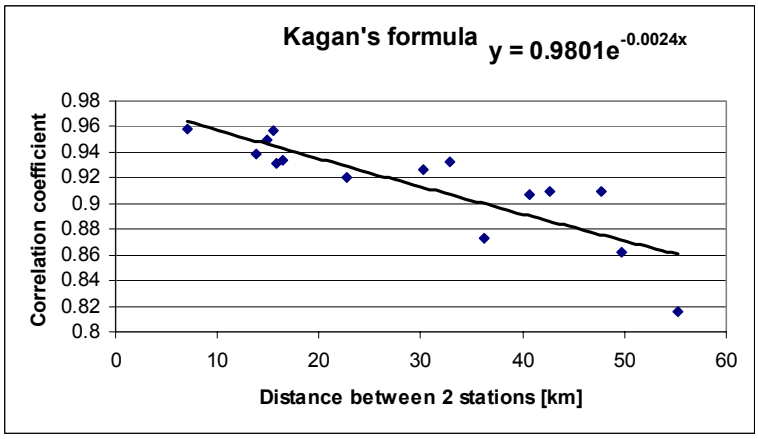

Figure 23 The formula of Kagan, tested with station 509108 as reference station

The formula of Kagan was tested for station 509108 as reference station. The formula of Kagan is an exponential function which equals ρ_0 at r=0 and which decreases gradually as r goes to infinity. The distance r_0 is defined as the distance where the tangent at x=0 intersects the x-axis. In other words the correlation between stations decreases as the distance increases. That the formula of Kagan indeed shows this can be seen from Figure 23.
The ρ_0 = 0.9801 and the r_0= 60 km. For gauge station 509247 which lies approximately 55 km away from the reference station the correlation coefficient is still 0.82. That is relatively good for this distance.

Also a comparison is made between the mean monthly rainfalls for the three gauges to see what the pattern is for each gauge. From Figure 24 a similar pattern is shown for all the three gauges.

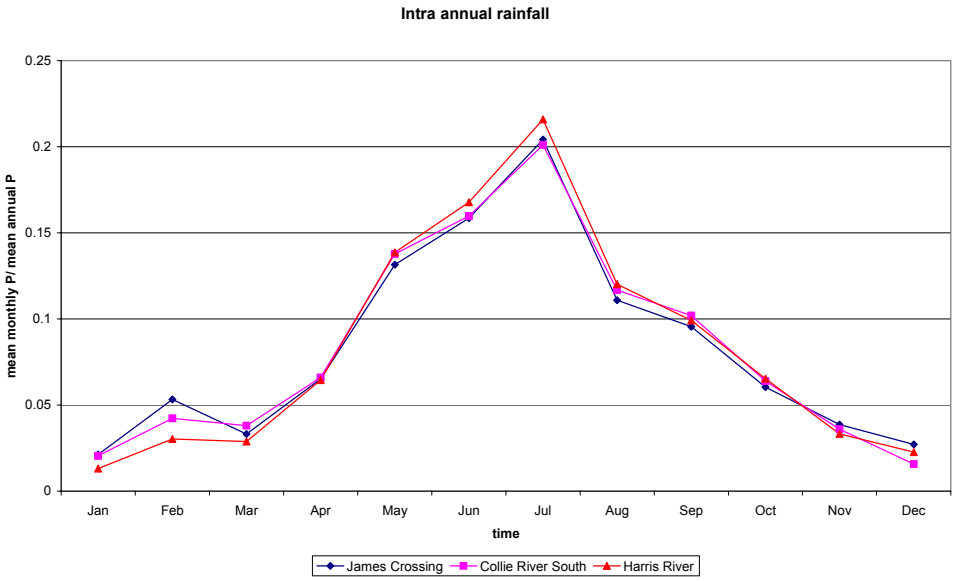

Figure 24 Intra annual rainfall Collie River South, East and Harris River

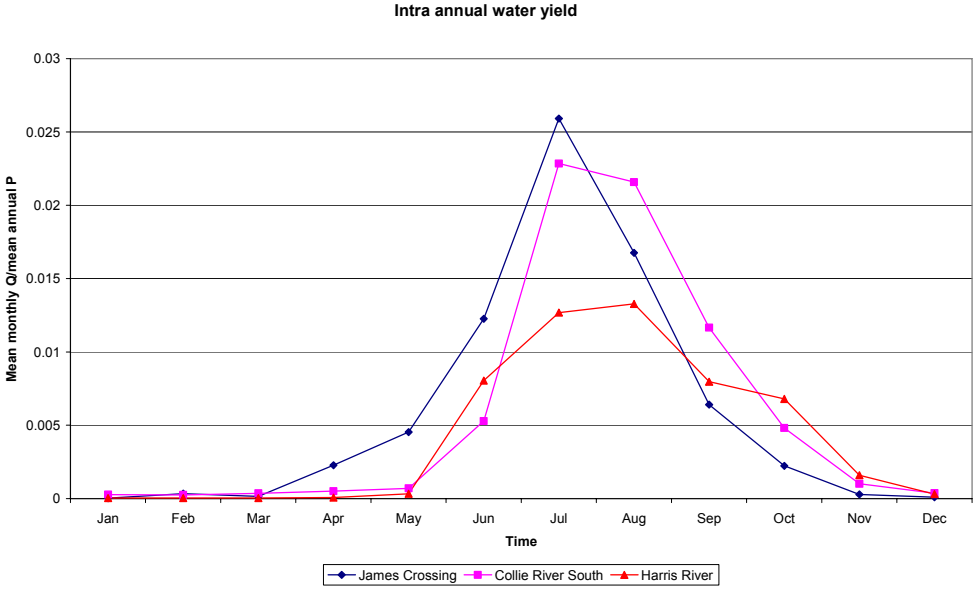

Figure 25 Intra annual water yield Collie River South, East and Harris River

The rain stations show the same pattern in the catchment. The amount of precipitation in a month is correlated for each station in comparison with the annual mean precipitation for that station. However, the stream flow stations show a different pattern. (Figure 25) The James Crossing is a small catchment and the catchment reacts strongly to peaks (e.g. in July). As soon as it rains, the runoff reacts immediately. So this indicates that the time that water is stored in the ground is relatively short. The other sub-catchments are larger and differences are more smoothed.

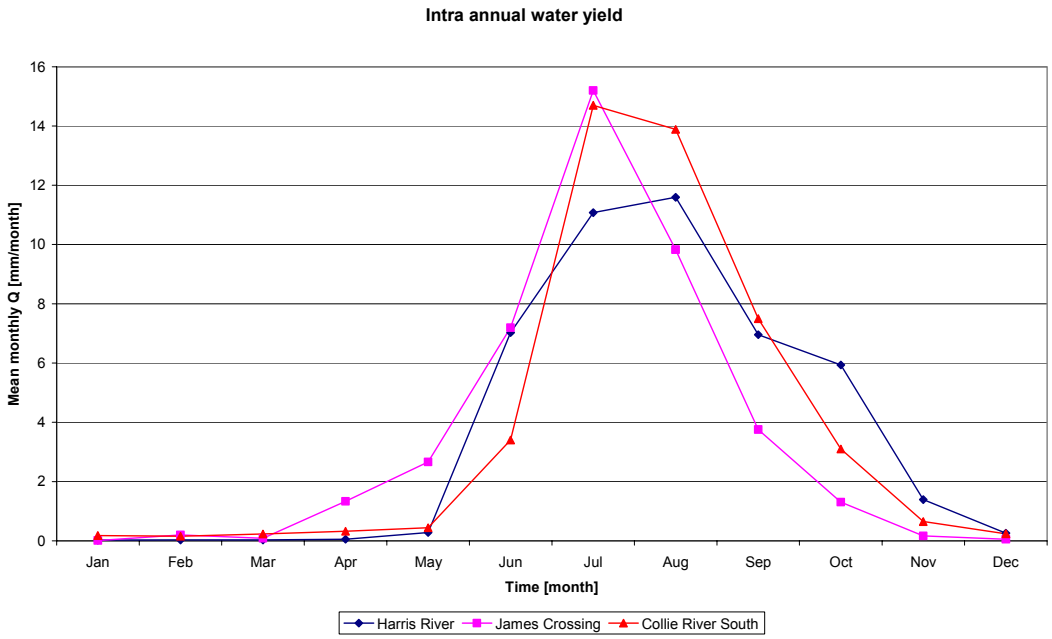

Figure 26 Intra annual water yield Collie River South, James Crossing and Harris River.

6.3.2. Discharge

In order to keep the analysis of the discharge logical, there are in this paragraph some annual analysis presented and are kept here for the clearness.
Based on the hydrographs of the different stations in the Collie River basin it can be concluded that this is an intermittent river. Figure 27 shows the measurement data from the stations in the Collie River South. The discharge increases after a precipitation event, shown with the cumulative precipitation line in the chart. When no precipitation occurs the line is horizontal. The years used are the hydrological years which start in March. At the end of the summer, the reaction of the discharge on a precipitation event is less than in autumn. This caused by the filling of the storages. During summer the evaporation and interception grade is much higher, so the storages are not full. Nevertheless, in autumn more precipitation occurred, so the storages are being filled. When the storages are full, the discharge in the river increases, more runoff takes place.
In the following, three stations will discussed, namely Collie River South, James Crossing and the Harris River. Each of these rivers is a branch of the Collie River Basin.
For the Collie River South, the average discharge between January 1985 and December 1990 was around 81970 m^3/day. However, if the peaks are not taken into account, the average discharge is around 12160 m^3/day (average base flow)

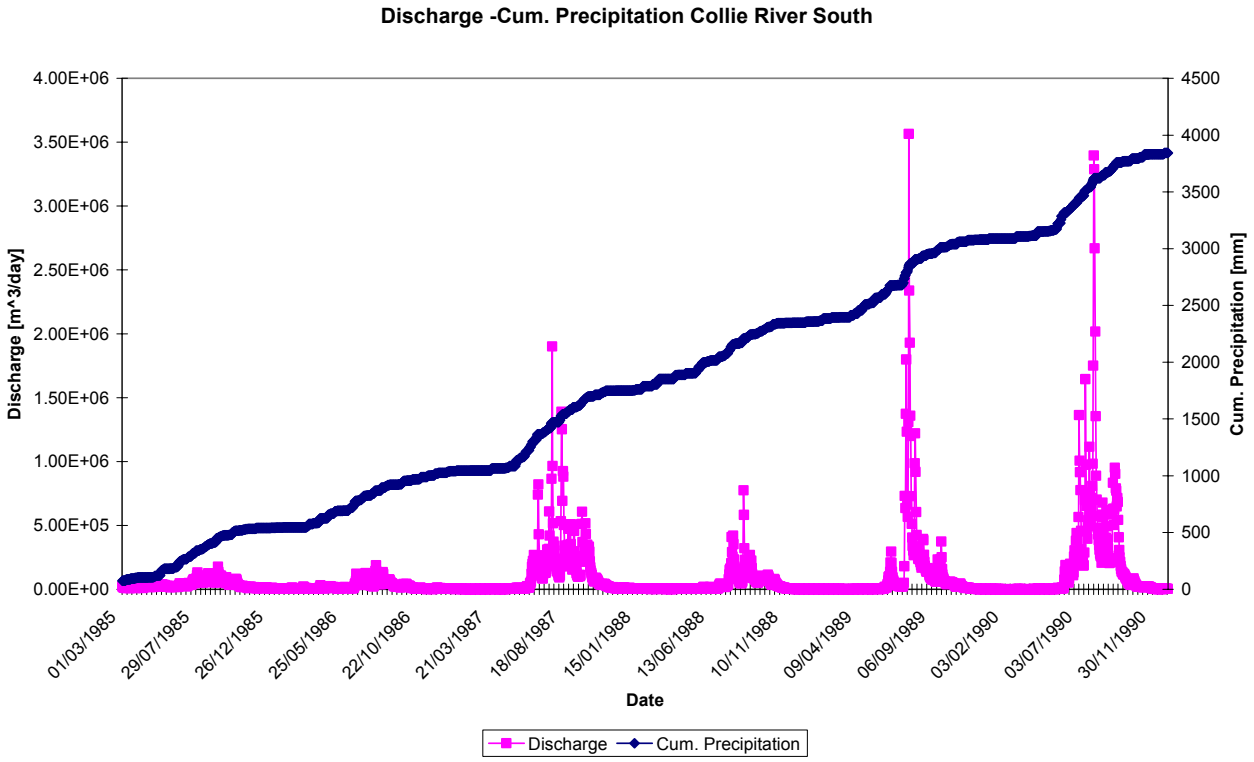

Figure 27 Discharge-Cum. Precipitation Collie River South

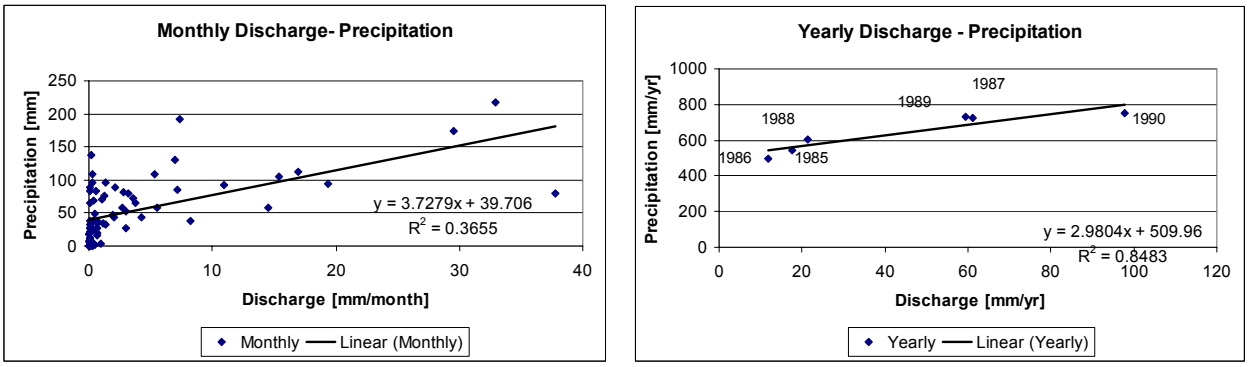

Figure 28 Monthly and Yearly Discharge Precipitation for Collie River South (Area 668 km2)

From the yearly discharge-precipitation chart (Figure 28) the threshold value when no runoff occurs can be determined. For this part of the Collie River Basin, the threshold value is 510 mm/yr. If the annual precipitation is below this threshold value, no runoff takes place. The precipitation is in that case stored in the different storages available in the catchment. For the monthly discharge-precipitation chart it can be observed that no logical relationship can be found. If looked at the yearly figures a relationship can easily be derived.

These analyses are also conducted to a different part of the Collie river catchment, namely the Harris River (see Figure 29). Just like in the Collie River South, the rainfall runoff relations differ between summer and winter. After the summer the storages can be filled, so a lower runoff occurs. In autumn and winter as the storages are being filled, the interaction time between precipitation and runoff is small. The average discharge is 46470 m^3/day, including the peaks; without peaks 17800 m^3/day.
The maximum discharge for this part of the basin lies around 1460 m^3/day. This occurred on 25 July 1987, while the maximum discharge for the Collie river south occurred on 21 July 1989 (3500 m^3/day).
A possible reason for changing locations of the maximum discharges from year to year can be found in strong spatial gradients of rainfall, potential evaporation and the vegetation cover.

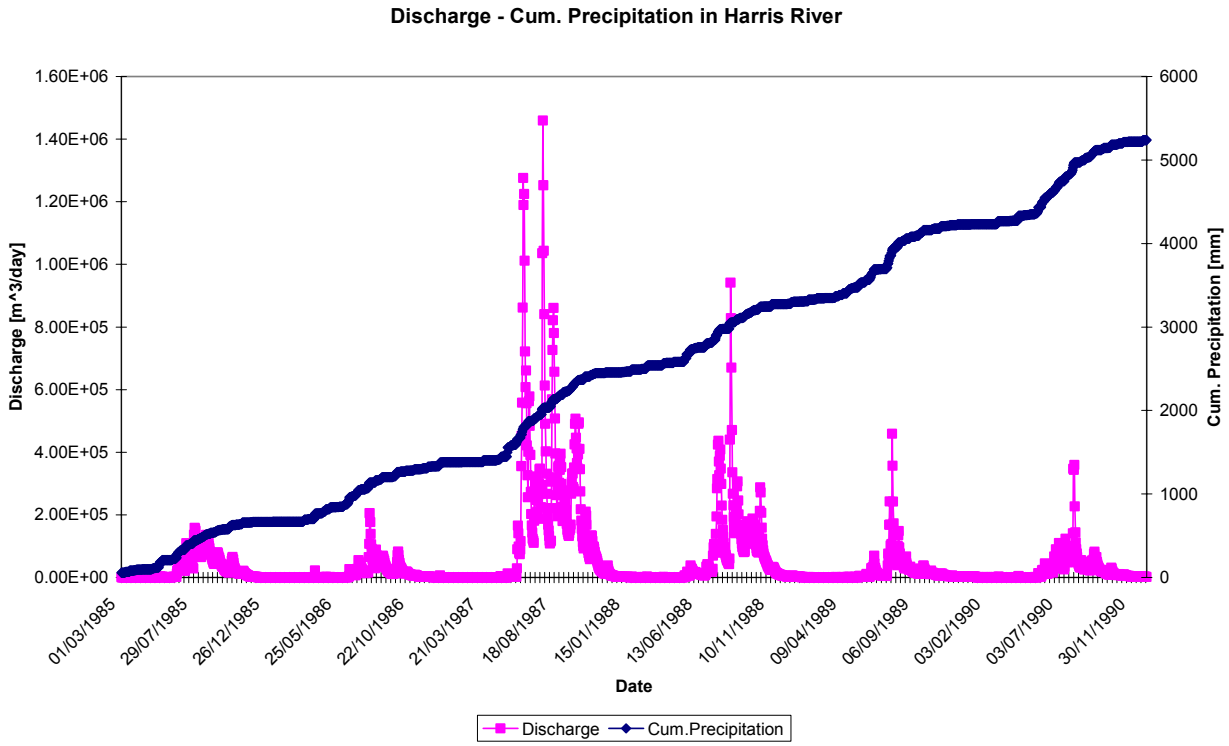

Figure 29 Discharge-Cum. Precipitation Harris River

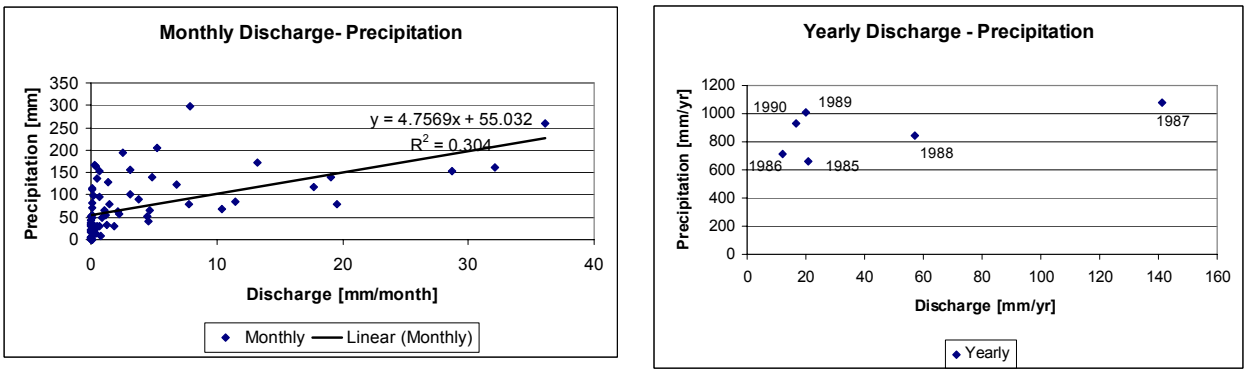

Figure 30 Monthly and Yearly Discharge- Precipitation for the Harris River (Area 382 k m2)

In contrast with the Collie River South the threshold value for the Harris River is higher, around 785 mm/yr. If however the last two years (the period in which the Harris Dam was constructed) are neglected the threshold value will be around 650 mm/yr (Figure 31). The relationship between the other years has substantially increased, so the correct threshold value is the one with neglecting the last two years. It should be noted that for the years after the construction of the dam the runoff coefficient has changed. So the mentioned value can not be used for the years after 1989.

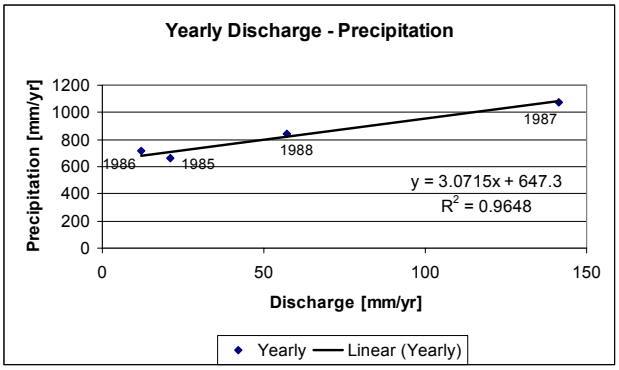

Figure 31 Yearly discharge for the Harris River, period 1985-1988, neglecting 1989-1990

For the James Crossing the same analysis has been conducted. It can be seen from Figure 32 that the same trend applies here for the precipitation. The average discharge is 19380 m^3/day (including the peaks), and without them it is 10140 m^3/day.

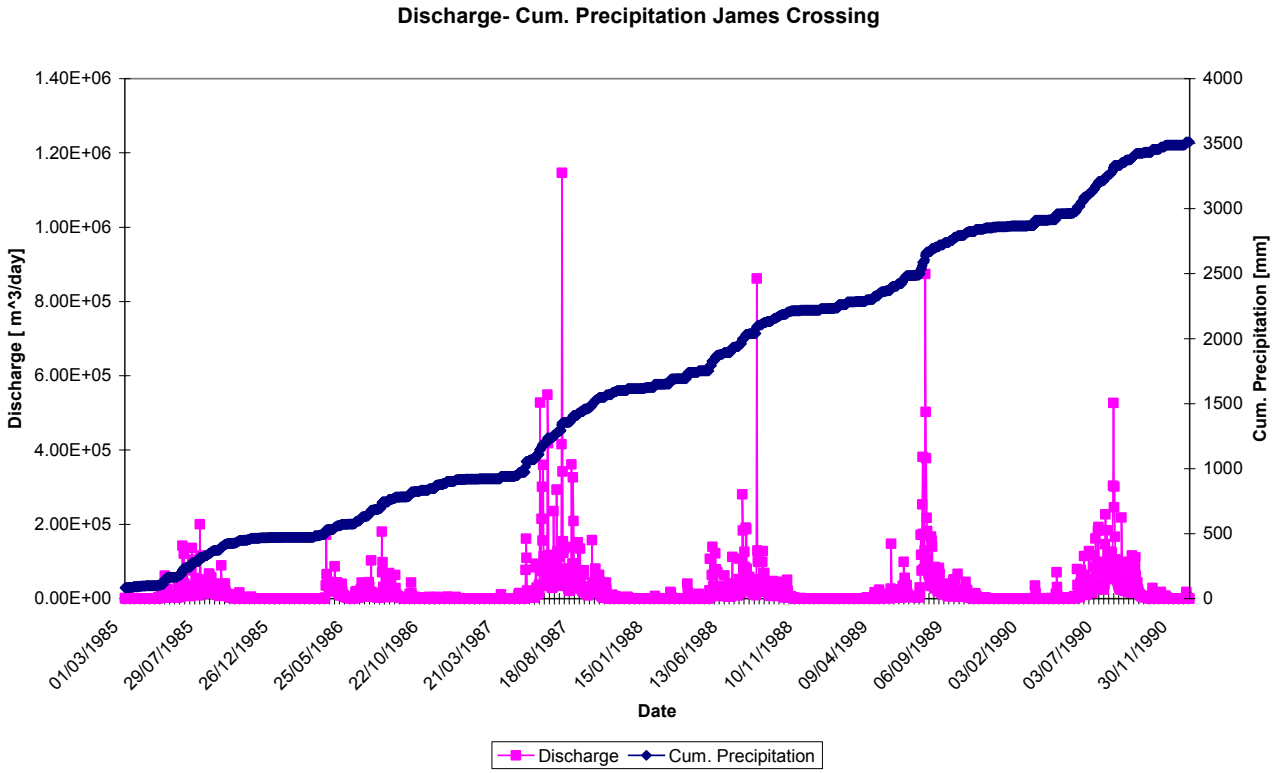

Figure 32 Discharge - Cum. Precipitation James Crossing

For the James Crossing the threshold value lies in the order of the 390 mm/yr. (Figure 33) If there is less precipitation no runoff will occur.

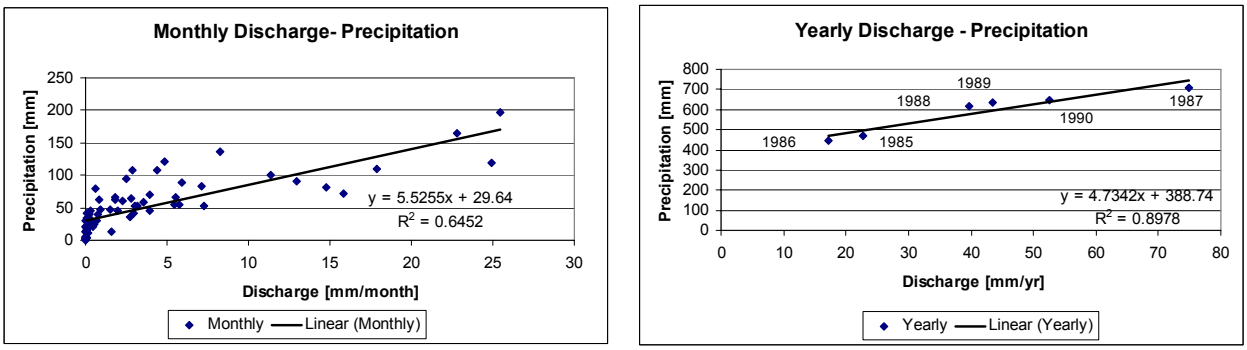

Figure 33 Monthly and Yearly Discharge-Precipitation in the James Crossing (Area 169 km2)

Multiple Linear Regression

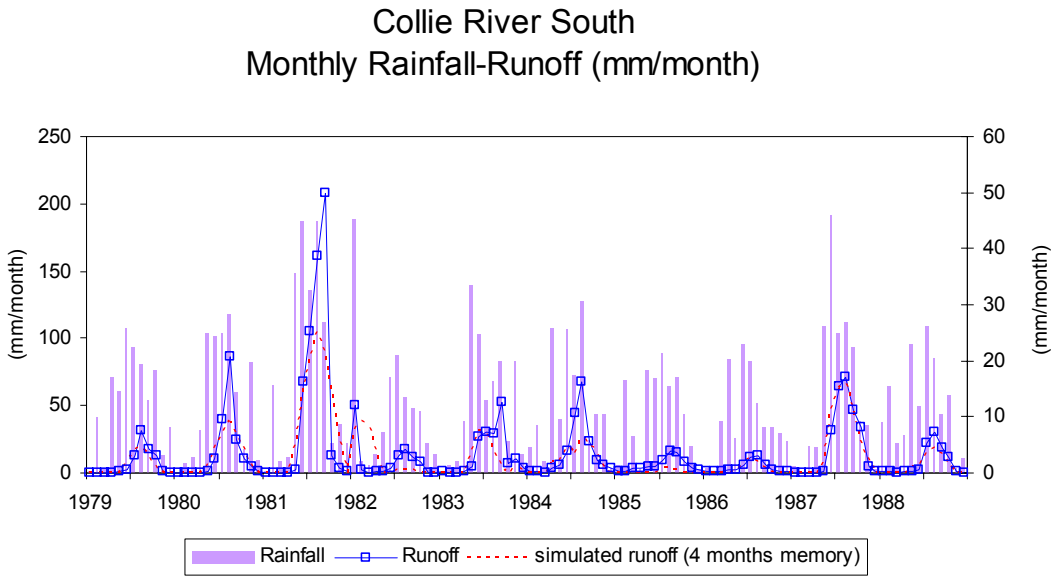

Figure 34 Collie River South, monthly rainfall-runoff

The rainfall- runoff relations are also reviewed with a multiple linear regression model. The relations based in the model are on a monthly basis. Runoff only occurs when the storages underground are full. There is a certain threshold value, in the model this has been chosen as 69 mm/month. In Figure 34 also a simulated runoff has been compiled based on four months of memory of both rainfall and runoff. Often the model underestimates, but sometimes the runoff is even overestimated. This can be caused by invariance in the underground or higher evaporation rate. As for the Collie River South, also the Harris River and James Crossing multiple linear regression calculations are made. (Figure 35, Figure 36)

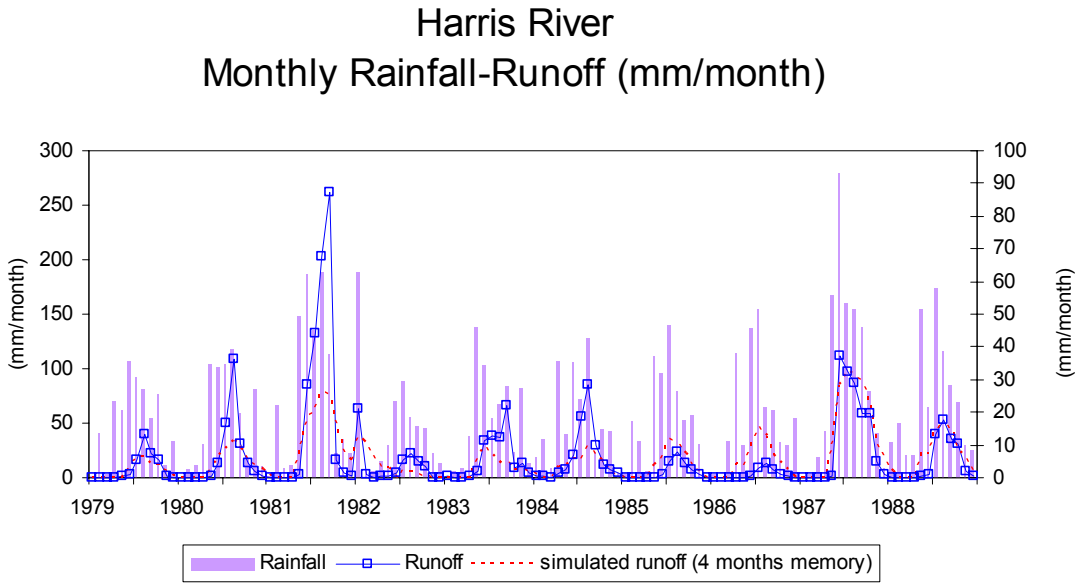

Figure 35 Harris River, monthly rainfall runoff, derived through multiple linear regression

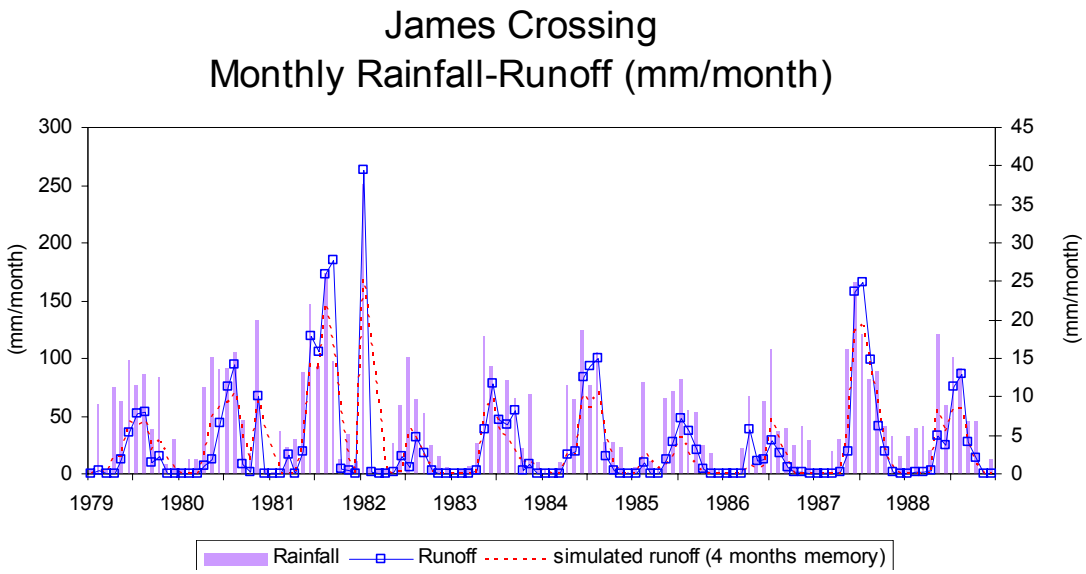

Figure 36 James Crossing, monthly rainfall runoff, derived through multiple linear regression

Table 4 Threshold values for the station using multiple linear regressions

	Threshold [mm]	R^2	Memory [months]	Coefficients 1	2	3	4	Σb_i
Collie River South	69	0.7640	4	0.1116	0.1085	0.0524	0.0684	0.3409
James Crossing	56	0.8699	3	0.1728	0.0643	0.0277	0	0.2648
Harris River	63	0.6527	4	0.1123	0.1185	0.0563	0.0520	0.3391

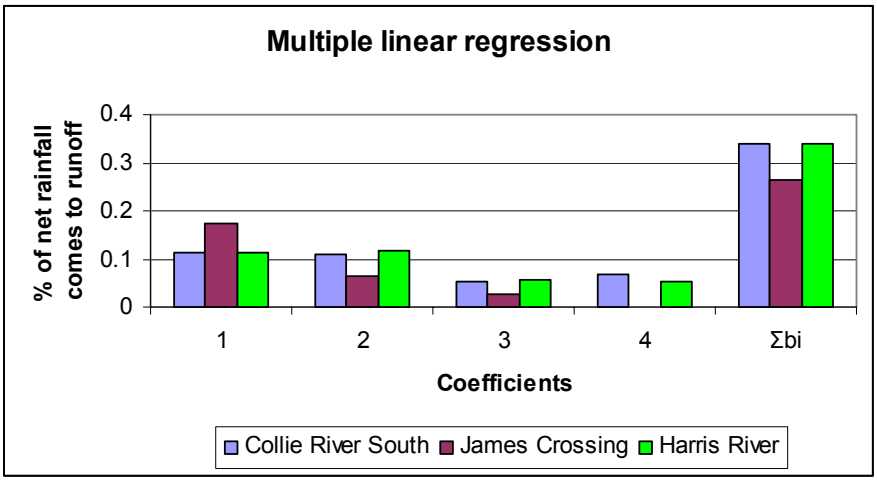

Figure 37 Results multiple linear regression, as % of net rainfall that comes to runoff

From previous analyses it was found that the filling of the Harris dam caused a lower measured runoff than normally could be expected. This was also found with the multiple linear regressions. In this case the threshold value for the Harris River was 103 mm, instead of the 63 mm that was found by neglecting the years of filling. In order to find what the runoff would have been if the Harris dam was not filling, the formula which was found for the period 1979-1988 was applied for the period 1985-1991. From Figure 38 can be seen that the simulated runoff is much higher than the measured one.
From the charts regarding the multiple linear regression the year 1982 is a strange year. In this year a tropical depression reached the Collie River Basin in January, leading to high runoff. This is due to a low number of rain-days, with a high precipitation rate.

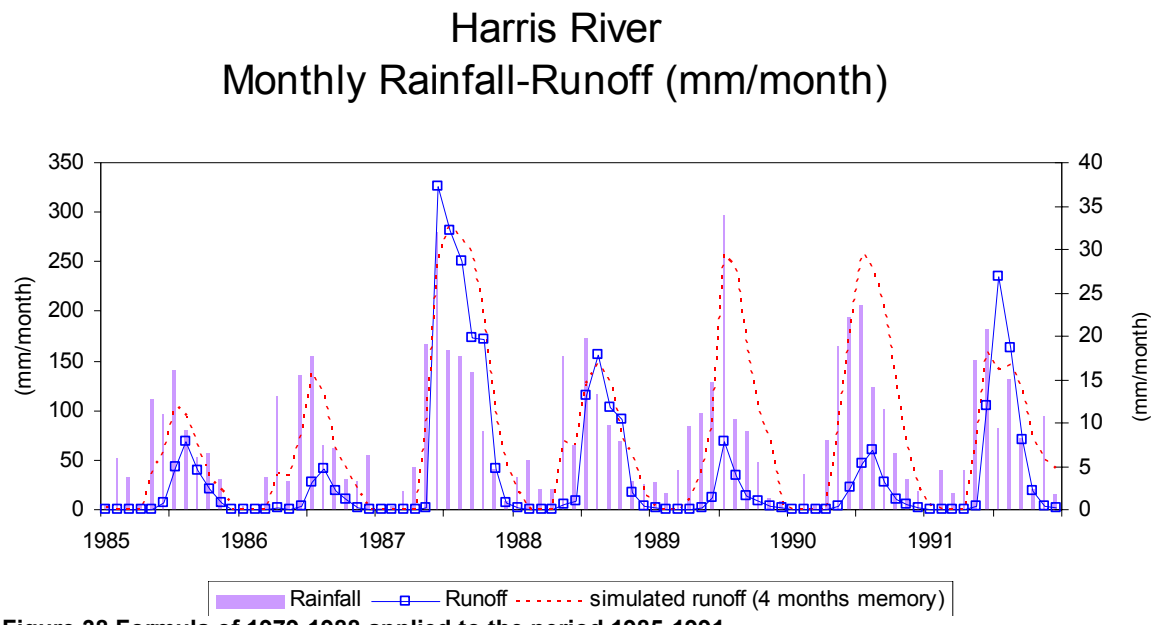

Figure 38 Formula of 1979-1988 applied to the period 1985-1991

The goal of the multiple linear regressions in combination with the threshold value is to have a small variability of residual values around the regression line relative to the overall variability. The residual value can range from 0.0 to 1.0. The R square (coefficient of determination) is 1.0 minus the residual value. For example the Collie River South has an R-square of 0.8130 (Table 4). Thus the variability of the Y-values around the regression line is 1.0- 0.8130 times the original variance. In other words the R-square is an indicator of how well the model fits the data.
The threshold represents the amount of interception that has to be reduced from the precipitation. The differences in the threshold value are caused by the large spatial gradients in precipitation and evaporation. (If the threshold represents interception capacity, the variable threshold values should be caused mostly by the variability of vegetation and ground cover.) In the Harris River the amount of interception is two times higher than in the James Crossing. This is due to the different vegetation that occurs in the Collie River Catchment.
From the above can be derived that in this catchment the fallen precipitation has an influence for four months. So in this catchment the groundwater process is dominated.
It should be noted that the given threshold represents the interception as well as the fast transpiration process. Fast transpiration is from shallow rooted plants (typically grass and annual crops) with a time scale of less than a month. This kind of transpiration only draws on the upper soil layer (until 50 cm depth). Besides the fast transpiration, transpiration also consists of delayed transpiration. The delayed transpiration is from deeply rooted plants (trees, shrubs, perennial crops), which have a time scale longer than a month and it draws on deeper soil layers. In this case the actual interception is smaller than the found threshold.

6.3.3. Runoff analysis

After extracting the threshold for the interception and fast transpiration processes the non-linear relationship disappears and a linear relationship was found.

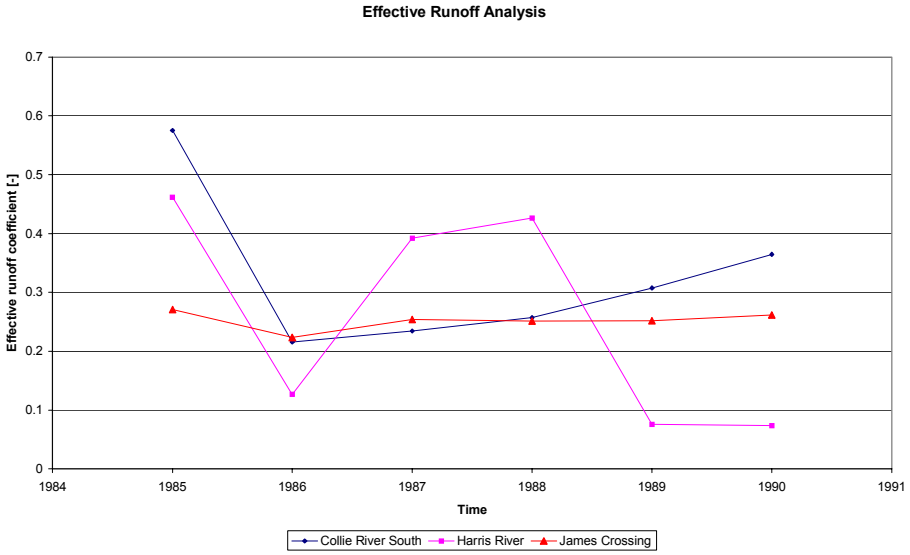

Figure 39 Effective Runoff analysis for three sub-catchments

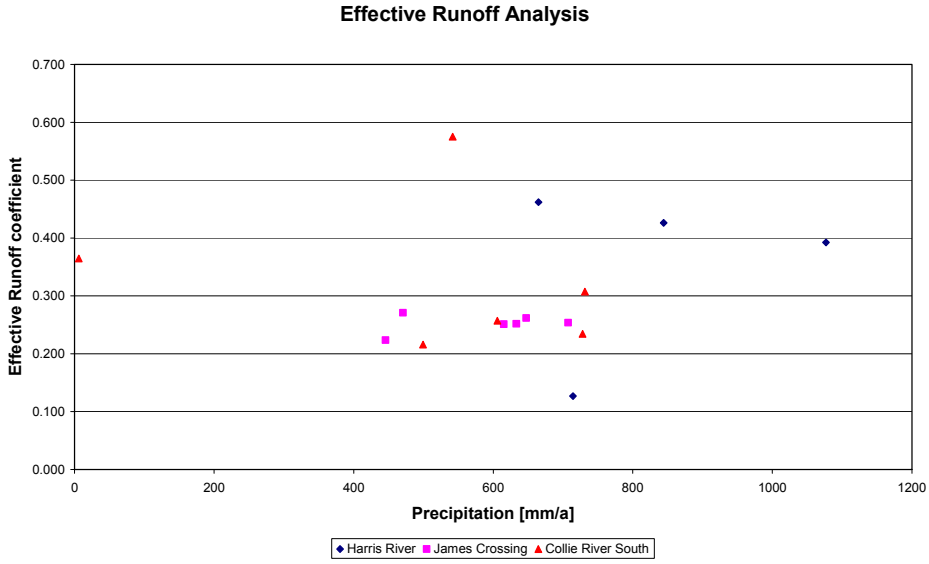

Figure 40 Effective runoff analysis for the period 1979-1988

As can be seen from Figure 40 the effective runoff coefficients show a more horizontal relationship, as should be expected. The conclusion can be drawn that the non-linearity in this basin is caused by the fast processes, such as interception and the fast transpiration (from shallow rooted plants; time scale less than a month).

6.3.4. Evaporation

The monthly variation in Pan Evaporation is between different years very limited. The distribution over the year is straightforward, as can be seen from Figure 41. In Figure 42 the Average Pan-Evaporation and Rainfall over a year can be found. In winter the rainfall exceeds the pan evaporation and the storages are filled during this period.

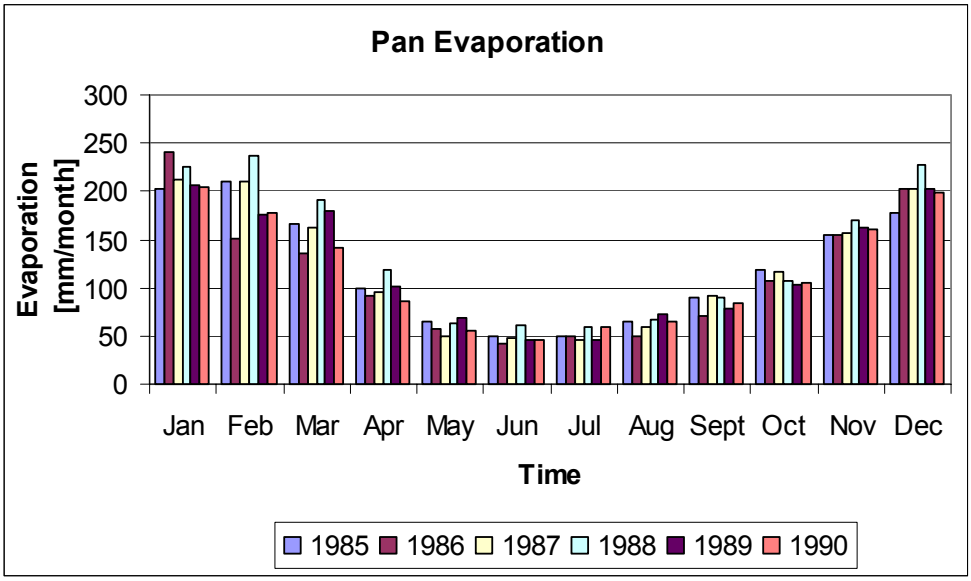

Figure 41 Monthly pan evaporation in the Collie River Basin

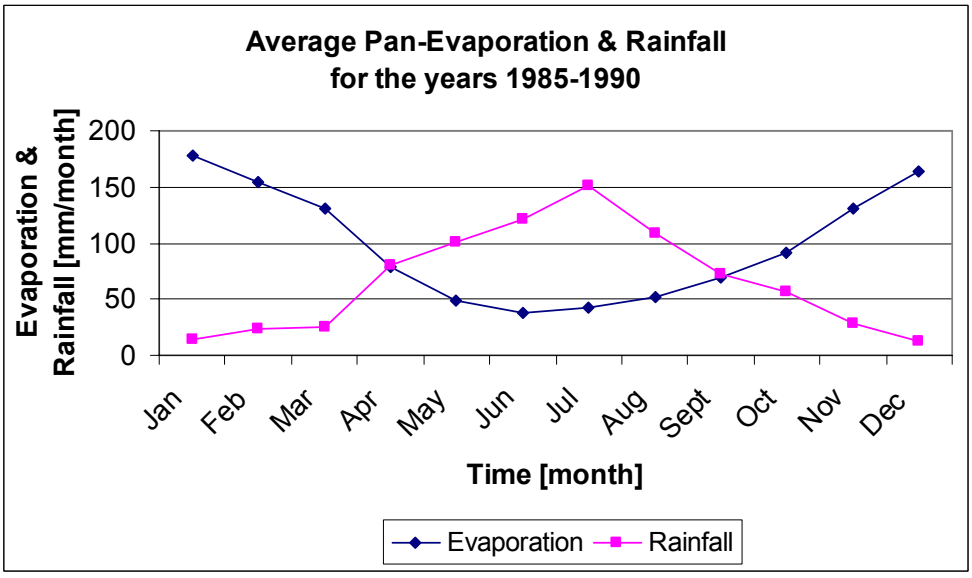

Figure 42 Evaporation and Rainfall for the years 1985-1990

6.4. Daily analysis

6.4.1. Precipitation

From the data of precipitation the conclusion can be drawn that 90% of the time no precipitation occurs or is captured by the rain gauges in the Collie river basin. Also as De Groen (2002) already derived, for every class of monthly rainfall P_m the probability of exceedance of daily rainfall P_r is in reasonable agreement with an exponential function:

$$F(P_r) = \exp\left(\frac{-P_r}{\beta}\right)$$

where

P_r is rainfall on a rain-day. A threshold can be introduced which makes that days with only trace rainfall are not considered rain-days. Here is P_r>1.0 mm

β is the scale parameter of the exponential distribution.

The average rainfall on a rain-day follows as the first moment

$$\mu_{P_r} = \mathrm{E}(P_r) = \int_0^\infty P_r \frac{1}{\beta}\exp\left(\frac{-P_r}{\beta}\right) dP = \beta \quad (\mathrm{mm/day})$$

In order to derive β the monthly rainfall is classified into several classes. For each class the probability of exceedance of daily rainfall has a reasonable agreement with an exponential function, as described above. For an example of this, the reader is referred to De Groen (2002), chapter 5.

With β, it is fairly easy to compute the monthly rainfall. The variance of the rainfall on a rain day can be expressed simply as β^2

$$\mathrm{Var}(P_r) = \mathrm{E}(P_r^2) - \mathrm{E}(P_r)^2 = 2\beta^2 - \beta^2 = \beta^2 \quad (\mathrm{mm/day})^2$$

This difference in exponential function can be caused by the different altitude of the station. All things considered the altitude differences often have influences on the duration curve.

6.4.2. Discharge

In Figure 43 the flow duration curve for three sub-catchments can be found. It can be seen that it suits an exponential function.

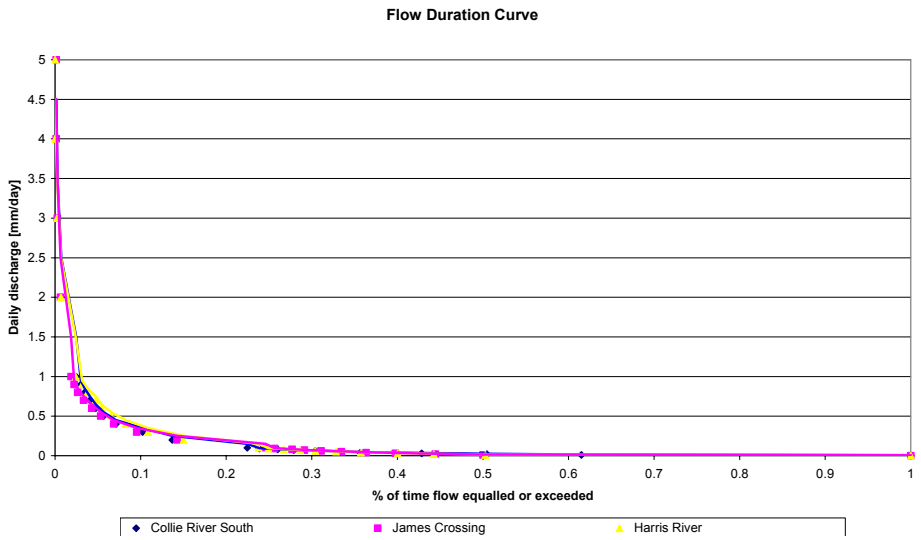

Figure 43 Flow duration curve Collie River South, James Crossing and Harris River

6.4.3. Runoff analysis

In the monthly analysis, the linear regression model was sometime not able to capture the peaks of runoff. This might be due to the fact that the precipitation took place in a relatively short period. In order to find out what was the reason, the analysis, described below, has been conducted.

As was derived by De Groen (2002) the scale factor β is equivalent to the mean rainfall on a rain-day

$$\beta = \mu_{P_r}$$

Trivially, the monthly average rainfall on rain-days equals the ratio of the monthly rainfall to the number of rain-days in the month;

$$\overline{P}_r = P_m / n_r$$

The expected mean rainfall on a rain-day is the same as the expected average rainfall on a rain-day:

$$\mu_{P_r} = \mathrm{E}(\overline{P}_r)$$

Drawing on the properties of the Markov process, the probability density function for β can be described as a function of monthly rainfall, by taking $\beta = P_m / n_r$.

The probability of occurrence of a rain-day is conditional on the occurrence of rain on the preceding day. It is possible to derive for different class intervals of monthly rainfall, the probabilities of this Markov property and the probabilities of exceedance of rainfall on rain-days. If a time series had the Markov property it means that the probability of occurrence of a certain state depends only on the state in which the system was during the previous time step. Here, a two state Markov process at daily time steps is used, with a dry day (P_t=0) and a rain-day (P_t>0) as the two states. In this dissertation a rain-day is defined as a day with recorded rain, not as one with rain above a certain threshold. The subscripts 1 and 0 are used for respectively a rain-day or a dry day.
The estimated probability p_{01} is straightforward:

$$p_{01} = \frac{a}{A}$$

Where
A is the number of days in the sample preceded by a dry day [-]
a the number of rain-days preceded by a dry day [-]

The estimated probability p_{11} is just as above, straightforward:

$$p_{11} = \frac{a}{A}$$

Where
A is the number of days in the sample preceded by a rain-day [-]
a the number of rain-days preceded by a rain-day [-]

Because a day is either a dry day or a rain-day,

$$p_{01} + p_{00} = 1$$

and

$$p_{11} + p_{10} = 1$$

Table 5 Transition probability of a rain-day after a dry day (p01) for three sub-catchments

	Collie River South		James Crossing		Harris River	
	p01	p11	p01	p11	p01	p11
1985	0,420	0,618	0,292	0,498	0,405	0,538
1986	0,344	0,524	0,343	0,508	0,354	0,582
1987	0,381	0,579	0,325	0,572	0,376	0,659
1988	0,455	0,622	0,304	0,568	0,433	0,613
1989	0,373	0,604	0,324	0,519	0,373	0,577
1990	0,310	0,584	0,348	0,512	0,337	0,638
mean	0,381	0,589	0,323	0,530	0,380	0,601

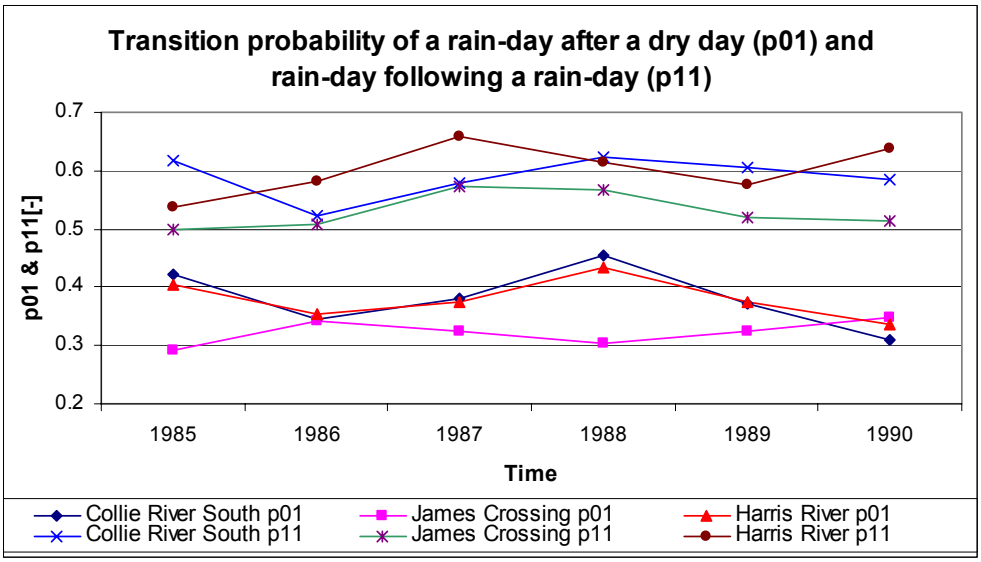

Figure 44 Transition probability of a rain-day after a dry day (p01) and rain-day following a rain-day (p11)

For the derivation of β the median of the average rainfall on rain-days is used, for reasons of simplicity and transparency. The scale factor can be expressed as a function of the monthly rainfall P_m:

$$\beta = \mathrm{M}(\bar{P}_r \mid P_m) = \frac{P_m}{\mathrm{E}(\bar{n}_r \mid n_m)} = \frac{P_m(1 - p_{11} + p_{01})}{n_m p_{01}} \quad \text{(mm/day)}$$

Where:

P_m	monthly rainfall
n_m	days in a month
p_{01}	transition probability of a rain-day after a dry day
p_{11}	transition probability of a rain-day after a dry day

This permits an easy determination of β as a function of P_m on the basis of the power functions between the monthly rainfall and the transition probabilities p_{11} and p_{01}. (Figure 45)

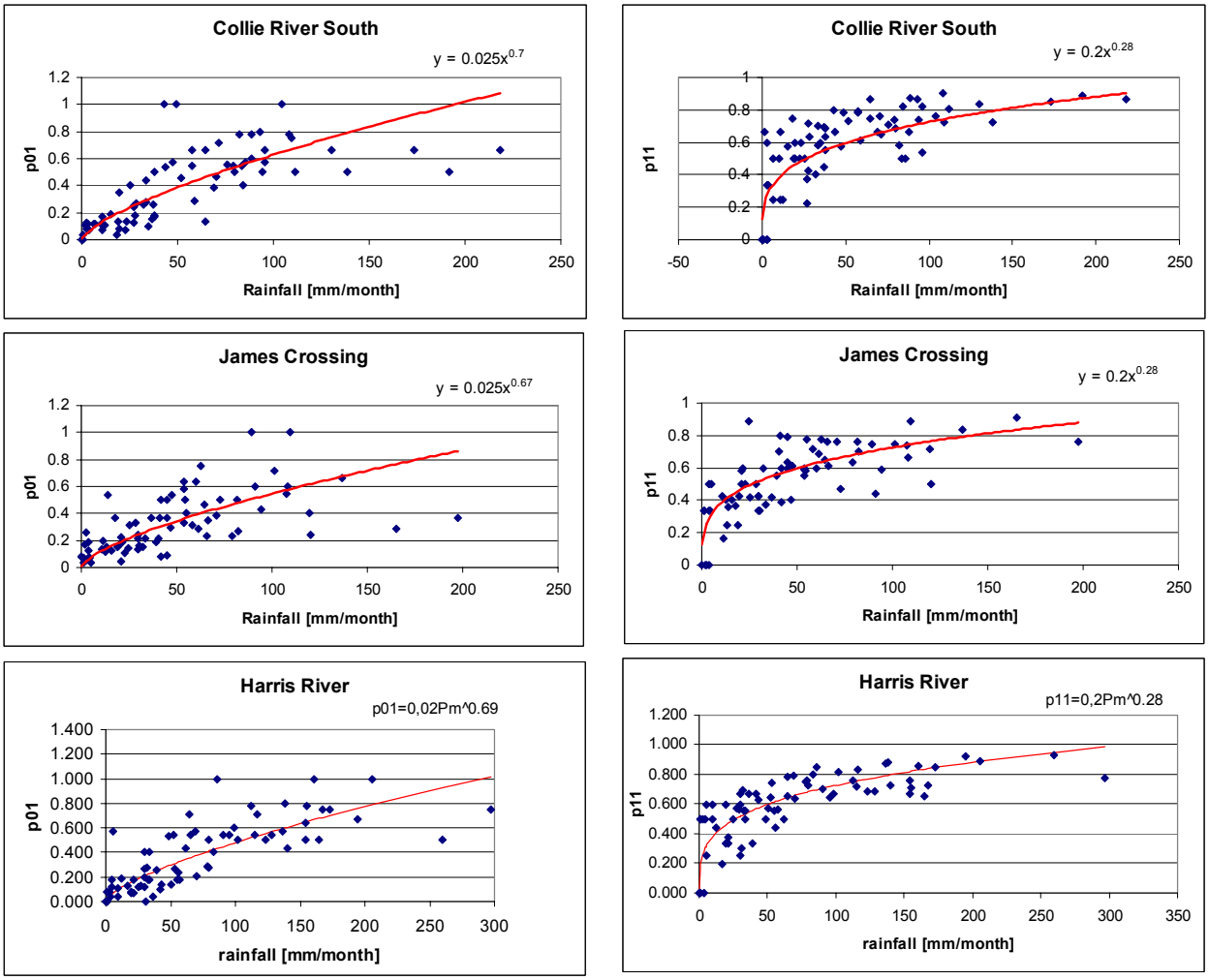

Figure 45 Transition probability p01 and p11 derived from data for Collie River South , James Crossing and Harris River

Through calibration, coefficients for the different station with daily data have been derived:

$$p_{01\text{collie-south}} = 0.025 P_m^{\,0.70}$$

$$p_{01\text{james\_crossing}} = 0.025 P_m^{\,0.67}$$

$$p_{01\text{harris}} = 0.020 P_m^{\,0.69}$$

It should be notes that p<1 and this is not the case for p01 for Collie River South, so this should be forced to be lower than 1. Also the formulae have the same form as the Budyko curve.
Only for very high monthly rainfall does the probability of the three stations derived from the observations deviate substantially from the fitted equations. This may indicate that months with extremely high rainfall are the results of a different climatic situation.

The relationship between monthly rainfall and p_{11} appears to fit almost the same power function for the three stations.

$$p_{11\text{collie-south}} = 0.2 P_m^{\,0.28}$$

$$p_{11\text{james\_crossing}} = 0.2 P_m^{\,0.28}$$

$$p_{11\text{harris}} = 0.2 P_m^{\,0.28}$$

The relationships between the monthly rainfall and p_{11} and p_{01} have strong similarities with those that were derived by De Groen (2002) for gauge stations in Zimbabwe. It was shown that the transition probabilities of rainfall occurrence after a dry day p_{01} and rainfall occurrence after a rain-day p_{11} can be expressed as power functions of monthly rainfall. This is applicable to other locations in the world.

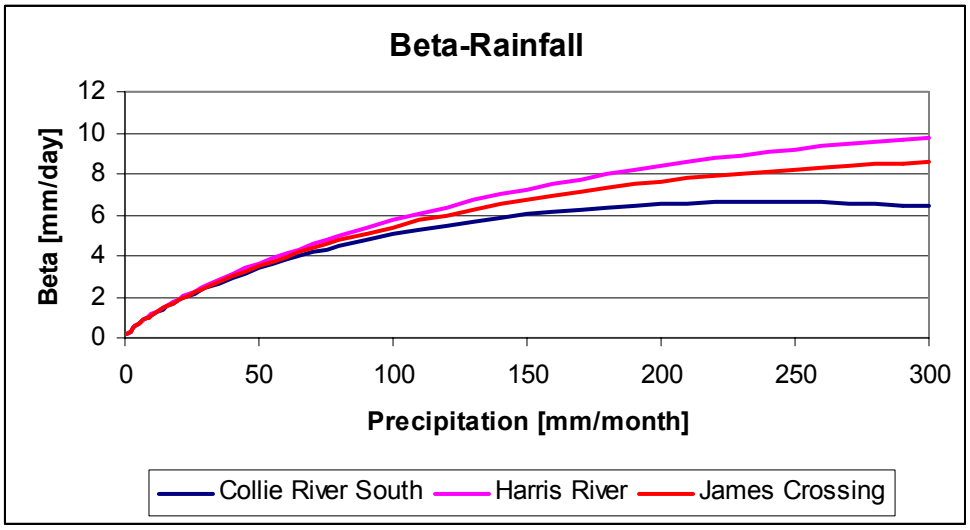

Figure 46 Beta rainfall for Collie River South, Harris River and James Crossing derived with the formula

The three formulae to calculate β for the sub-catchments are found. They are:

$$\beta_{Collie-South} = \frac{P_m(1-0.2P_m^{0.28}+0.025P_m^{0.70})}{n_m 0.025P_m^{0.70}}$$

$$\beta_{Collie-East} = \frac{P_m(1-0.2P_m^{0.28}+0.025P_m^{0.67})}{n_m 0.025P_m^{0.67}}$$

$$\beta_{Harris} = \frac{P_m(1-0.2P_m^{0.28}+0.020P_m^{0.69})}{n_m 0.020P_m^{0.69}}$$

Table 6 β found for different precipitation classes for the three sub catchments

P	β Collie River South	β James Crossing	β Harris River
0-50	2,25	2,36	2,64
51-100	4,11	4,32	4,59
101-150	5,47	5,66	5,87
151-200	6,79	6,95	7,09
201-250	8,11	8,22	8,31

Runoff between years for the three stations

For the readability of the figures, please refer to appendix 9. With this appendix for each branch the most striking aspects will be discussed, whereby the reasons why the multiple linear regression model could not fully capture the runoff are explained. Finally a comparison between the three branches will be given.

Collie River South

In 1989 a relatively high amount of precipitation fell in just a few days. This leads to a high surface runoff. This specifically is valid for the months June, July and August. The runoff in June 1990 is also considerably large. This is also due to the fact that the precipitation has fallen in just a few days. In this case there is just one month in which this occurs; the rest of the runoff is comparable with the other 'normal' years. Finally in 1987 a similar situation occurred, in this case for more months, leading to a runoff, which is higher than normally could be expected.

James Crossing

In 1987 in the months June and July, high runoff was measured. The monthly rainfall however was normal. The explanation for this lies in the fact that the precipitation fall in a relatively short period, leading to surface runoff. Something similar happened in 1990, when in July a high runoff was measured. The precipitation was in this month 100 mm. In this case the precipitation occurred in more or less average rain-days (a bit below). In this case the storages were already filled in the preceding months, leading to surface runoff.

Harris River

In the Harris River something different occurs to the other branches of the Collie River Basin. Here a high runoff occurs, when there are a high number of rain-days. For example, in the year 1987 in the months June, July and August 150 mm/month fell. The number of rain-days lies in the order of 20-25 days. This is more are less as could be expected for this amount of precipitation. So the reason why there still occurs a relative high runoff is not explained. In 1988 there were a high number of rain-days, with normal precipitation. However there too occurs high runoff. The reason for the high runoff might lay in the fact that the preparation for the dam construction had already been started.
In 1990 there appeared something different. In July there fell 300 mm precipitation in 24 days. This should have lead to a high runoff in this subcatchment. However, in the measured data, this is not shown anywhere. The reason for this, might lay in the fact that the dam was filling at that time.

Overall remarks

In general it can be said that there were two wet years, 1987 and 1990. All the stations show a higher runoff during these years. This is mainly caused by the temporal distribution within a month. The number of rain-days determines whether the runoff is relatively high or normal. The branches all react in more or less the same manner; however there are differences, which are caused by the spatial gradients in evaporation, precipitation and vegetation cover and the number of rain-days in a month. Finally local changes in for example vegetation or the construction of the Harris Dam caused differences between the branches. But generally they react in more or less similar way to precipitation.
In 1981 in all the branches occurred high runoff in especially August and September. This is mainly caused by the relative low number of rain-days during these months. Therefore the model has more difficulty to fully capture this process (see Figure 47)
1982 was a very special year. In January the remains of a tropical depression came to Western Australia and caused high precipitation in just a few days. Due to this high runoff occurred during this month. The annual rainfall is similar to the other described years; the special thing here is that the precipitation fall in a relatively short period in January (200-300 mm).

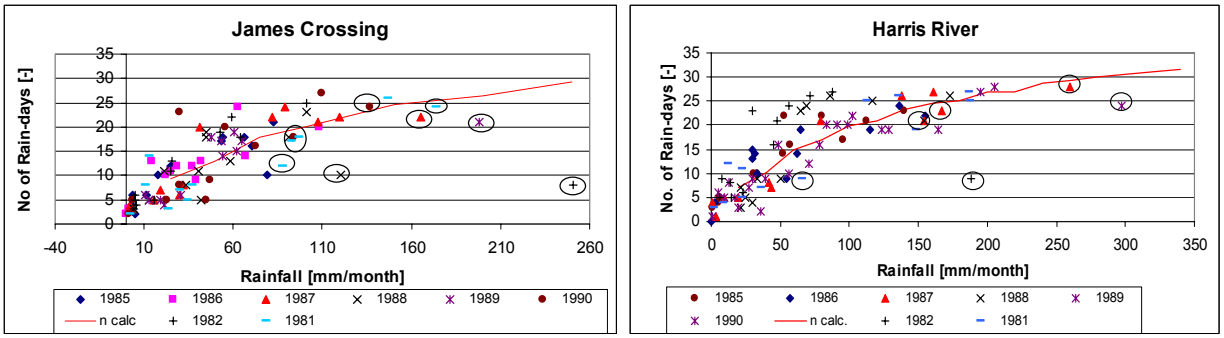

Figure 47 For the years 1981 and 1982, the number of rain-days are few in comparison with the precipitation rate

6.4.4. Evaporation

For the daily analysis of evaporation, we will look in more detail to the interception. This analysis shows that there is a strong correlation with the Budyko curve, which was presented in paragraph 6.2.4

Interception

Interception on a daily basis is defined as the amount of daily rainfall that does not exceed a certain daily threshold. This daily threshold *D* depends on local land cover conditions. Using this definition, De Groen (2002) derived that the monthly interception equation is:

$$I_m = P_m \left(1 - \exp\left(\frac{-D}{\beta}\right)\right)$$

I_m monthly interception [mm/month]
D daily threshold [mm]
β mean rainfall on a rain-day [mm/day]

This formula has strong similarities with the in already presented Budyko-curve (Figure 20). Because β is the ratio of the monthly rainfall P_m to the number of rain-days n_r, the above equation can be transformed to:

$$I_m = P_m \left(1 - \exp\left(\frac{-D * n_r}{P_m}\right)\right)$$

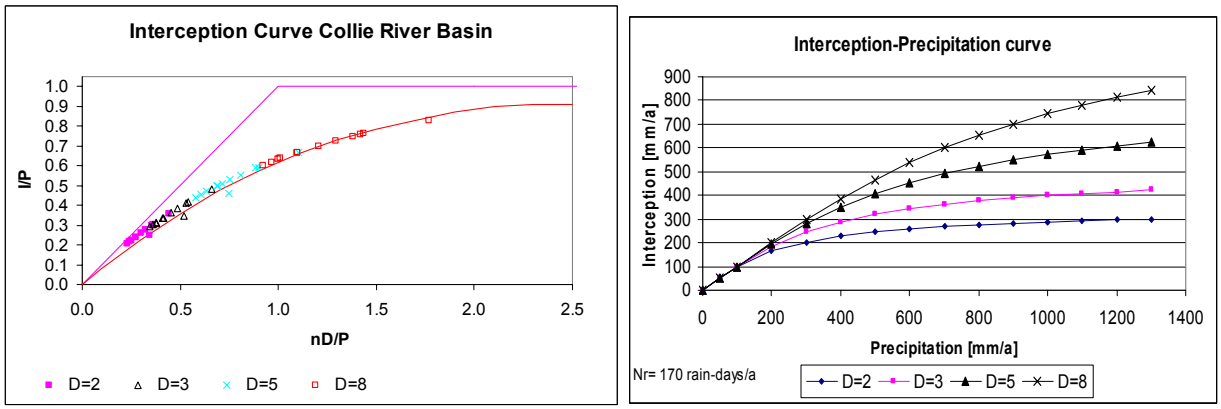

Figure 48 Interception curve for D=2;3;5 and 8 mm and Interception-Precipitation curve (common threshold value for this basin is around 3 à 4 mm)

Another way of representing the interception, instead of taking a threshold value, is taking the daily pan evaporation value, only on the rain-days. In that case is assumed that when it is day where it rains very smoothly all over the day, the rainfall is not that high, but more-over not much water has evaporated. Is it on the other hand a warm day, with a short thunderstorm, the evaporation rate can be much larger, and thus the interception rate.
For the below analysis, the rain-days has been extracted for the year 1979. The daily pan evaporation has been measured during this period. The pan evaporation on rain-days is never higher than 8 mm, as was found in the available data. The following formula was used to calculate the interception curve

$$I_{daily} = P_{daily}\left(1 - \exp\left(\frac{-E_{pan,daily}}{P_{daily}}\right)\right)$$

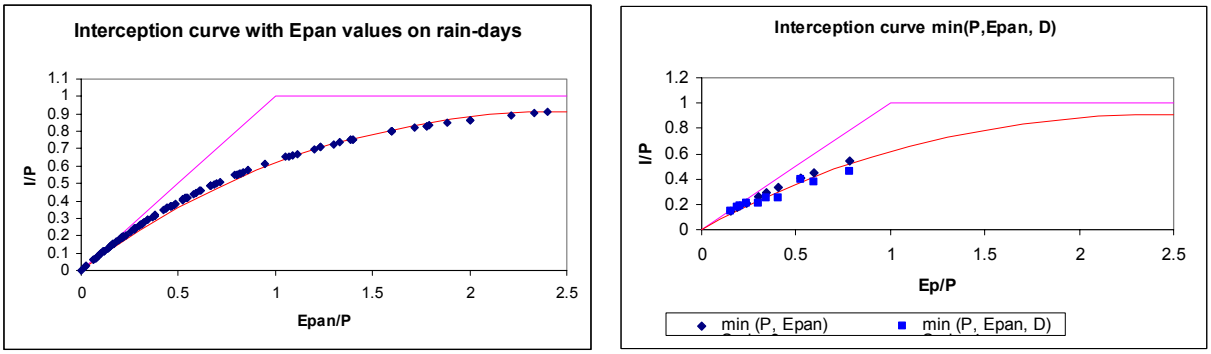

Figure 49 (a) Interception curve with daily Pan Evaporation on rain-days. The red line is the analytical derived line and is the same, as in the Budyko and interception curve. (b) Interception curve with I = min (P, Epan, D). It shows that this also follows the analytical derived line.

Figure 49 shows that also the pan evaporation on rain-days can be used as an estimate for the amount of interception. As was derived by De Groen, the daily pan-evaporation also follows the exponential function. In this figure it is also shown that if I= min(P,Epan, D) the analytical derived line is more or less followed in a similar manner as was found in an earlier stage.

7. The model description

To be able to predict the discharge after a precipitation event and to evaluate the REW approach related to the rainfall-runoff relation a REW-model was made, as mentioned before. In this thesis the CREW model developed by Lee is used.

7.1. Model structure

The code named *CREW.*for is a program solving governing equations of the REW approach, that is, mass and momentum balance equations governing water flow which are defined at the sub-catchment scale called REW by Reggiani et al (1998, 1999). Hereafter, the model based on the REW approach will be named CREW by the authors of this model. CREW stands for *C*ooperative Community Catchment model based on the *R*epresentative *E*lementary *W*atershed approach.
About the numerical scheme used to implement CREW model; CREW model uses adaptive step size control numerical scheme incorporated with Runge-Kutta ode solver to solve ordinary differential system of the REW approach. The main code part related to adaptive Runge-Kutta ode solver is from chapter 16.2 of the book called "*Numerical Recipes in Fortran, 2nd Ed., W.H. PRESS".* CREW model directly borrowed the three subroutines from the book: subroutine rkqs, subroutine rkck, subroutine odeint (respectively page 712-714). Therefore, the user is encouraged to refer to the book to understand the numerical part of the code fully.
Figure 50 is describing the structure of the code.

There are 5 input files (see also Appendix 10), which are called:

- GENERAL.INFO.inp includes general information to handle model running
- GEOINFO*.inp includes geometric information for the catchment. Note that * should be the same as the value of nREW's
- INITIAL_STATES.inp includes initial state variables user specified
- PARAMETERS.inp includes model parameters
- REpQ.inp includes observed climatic data
    - The precipitation (daily);
    - The (open water) evaporation (daily)
    - Runoff at the outlet of the basin (daily)

The model uses several subroutines (see
Figure 50) and functions. The subroutines will be shortly described.

- *Odeint* : is Runge-Kutta driver with adaptive step size control. (See page 714 of Numerical Recipes in Fortran, 2nd Ed, for the details)
- *Rkqs*: is stepper routine of the subroutine odeint. (See page 712 of Numerical Recipes in Fortran, 2nd Ed, for the details)
- *Rkck*: is the routine to take a Cash-Karp Runge-Kutta step. (See page 713 of Numerical Recipes in Fortran, 2nd Ed, for the details)
- *Datain*: introduces climate data (rainfall, potential evaporation, observed discharge) into model space
- *Paras*: reads parameter file named PARAMETERS.INP and initialize parameter values.
- *Geoinfo*: reads geographic information from the file named GEOINFO*.INP and initialize values of the variables related to geometric setting of the REW.
- *Istates*: reads information on initial state variables from the file named INITIAL_STATES.INP.
- *Derivs*: calculates mass and momentum balance equations of the REW approach.
- *States*: calculates state variables updated by calculated derivates at the subroutine derives.
- *Psvwb*: for printing the simulation results out to the output files.

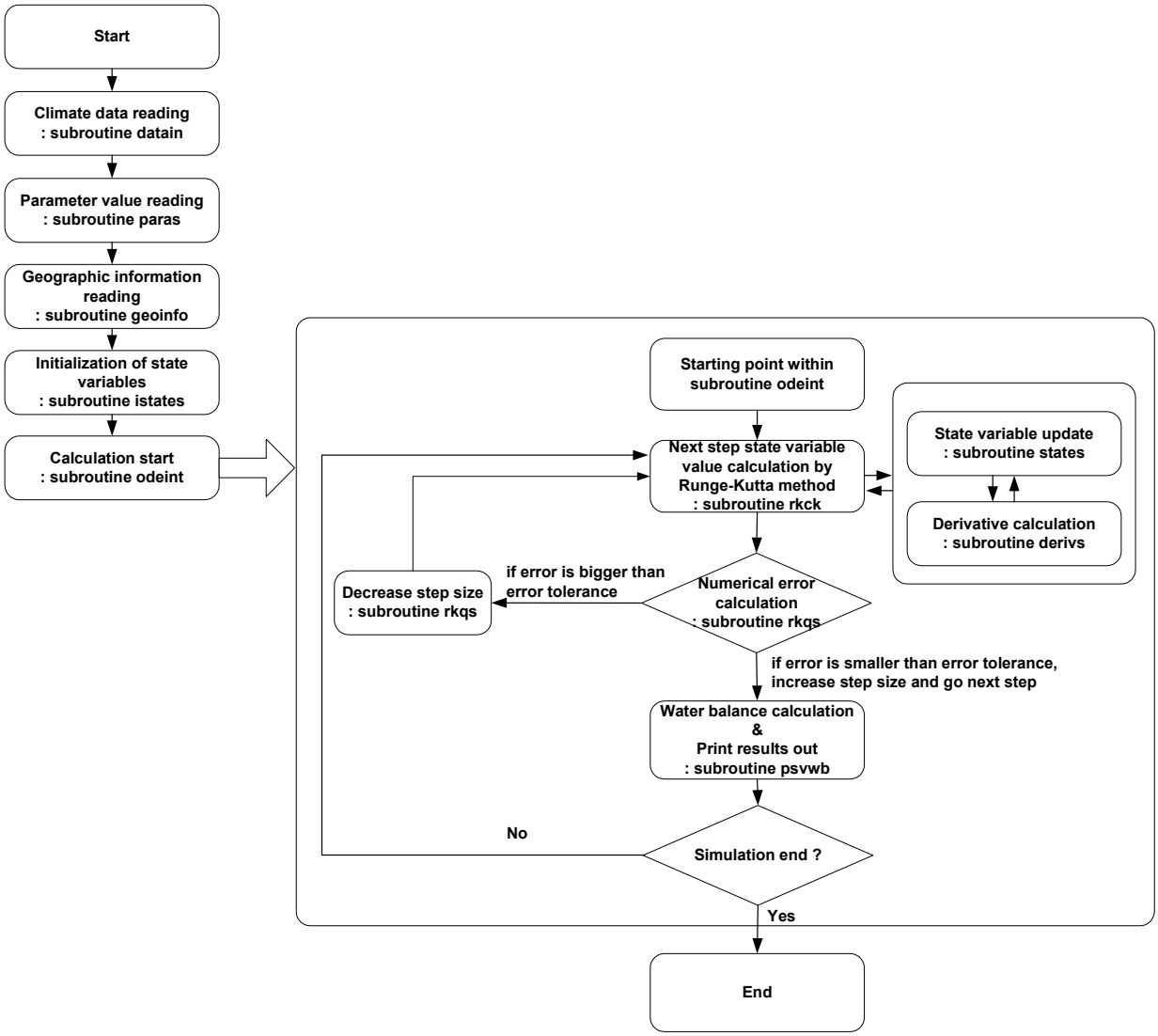

Figure 50 Structure of the model code

7.2. General info

Current version of the model is developed with Fortran compiler, called Fortran PowerStation 4.0 Microsoft Developer Studio, to solve mass and momentum balance equations and it does not include energy balance equations at all. The current version of the model adopts closure relations developed by Lee *et al.* (2005b). The model provides water fluxes at each REW, state variables at each REW and efficiency measure as model simulation results. Moreover, the model checks the water balance errors at sub region of the REW and the water balance error for all REW's. So the user can easily check possible water balance errors.
This current version also provides derivative values of state variables within a REW (user specified). In this way the user can find which governing equation is making instability in terms of numeric. This current version also uses the SI unit system, so all data will be converted into the unit system. At this moment the model has only been tested with hourly data on a small catchment in Western Australia (Susannah Brook). Until now it is unknown how many REW's and how much data the current model can cope with.
With the first version that was handed for this thesis, it was not possible to have more than one input file, containing the runoff, precipitation and evaporation. During the research it was evident that for the Collie River Basin the variability of the precipitation plays an important role in capturing all the processes in this basin. Therefore it became possible to have a heterogeneous precipitation field in the model. In appendix 10 also the geometric information of the various REW's scenario's can be found.

8. Implementation of the model & challenges encountered

The CREW model has never been tested on a catchment of the scale of the Collie River Basin. Several challenges will be encountered and part of this thesis is to recognize them and try to find a solution for them. In order to be able to capture all the processes correctly in the model, in the beginning one REW is used and subsequently this is refined up to 27 REW's.
This chapter deals with the implementation of the model to the Collie River Basin and the issues that are dealt with during this process.

8.1. Parameters & Optimization closure relation

As the Collie River Basin has been thoroughly studied over the last decades quite a few parameters are verified over the time. So, these parameters are used in this research and no attempt has been made to change the parameters significantly, as this may result in a misconceived simulation of this specific basin.
For instance, although the saturated hydraulic conductivity is a very sensitive parameter in the CREW model, previous research have found more or less the same value for this parameter. So this value has not been changed from the found value, in order to get reliable results for the basin.

Table 7 Values of parameters found in literature and used as input in CREW- model

Parameter	Value	Reference
U-zone pore disconnectedness Index (Sandy Loam)	3.6	Bras (1990)
Pore size distribution index (Sandy loam)	3.3	
Vegetation effect of LAI (k_v)	1.2	Jothityangkoon (2001)
Canopy density	0.7	
U-zone saturated hydraulic conductivity (m/s)	0.0000347	
Porosity	0.4	
Manning roughness coefficient C-zone ($m^{1/3}$*s)	0.030	
Manning roughness coefficient O-zone ($m^{1/3}$*s)	0.015	

Also with regards to the *Geoinfo.inp* file, special attention should be paid to the numbering of the REW's. The REW's should be given a number in such a way that the ones which are located at the downstream part of the basin have the lowest number. This should increase going upstream. This because of the way the model calculates the in- en outflow of the REW's. If this is done incorrectly, this will lead to less accuracy.

The parameter range for some parameters used during the calibration and validation will be given in paragraph 9.5.

Optimization closure relation
During the calibration of the model it was found that the unsaturated zone momentum balance equation contained several errors, e.g. sign errors. With the help of Mr. M. Hassanizadeh (University of Utrecht, the Netherlands) these errors were corrected. Here below this process is described.

$$-\underbrace{\rho\varepsilon s_u y_u \omega_u g}_{\text{gravity}} + \underbrace{\rho g \varepsilon \omega_u [\frac{1}{2} y_u + |\Psi_b|(s_u)^{\frac{1}{\mu}}]}_{\text{force top}} - \underbrace{[K_{sat}(s_u)^{\{3+\frac{2}{\mu}\}}]^{-1} \rho\varepsilon g y_u \omega_u v_{u,z}}_{\text{resistance force}} = 0 \quad \text{(a)}$$

After rearranging the above equation with regard to $v_{u,z}$

$$v_{u,z} = K_{sat}(s_u)^{\{3+\frac{2}{\mu}\}} \left[s_u + \frac{1}{2} + \frac{|\Psi_b|(s_u)^{\frac{1}{\mu}}}{y_u} \right] \quad \text{(b)}$$

With the above form, the unsaturated zone saturation degree will always be greater than ½ at the equilibrium state. At equilibrium state however, the saturation degree in the unsaturated zone can be either fully dry or fully saturated.

Here below the unsaturated zone is considered under hydrostatic conditions, which leads to the following equations

$$-\varepsilon s_{top}\omega_{top}p_{top} - W_u + \varepsilon s_{bott}\omega_{bott}p_{bott} = 0 \quad \text{(I)}$$

$$\text{Let } p_{bott} = p_{atm} = 0$$

$$p_{top} = p_{u,centroid} - \frac{1}{2}\rho g y_u \quad \text{(II)}$$

$$W_u = \varepsilon s_u \omega_u \rho g y_u \quad \text{(III)}$$

$p_{u,centroid}$ is the average pressure of the unsaturated zone which is also equal to $p_{air} - p_{u,c}$, where $p_{u,c}$ is the average capillary pressure of the unsaturated zone, given by

$$p_{u,c} = \rho g \psi_b (s_u)^{-\frac{1}{\mu}} \quad \text{(IV)}$$

Substitution of these equations in (I) yields

$$-\varepsilon s_{top}\omega_u \left[(p_{air} - p_{u,c}) - \frac{1}{2}\rho g y_u \right] - \varepsilon s_u \omega_u \rho g y_u = 0 \quad \text{(V)}$$

Let $p_{atm} = 0$ and assume $s_{top} = s_u$ (This is a gross assumption).

This results in:

$$-\varepsilon s_u \omega_u \rho g \left[\psi_b (s_u)^{-\frac{1}{\mu}} + \frac{1}{2} y_u \right] - \varepsilon s_u \omega_u \rho g y_u = 0 \quad \text{(VI)}$$

This is the hydrostatic equivalent of equation (a). It can be seen that the sign of the ψ_b is wrong.

Solution of (VI) for saturation s_u yields

$$s_{u,eq} = \left(\frac{2\psi_b}{y_u} \right)^{\mu} \quad \text{(VII)}$$

The thicker the unsaturated zone, the smaller the average saturation; the larger ψ_b (e.g. clayey soil), the larger average saturation.

In equation (a) s_u is missing in the term representing “force top”.

Now, let’s consider flow conditions. To the force balance (I), we have to add a force entered by the solid phase on the flowing water; so that (VI) becomes:

$$-\varepsilon s_u \omega_u \rho g \left[\psi_b (s_u)^{-\frac{1}{\mu}} + \frac{1}{2} y_u \right] - \varepsilon s_u \omega_u \rho g y_u + \hat{\tau}_{u,z} = 0 \quad \text{(VIII)}$$

Let $\hat{\tau}_{u,z} = -Rv_{u,z}$, as a result we obtain:

$$-\varepsilon s_u \omega_u \rho g y_u + \varepsilon s_u \omega_u \rho g \left[\psi_b (s_u)^{-\frac{1}{\mu}} + \frac{1}{2} y_u \right] = R v_{u,z} \quad \text{(IX)}$$

This means that if y_u increases (drainage of unsaturated zone), then $v_{u,z}$ will be negative (downward flow. At the same time, the capillary pressure increases (due to the decreasing saturation) and opposes the drainage. Comparison of (IX) with (a) shows that the sign of the r.h.s. of (a) is wrong.

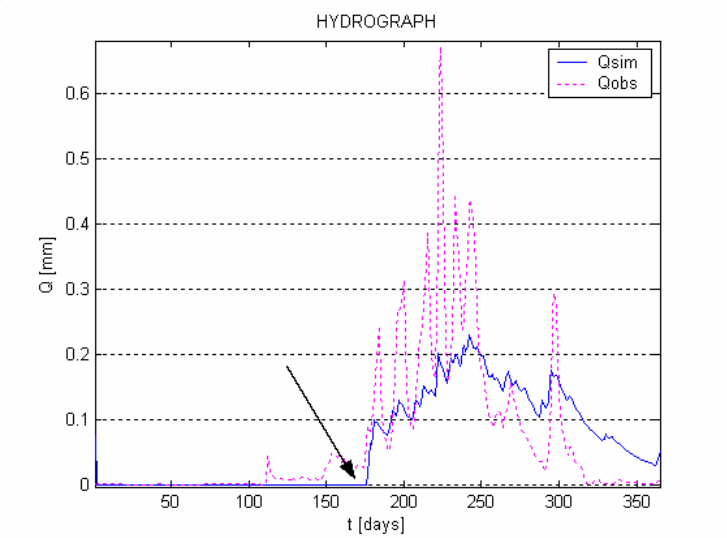

With the above changes, the new equation for $v_{u,z}$ becomes:

$$v_{u,z} = \frac{K}{y_u} s_u \left(\psi_b (s_u)^{\frac{1}{\mu}} - \frac{1}{2} y_u \right) \quad \text{(c)}$$

With the new equation the results shows improvements, because with the old equation in the dry period the runoff was zero, while this is in reality not the case. The simulated runoff would abruptly start again, while the observed runoff showed a very low runoff (baseflow) in the dry periods.

Figure 51 Results of CREW model with old version of formula, the runoff starts abruptly on day 176 in year 1979.

8.2. Derivation REW's based on Strahler order

For this research the numbers of REW's are derived on the basis of Strahler order. For this process a program named PCRaster was used. This program is a result of eight years of research in a research group formerly known as GISLA (Geographical Information Systems for Landscape Analysis) at the department of Physical Geography at Utrecht University, the Netherlands.
The PCRaster Environmental Modelling language is a computer language for construction of iterative spatio-temporal environmental models. It runs in the PCRaster interactive raster GIS environment that supports immediate pre- or post-modelling visualisation of spatio-temporal data. In Appendix 11 a user's manual for PCRaster and the developed script can be found.

In the script used for the derivation it is also possible to take into account the slopes of the catchment. In that way, flat areas can be identified and if necessary treated differently than a REW, as this decreases the velocity and increases storage capacities.

8.3. Computation time

In the beginning of calibration the computation time was very long. For 5 REW's it could take an hour before two years of climatic data were simulated. For 27 REW's it could easily take 3- 4 hours. Several options were investigated, e.g. routing and choice of parameters. It is evident that the amount of REW's also plays a big role in this process. When there are more REW's, more sub-catchments have to be calculated.
Parameters do not control the computation time but influence the processes simulated, thus giving rise to different errors in each computation time step. Therefore different parameter sets can lead to different computation time.
By using the adaptive step size control for Runge Kutta the time it takes for each computation time step depends on the accuracy and the errors.

8.4. Equifinality

As was stated by Savenije (2001) equifinality can be applied to two situations. The first one was shown in chapter 6, namely the complexity of hydrological processes, may become at a higher level of aggregation irrelevant. Nowadays this might become disturbing, because people, who refuse to believe this fact, use powerful computers to simulate hydrological behaviour in highly fragmented distributed models. By using a downward approach, as in chapter 6, processes that occur at a more detailed level can be explained to the occurring processes at that level.

Equifinality also arises when in a hydrological model many different parameter sets are equally good at reproducing an output signal. Such models, often distributed models with a large number of parameters, are quite good at mimicking hydrological behaviour. They are however not the most appropriate tools to predict what will happen if certain characteristics of the catchments change.
During this research, the last type has occurred. By using different parameter sets the same output signal, e.g. simulated hydrograph have been found. It should be noted that the value of one parameter used cannot physically exist. (U-zone pore disconnectedness index, value used was 12.0, eventually found in literature, for sandy-loam; 3.6).
This however was not known at the time of executing the simulations. When discovered, the same runs were executed with the correct parameter sets.
Hydrologists have tended to look at the hydrograph results, for both the simulated and observed results. However, this is not sufficient any more to judge the accuracy of the model. Attention should also be paid to the water balance and e.g. saturated area fraction. By looking at more parameters a better judgment can be made about the accuracy of the model predictions.
Here, a closer look has been taken to the following parameters, e.g. variable source area fraction (ω_o). With the first parameter sets, this resulted in a very low value for the ω_o (10^{-5}), which is not very common. With the second parameter set, the value for ω_o was around 0,015.

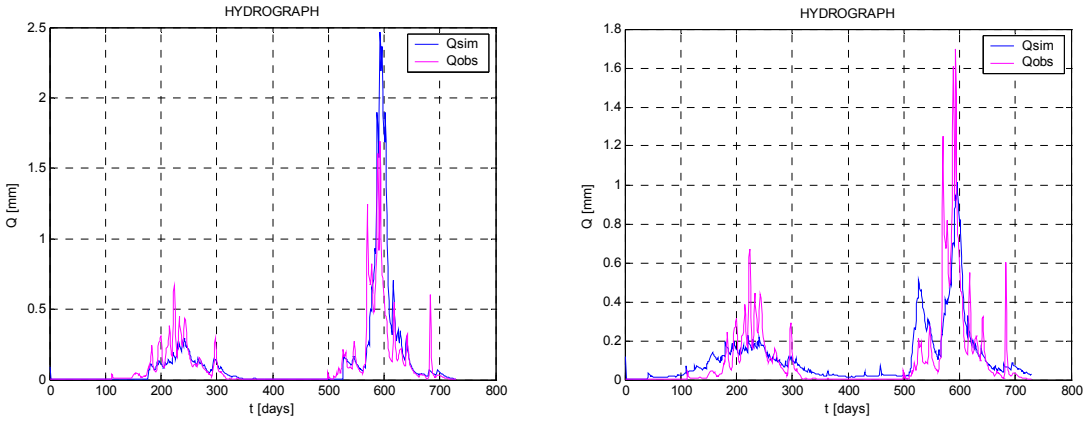

Figure 52 Equifinality: Parameters used which are not physically possible (left figure), and right figure shows the results with the right physical parameters. Special attention has been paid to the variable source area fraction.

8.5. Heterogeneous precipitation field

In the Collie River Basin, the precipitation varies between 600 mm in the east till 1200 mm in the west. That the CREW model will have difficulty capturing the runoff with averaged rainfall is without doubt. Therefore instead of one column of precipitation for the whole basin, this should be specified for each REW.
In order to give an idea what the differences are in this catchment, the precipitation for the 26th of June 1980 has been given in Figure 53.

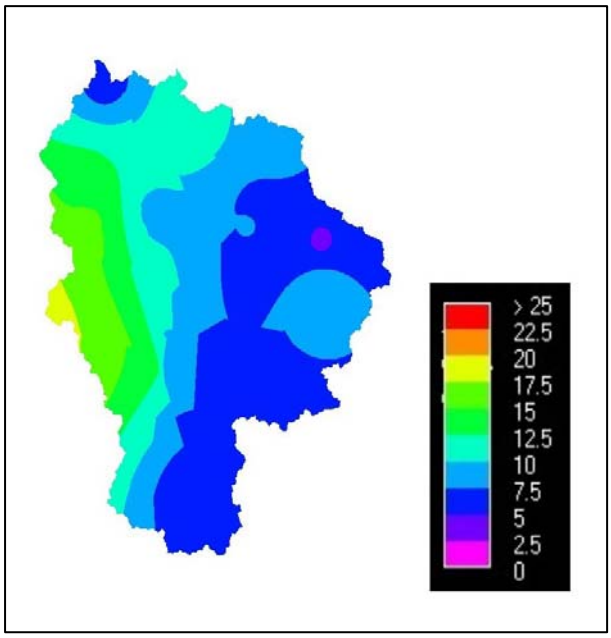

Figure 53 Precipitation field in the Collie River Basin for 26th of June 1980

The same areal difference also exists for the evaporation. Only the restraint is that just one gauge station is available with this data.
The necessity for this heterogeneous precipitation field has been found after calibrating for 1, 5 and 27 REW's with only areal precipitation as input. The base flow was in a way captured, but the peaks were underestimated. With one REW, the input data for precipitation has been changed, to find if the model was sensitive for differences in precipitation. It was found that by giving the gauge station in the east dominances in the areal precipitation, the CREW model was able to give better results for the peaks (see Figure 54). The model still captures the small peaks not well, but this is suggested to be caused by occurrence of quick flow.

In order to get a heterogeneous precipitation field, interpolation techniques have to be used to get the precipitation for each defined REW. Therefore scripts have been developed that automate the process of using interpolation techniques to develop values for rainfall and evaporation for each REW. In this case, the programs Matlab and PCRaster are used.
The script uses inverse distance as interpolation technique. More info about creating these files can be obtained from appendix 11.

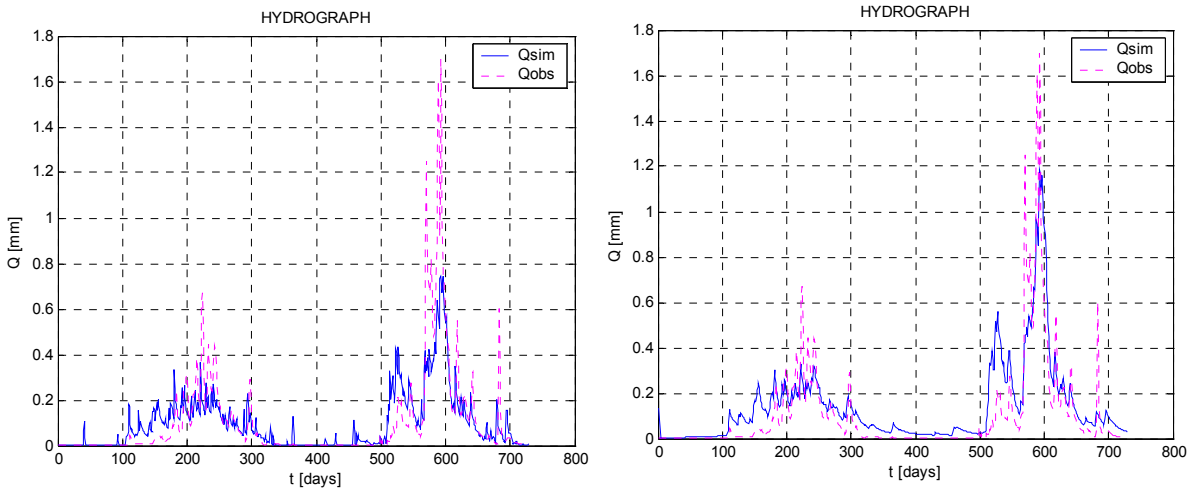

Figure 54 The importance of a heterogeneous precipitation field. Left the homogeneous precipitation field and right the heterogonous field. With the latter the peaks are better captured.

8.6. Vegetation

Differences in catchment water yield under different vegetation types can be explained in terms of differences in the various terms of the hydrologic balance (see also chapter 3) and the way they are affected by the structural and functional characteristics of the vegetation. Each comparison or analysis must take into account possible differences in the amount of water intercepted and evaporated from canopies, the pattern and duration of L^* [a function of stand density and leaf habit (e.g. deciduous, evergreen)], and the depth of the rooting zone, which determines the capacity of the vegetation to access deep groundwater. The rates of transpiration from the vegetation, at any particular season, will be determined by factors such as, energy balance, aerodynamic and canopy conductance. Runoff and drainage are strongly dependent on the condition of the soil surface and the water content of the root zone as well as precipitation patterns.
In the Collie River Basin four major vegetation systems were distinguished (chapter 5) and the variation in vegetation corresponds to changes in soils, climate and physiography
After World War II parts in the Collie River Basin were cleared for mining, but mostly for agriculture. This lead to a significant increase in groundwater level as well as salinity, due to the fact that ancient marine water without the deep root systems of the jarrah could come to the surface, (Mauger *et al.*, 2001). In case of a high precipitation rate this could lead to Hortonian overland flow at the agriculture lands. On most of the cleared lands, there are gullies that indicate this.
The jarrah forest in Western Australia appears to have a sufficiently deep and efficient root system to access the deeper water stores and to maintain a vigorous overstorey.
Evapotranspiration rates were close to 60% of reference Penman evaporation and transpiration and 78% of equilibrium evaporation and transpiration throughout the year. Despite a reduction of leaf area by one-third of the spring value and a reduction of 30% in soil moisture, the forest maintains high leaf conductances during summer. In this way, the forest avoids periods of major water stress during the dry season (Silberstein *et al.*,2001).
Due to spatial and temporal variability in vegetation there are differences in infiltration capacities, interception, and evaporation. In order to be able to improve the simulation results on the Collie, these should be taken into account.

8.7. User Guidance

As the CREW model has been recently developed, so far two people have worked with the model. As it is the intention of the developers to release it next year for everyone who is interested, it was necessary to make a supplement of the existing user guide. In the user guidance everything which can lead and have led to indistinctness during the modelling can be found. The user guidance can be found in appendix 12.

Note: the reference to the appendix containing the PCRaster manual can be found in appendix 11.

9. Model results

In the previous chapter the challenges which occurred while implementing the model to the Collie River Basin have been described. The results will be presented next, based on the current model code. In order to give a full overview of the process, and the differences between using more or less REW's the results for several refinements are being presented here. Based on Strahler order, the following REW's were defined: 1, 5 and 27 REW's. In case additional refinement is necessary, the next step would have been 139 REW's. Due to time limitations, the results for this scenario could not be examined.

The precipitation input data have all been corrected with the computed interception of 2 mm/day, found with the multiple linear regression model (chapter 6). So in that way interception has been taken into account. Manual calibration was used for estimating model parameters instead of automatic calibration methods. In this chapter for the different scenarios will be manually calibrated and finally validated. To evaluate the calibration the coefficient of efficiency of Nash and Sutcliff is taken into account. For an efficiency of 1 means that the model produces discharge data which are exactly coinciding with the observed data. A deeper insight in what the model can tell e.g. about the different zones is given in the paragraph 9.4.

9.1. 1 REW

For 1 REW, the model has been calibrated with a homogeneous precipitation. After a few simulations, with 6 years of climatic data, the decision was taken to reduce the years to two, because the calculation took to long (around five hours). Figure 55 shows the lay-out for 1 REW. During the calibration attention has been paid to the hydrograph, saturated area fraction and the water balance, as well as the computation time. The computation time was during the calibration reduced from one hour to several minutes. As the computation time is important for the model to succeed, this might have an effect on the results, but should be limited.

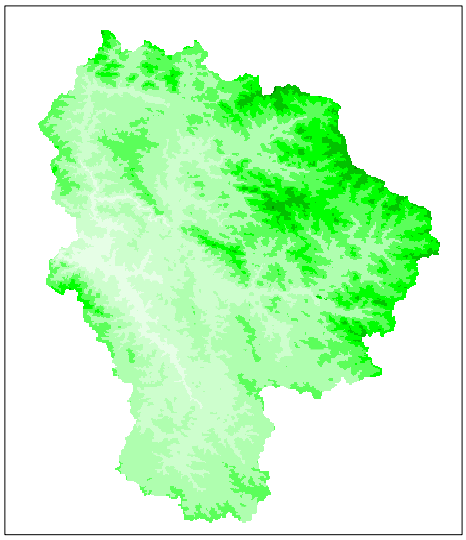

Figure 55 A simple beginning, just 1 REW

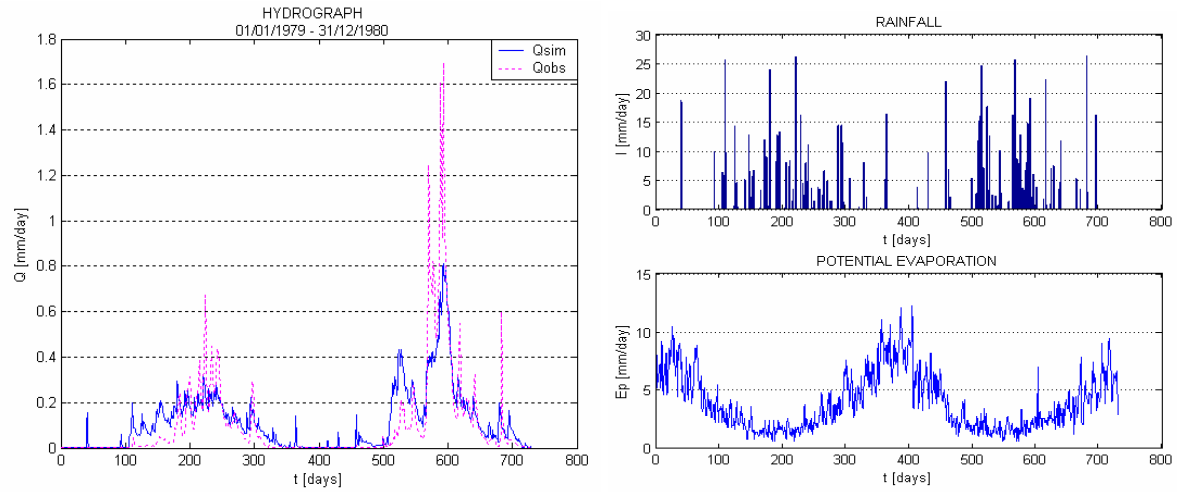

Figure 56 Model results for 1 REW, using average precipitation of the Collie River Basin, years 1979-1980

The model is used to calculate the discharge between 1st of January 1979 and 31st of December 1980. It can be seen from Figure 56 that the model reacts strongly to high precipitation, although some peaks are still missed, e.g. at day 700. Half February 1979 a large quantity of precipitation fell and while in reality this does not lead to runoff, the model does simulate this effect. The same applies for the precipitation fell in spring and summer (1979/1980). Here the model also expects runoff. This indicates that the sub surface storages are not well simulated at this time. During the winter of 1979 and 1980 the runoff was underestimated, this indicates that the saturated area fraction has to be modified. With 1 REW this was not sufficiently possible, because changes also lead to higher computation time. The latter was tried to minimize.

The base flow is in general well estimated, apart from the 4 peaks in spring & summertime. The saturated area fraction is around the 0.015. In this case the water balance (WB) has generated mass without a source, e.g. precipitation, namely 0.3490707E-05. In this case WB/P is 0.3514940E-05 (0.0003514940%). This can be interpreted as the water corresponding to 3.514940E-04% of precipitation has been generated without a source. As this value is small, this is acceptable. The Nash-Sutcliff efficiency (NSE) is 0.66; which is reasonably good.

Based on the annual water balance predictions, all the rainfall falling on the concentrated overland flow zone is infiltrated, and so the main runoff generation mechanisms contributing to streamflow are subsurface storm flow and saturated excess overland flow; this accurately reflects the situation for the Collie River Basin. There occurs no Hortonian overland flow. During the calibration the land clearing areas have not yet been taken into account, so as these areas are the only Hortonian prone areas in this catchment, it is logical that it is not yet occurring.

9.2. 5 REW's

The model is used to calculate the discharge for the period between 1st of January 1979 until 31st of December 1980. Two kinds of calibrations were executed. The first one with a homogeneous precipitation field, where the rainfall has been averaged over the area, and the second one uses a heterogeneous precipitation field.
Especially the latter should show reasonable results for the peaks in runoff in this basin, as now the spatial variability of the precipitation has been taken into account. In Figure 57 the division of the 5 REW's is presented.

Figure 57 5 REW's

9.2.1. Homogeneous precipitation

By calculating the discharge with more REW's more variation between the parameters can be established resulting in a better base flow. Until now CREW still has some difficulties in capturing the peaks (see Figure 58). In the second year, 1980, there is an overestimation runoff for the months May and June. During this period the model calculated that more water came to runoff. As this is early winter time, this indicates that the vegetation and its variability are important in this period. In wintertime all the fauna starts to grow, which leads to more withdrawal from the sub surface by the roots of the fauna.

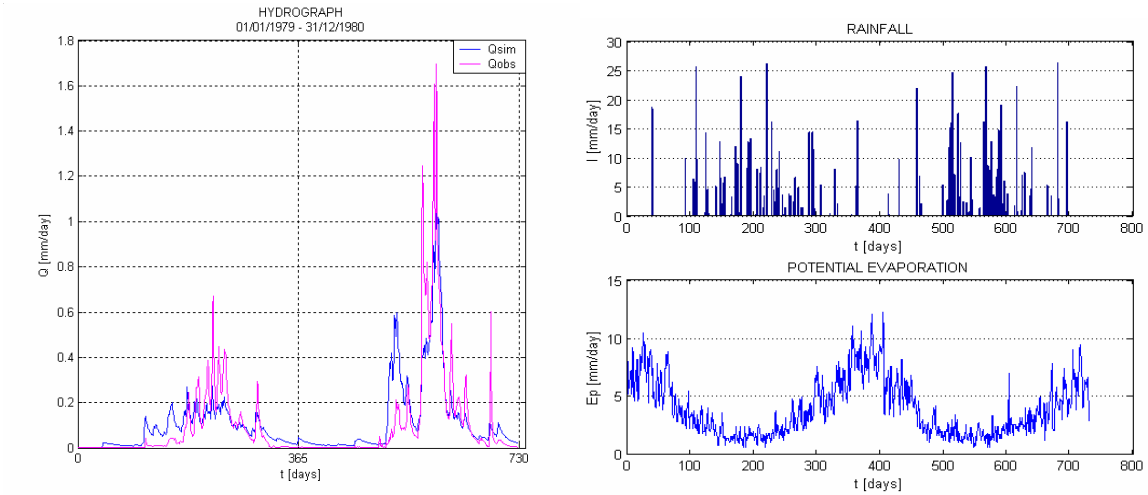

Figure 58 Model results for 5 REW's for the years 1979-1980, with the left figure based on 1st REW (near outlet)

The saturated area fraction is around 0.010. Here the water balance (WB) shows that there has been mass generated without a source, namely .1014849E-06. By looking at WB/P it becomes clear that WB/P is 0.00001014849%. This indicates that water corresponding to 1.014849E-05% mass has been generated during the simulations. This value is smaller than at 1 REW and is acceptable. The NSE for this specific case is 0.69.

9.2.2. Heterogeneous Precipitation field

For the first time the model simulates the spatial variability of the precipitation. As expected the peaks, especially in the second year, are better estimated (see Figure 59). In the first year the model underestimates the peaks, caused by the initial conditions of the model. To eliminate the importance of the initial conditions, it is decided, that for the heterogeneous fields, the simulated data is increased with one year. The first year is affected by the initial conditions, whereas the other years show reasonable results, especially for the peaks.

Year 1981 was found, with the top-down analysis, to be a ‘strange’ year. The annual rainfall was normal, while the number of rain-days, especially in winter, was limited. This resulted in high runoff for a few days (a higher rainfall intensity).

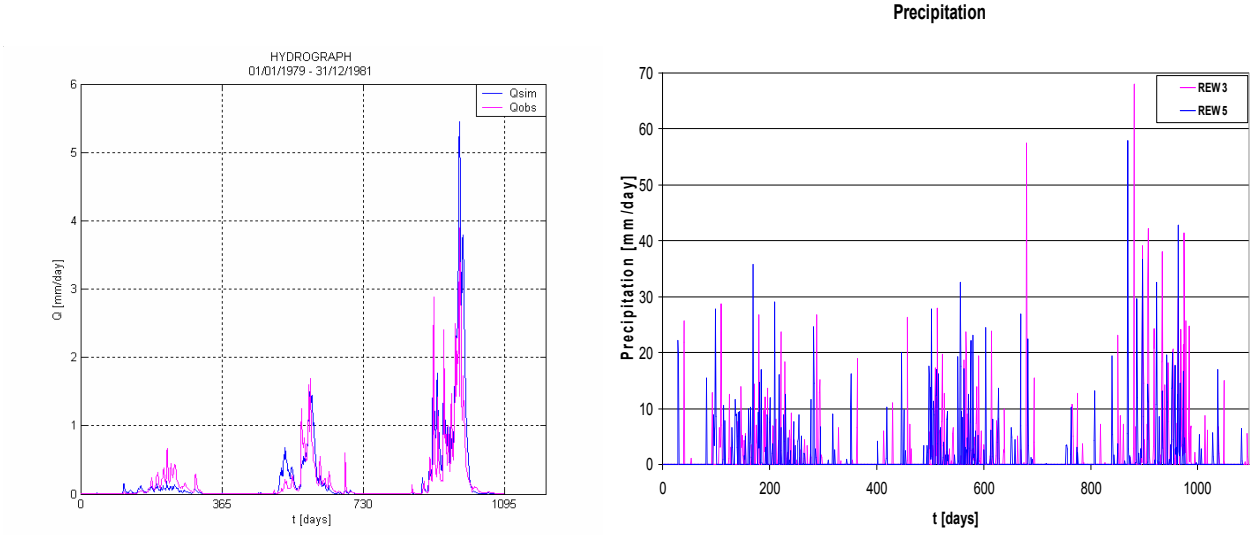

Figure 59 Results for 5 REW's with a heterogeneous precipitation field and left figure shows the differences between two precipitation fields

As was observed with results for the homogeneous precipitation field, the start of the growth of the fauna in early wintertime reduces the runoff, which is not yet incorporated in the model.
In comparison with the homogeneous precipitation field it can be seen that the second peak in the 1980 is better represented. Also the simulated base flow in the summer 1979-1980 is more representative to the observed discharge. With the homogeneous precipitation field, the peaks in the first years are better predicted and also the first peak in 1980 is less overestimated. The routing also predicts reasonable. The peaks in runoff, which are simulated, agree with the observed peaks.
Here, the water corresponding to 5.567952E-03% of rainfall has disappeared from the system and the NSE 0.43. This low efficiency is caused by the large overestimation of the last peak in 1981. If only the first 905 days are considered the NSE is 0.68. This is an increase of 150%.
Figure 59 shows the precipitation for two different REW's, derived using the inverse distance as interpolation technique.

9.3. 27 REW's

It was shown with 5 REW's that the heterogeneous precipitation field improved the runoff, especially for the peaks in wintertime. By identifying more REW's the spatial variability of the precipitation is better captured, especially in case there are sufficient and well distributed rain gauges available within the study area..
Although the homogeneous precipitation does not give satisfying results, the results will be shown also for 27 REW's, so comparison between 5 and 27 REW's can be made for both precipitation fields.
It should be noted that by defining more REW's more streams are identified. Figure 60 shows the division of the 27 REW's. Also here the early winter peak is caused by the influence of vegetation on runoff.

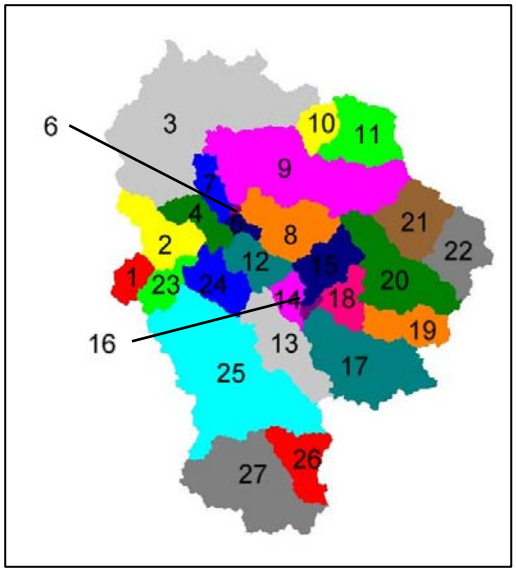

Figure 60 27 REW's based on the Strahler order

9.3.1. Homogeneous precipitation

Similar to the case of 5 REW's the peaks in May and June are overestimated, whereas the peak in August is underestimated (see Figure 61). The results for 5 REW's are actually better then for the case of 27 REW's. The simulation for year 1979 is affected by the initial conditions, so little attention should be paid to this. However it should be noted that the peaks are indeed identified but underestimated. The NSE is 0.66 and 1.681254E-04% of the rainfall has been disappeared from the system.

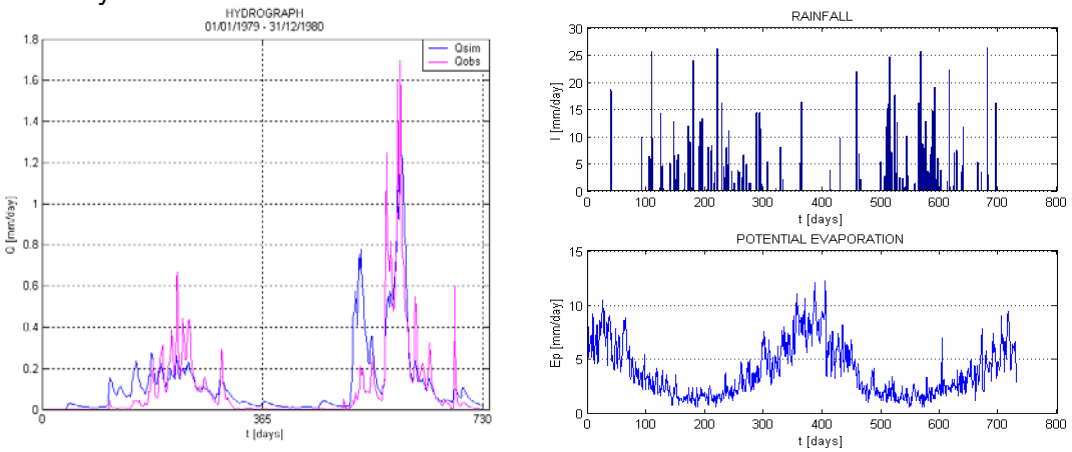

Figure 61 Results for 27 REW's using a homogeneous precipitation field

From the calibration of 5 and 27 REW's, it can be concluded that by using a homogeneous precipitation field the peaks in the Collie River Basin can not be well simulated.

9.3.2. Heterogeneous precipitation field

The observed data is also three years, namely 1979 – 1981, to minimize the influence of the initial conditions. In this way the effect of the initial conditions after the first year is minimized. In the first year the peaks are all underestimated, due to the initial conditions. After the first year the peaks in May-June are still overestimated, as was the case with the homogeneous precipitation field, whereas the peak in August is well simulated. Similar for the simulation of 5 REW's this is due to the not incorporated dynamic vegetation.

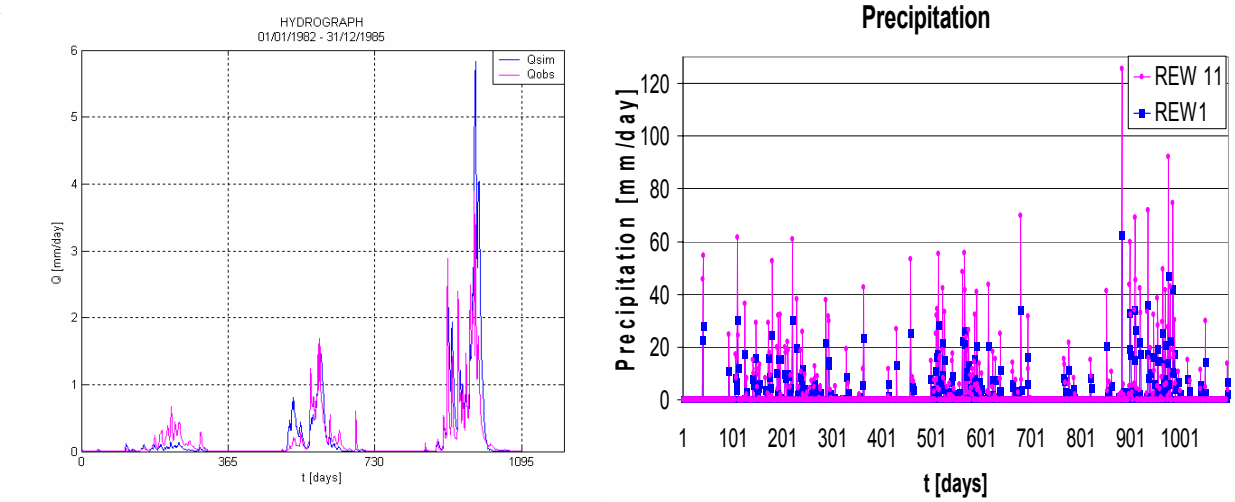

Figure 62 Results for a heterogeneous precipitation field for 5 REW's for the years 1979-1981

The results for the year 1981 show that peaks are well simulated, although de peaks in July-August are overestimated. Also it can be seen that the simulated discharge shows more delay than the observed discharge. This indicates that routing may play a role in this part. By looking at the delay time (6 days) and the length of the river channel (213km), the importance of routing can be roughly estimated. During the calibration the cross sectional areas for the streams are the same, whereas in reality the river close to the outlet is larger than in the upstream parts.

Comparing the results for 27 REW's with 5 REW's shows the NSE has decreased till 0.24. Again this indicates that more REW's don't guarantee a better performance. For this case the amount of precipitation that has disappeared from the system is 8.352401E-03%, which is reasonable low.

9.4. Validation

As the calibration has finished now, it is time to see whether model with the same set of parameters obtained after calibration also performs on a similar level of accuracy on other data sets of the Collie River Basin. For the validation the choice has been made only to test the cases with 5 and 27 REW's for the heterogeneous precipitation field, as they showed the most promising results. For the 1 REW case, it is the intention to see in what way the long-term water balance develops. In this paragraph in more detail the results of the validation and how the model helps to improve our understanding of the catchment are described. In Appendix 13: Model results, some results are shown for both cases.

9.4.1. 1 REW

For this case the model will be verified for 12 years, including 1979 and 1980 (the years for calibrating). However, the intention is to see in what way the long-term balance develops and after how many years the Collie Catchment stabilizes. From the hydrograph (Figure 63) it can be seen that the model simulates the base flow well. The peaks are often underestimated by the model.

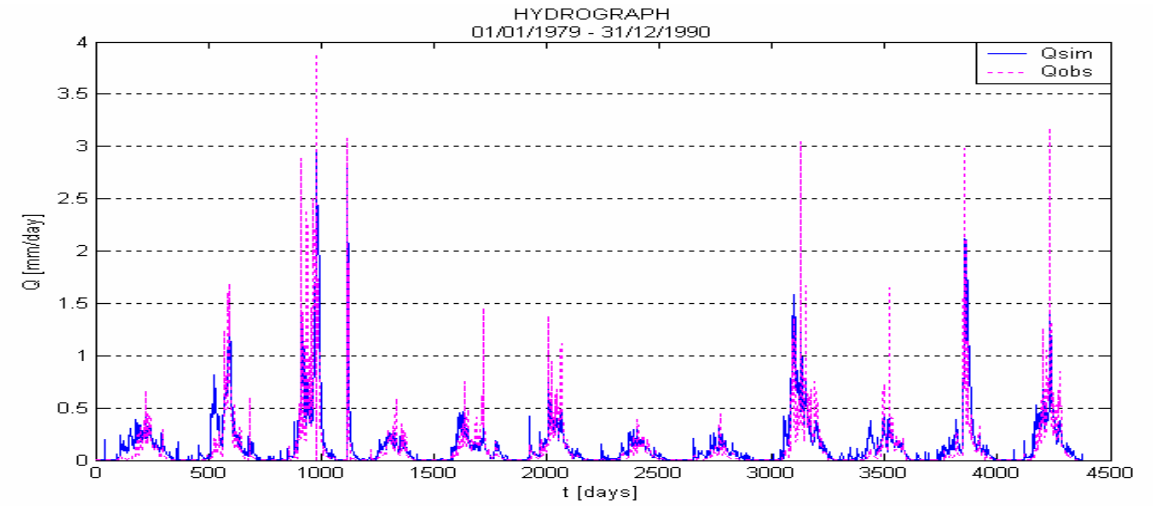

Figure 63 Hydrograph for 1 REW for the period 1979-1990, NSE= 0.61 and interception part is accounted by [2 mm/day]

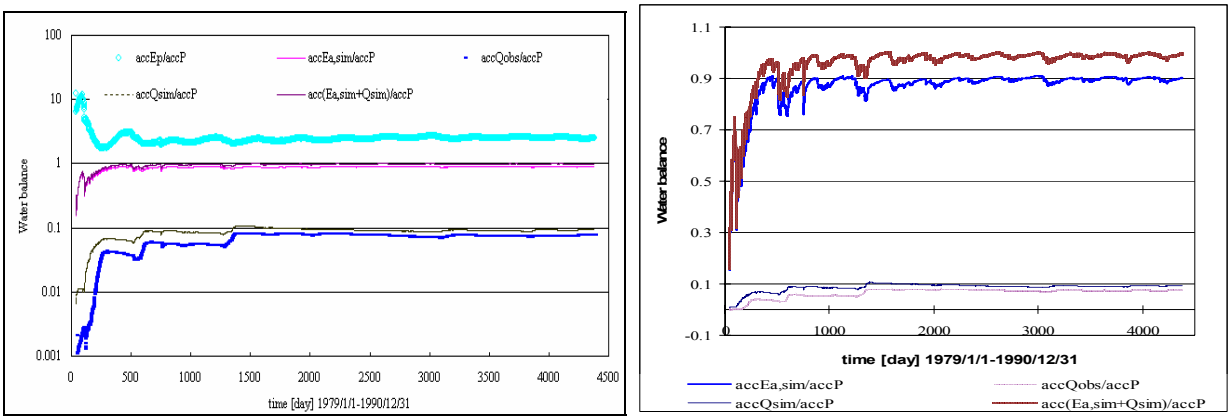

Figure 64 Water Balance analysis for 1 REW

From the water balance analysis (shown in Figure 64) it can be seen that acc(Ea+Q)/accP approaches 1.0, which means long term water balance is preserved. It is also observed that the Collie River Basin is stabilized in terms of long-term water balance after some unstable period, approximately 4 years. Also it can be observed that accEp/accP is 2.485 which mean Collie catchment is an (semi-)arid catchment. This is also shown in chapter 6.

9.4.2. 5 REW's

For the validation of 5 REW's with a heterogeneous precipitation field, the years 1982 till 1985 were simulated. In January 1982 a tropical depression reached Western Australia, which caused high rainfall in three days. This led to a substantial increase in runoff. From Figure 65 it can be seen that the model overestimates the runoff. This is partly due to the initial conditions, as well as the influence of the vegetation cover.
The NSE index is 0.39 when the tropical depression (early 1982) is neglected.

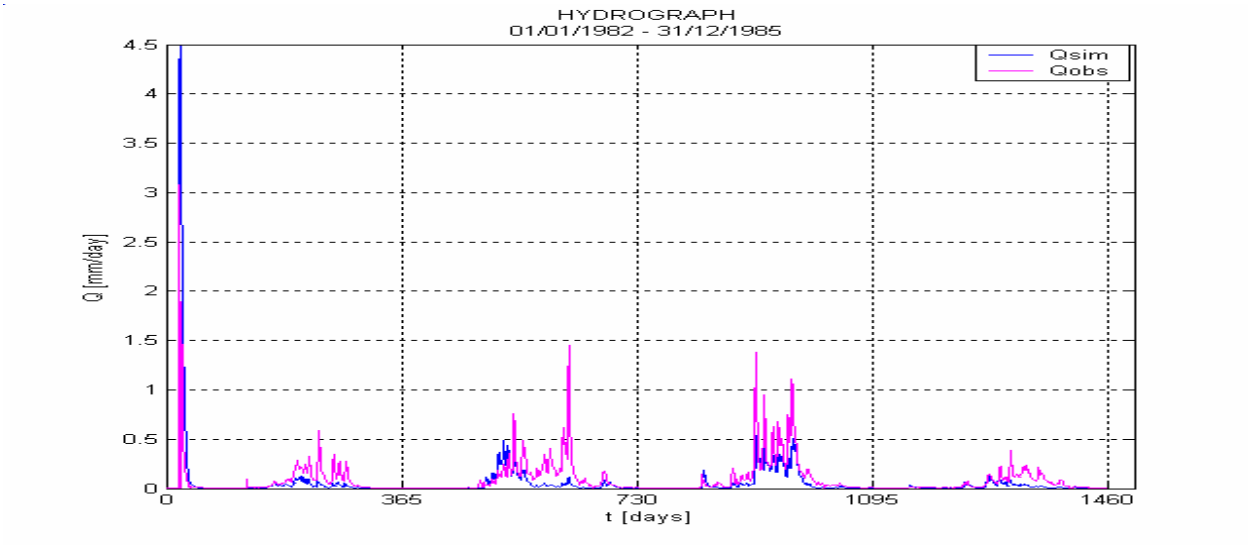

Figure 65 Validation of 5 REW's for the years 1982- 1985

From the model results the following can be derived: the S-zone storage fluctuates according to the precipitation events and dry periods. In times that precipitation occurs, the storage increases and decreases during a dry period. The fluctuation is in the order of centimetres (which fluctuates around the depth of 1.4 m). The same trend can be observed for the U-zone, where the fluctuation is in decimetres (range 0- 0.4m). For the O-zone a capricious development of the storage can be seen. It fluctuates strongly throughout the year, and it lies in the order of 0- $2*10^{-6}$ m. As is expected, the storage in the R-zone increases during winter, as a result of the runoff. (For more information see Appendix 13: Model results)
In the time of precipitation, the U-zone vertical velocity increases, so water is infiltrated in the U-zone and percolates to the S-zone. In case of precipitation the saturated overland flow mechanism is triggered.
For the O and C zone, there is rainfall and evaporation. During summer this is a negative value (evaporation), whereas in winter the net value is positive due to the precipitation.
The average thickness in the S and U- zone are correlated and increases during precipitation and due to a residence time of 4 months (see chapter 6) the thickness decreases with a delay time in dry periods.
The saturation degree of the U-zone shows, that for the tropical depression in 1982 this increased until 0.34, whereas in normal years the saturation degree in wintertime is around 0.22. During summertime this drops down till 0.1, due to the drying of the soil due to the evaporation.

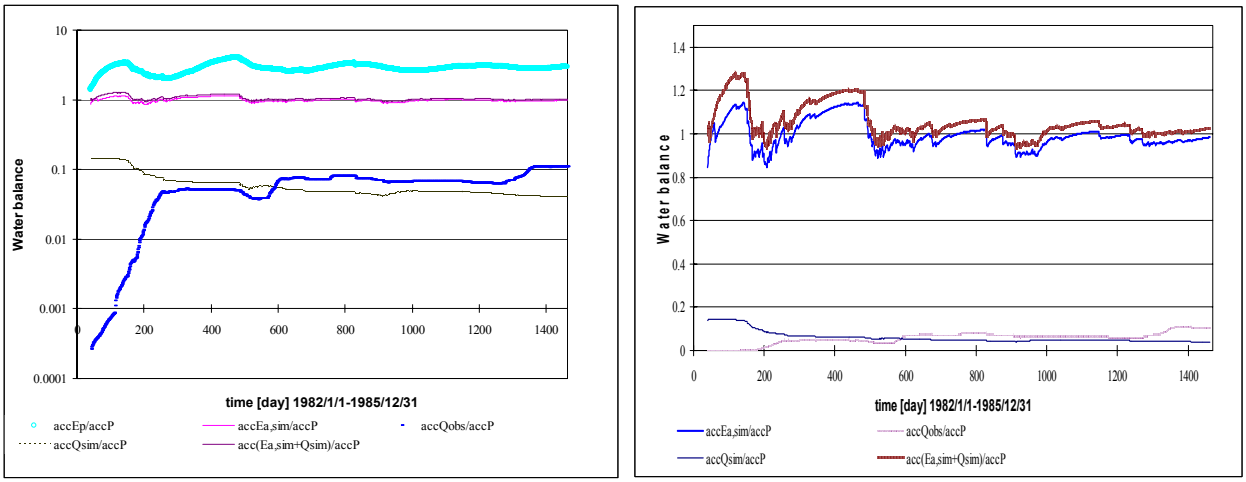

Figure 66 Water Balance Analysis for 5 REW's (heterogeneous precipitation field)

From Figure 66 it is observed that the long term water balance approaches 1.0, so the balance is preserved. It also shows that it starts to stabilize after an unstable period. At the end of the simulation period the simulated discharge is lower than the observed one. The difference is larger than in the previous years (first year is due to initial conditions). Further more it was found that for the simulated years the accEp/accP is 2.9 which indicate that the basin is (semi-)arid.

9.4.3. 27 REW's

For this case similar results were found for the calibration for the years 1982-1985 with 5 REW's. The major difference is that here the model overestimates the peak in early January in the first year even more (Figure 67). This might be caused to the larger number of streams in this simulation and the initial conditions. For the remaining years the model underestimates the peaks, but it is reasonable. After neglecting January 1982 the NSE is 0.37, which is almost similar to the validation of 5 REW's.

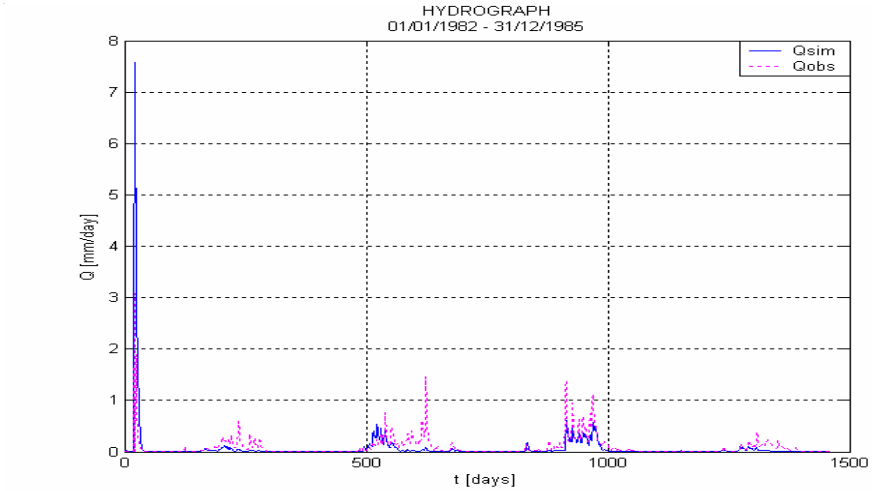

Figure 67 Validation of 27 REW's for the years 1982 - 1985

Similar to 5 REW's the following can be observed from the model results: The S-zone storage is slightly higher than for 5 REW's, namely 1.4001 m, but follows the same trend. The same applies for the storages in the U (0-0.4 m), O (0- $2*10^{-6}$ m) and R (0- $2*10^{-3}$ m) -zone. The U-zone vertical velocity increases during wintertime, so water infiltrates with higher velocity in the soil. Saturated overland flow mechanism works during precipitation events. (for more information see Appendix 13: Model results)

In this case there is no rainfall or evaporation in the R-zone, whereas this is the case for C en O-zone. For the latter the balance is negative for summertime, whereas in wintertime more precipitation falls than is evaporated.

Looking at the properties for the R-zone, it can be seen that the perimeter (peak 15m, baseflow 0.5m), top width (peak 3m, baseflow 0.5) and average depth (peak 0.7m, baseflow 0.1m) increases during wintertime (when most of the precipitation falls). This was also found for 5 REW's, though somewhat smaller.

The average thickness of the U and S-zone are correlated with each other, but instead of increasing during peak events, the thickness decreases. No logical solution for this phenomenon could be found, but after an investigation it appears that this occurs when a heterogeneous precipitation field is used. So the explanation might lie in the fact that by using the heterogeneous field for 27 REW's something is incorrect. It should be noted that in case of 5 REW's & heterogeneous field, the average thickness increases during precipitation events as should be expected. This error should be investigated in more detail.

The saturation degree for the peak in January 1982 is around 0.36, slightly higher than for 5 REW's. During the other peaks this value is around 0.21 and during summertime this decreases to 0.09.

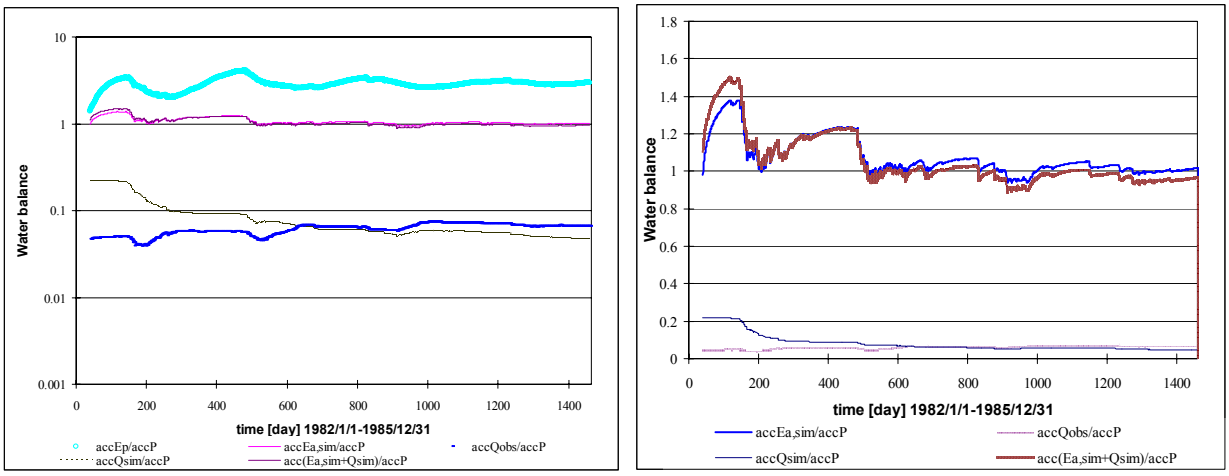

Figure 68 Water balance for 27 REW's (heterogeneous precipitation field)

The long-term water balance is preserved, as shown in Figure 68, as acc(Ea+Q)/accP approaches 1.0. After the first two years, which were unstable, the model starts to stabilize. The model overestimates the accumulated discharge in the first two years, due to the peak in January 1982, and underestimates in the final years. So further calibration is necessary, but to improve results also routing and dynamic vegetation should be taken into account.
Further more, it was found that for the simulated years the accEp/accP is 2.8 which indicate that the basin is (semi-)arid.

9.5. Conclusion

Comparing the results of CREW with the multiple linear regression model, used in chapter 6, the conclusion can be drawn that the efficiency of both models are comparable. While CREW requires a lot of information about the climatic data, geology, soil and physical parameters, the other model requires only data on the discharge and rainfall, which is less data intensive.
The CREW model gives more information about the catchment and the responses in the subsurface. It depends on the purpose and the demands of the user, which model is most suitable.

With the results of the calibration and validation the conclusion can be drawn that with a heterogeneous precipitation field the results, more specific the peaks, are improved. However it appears that the temporal and spatial variability of the vegetation also plays a significant role in the runoff process. Also important is the routing, until now this is constant over the whole catchment, but it is obvious that the cross sectional area of the downstream river is larger than the upstream part. There also exists a time delay of a few days in the simulated runoff, this is caused by routing.

With all the simulations it is observed that the first year is poorly simulated, which is caused by the initial conditions. After the influence is minimized, the model simulates the runoff reasonably well, taken into account, that several processes are neglected at this stage.
The results for 5 and 27 REW's give similar results. So more REW's is not always a sign that the results will improve. Until now the interception has been manually extracted from the data, but in newer versions of the model this can be taken into account.

For peak flows the saturated excess overland flow, is an important streamflow generation mechanisms (mentioned in paragraph 5.7). The model also generates that this is the case.

From literature a number of parameters were found (see paragraph 8.1). During the calibration process those were not changed. The parameters and state variables that were changed are listed below (Table 8).
It depends on the information that is already available from a catchment how data-intensive it is. Moreover, the difficulty of measuring certain parameters and state variables causes uncertainty in the modelling results. As it was the intention of REW to overcome the problems with data-intense models, it appears, that until now this has failed e.g. hydraulic conductivity for U and S-zone. It is possible, that with testing and calibrating the model to several different catchments all over the world, that some parameter ranges can be defined and better measurement techniques become available.

Table 8 Parameter & State variables range used for calibration of the model for the Collie River Catchment

Parameter/ State variable		from	to	comment
Parameter				
alpha_su(nREWs)	Recharge & Capillary rise	1.0	1.0216	1,0 for Darcy flux
alpha1_os(nREWs)	Seepage flow	0.009	0.015	
alpha2_os(nREWs)	Seepage flow	1.0	1.05	
alpha3_os(nREWs)	Seepage flow	6.0	24.0	
alpha_uc(nREWs)	Infiltration	0.06	0.06	
alpha_uwg(1)	Evapotranspiration	50.0	180.0	
alpha_oc(nREWs)	Concentrated overland flow	0.01	2.0	
alpha_ro(nREWs)	Saturated overland flow	0.01	2.0	
beta1_wo(nREWs)	Saturated surface area	0.133790	0.05d0	Derived with formula for ω_0
beta2_wo(nREWs)	Saturated surface area	3.21114E-52	0.3	"
beta3_wo(nREWs)	Saturated surface area	0.4	53.32	"
State variables				
zmr(nREWs)	flow cross sectional area in R-zone	0.0232	2.5	
vr(nREWs)	flow velocity at R-zone	1.50	3.70	
su(nREWs)	saturation degree at U-zone	0.10	0.12	
qbsteady(nREWs)	steady outflow from S-zone to R-zone	5.7870E-12		
yc(nREWs)	average thickness of C-zone	0.0	0.0	
vc(nREWs)	flow velocity at C-zone	0.0	0.0	
yo(nREWs)	average thickness of O-zone	2.0		
vo(nREWs)	flow velocity at O-zone	0.00001		

10. Overview of closure relations

In this chapter an attempt has been made to give an overview of the at the moment existing closure relation by indicating if they are adequate for a certain catchment with its particular climate, geology, topography and data-availability.
This overview is based on the various criteria which are discussed after the presentation of Table 9, which shows the criterions and the three existing models.

Table 9 Overview of applicability of the different developed closure relations

	Reggiani	Lee	Zhang	
Demand on data				
High	■			
Average		■		
Low			■	
Physical basis				
Common sense	■			
Porous conceptual model			■	
Pure physical		■		
Climate				
Temperate	■		■	
Tropical wet		■		
Tropical dry	■			
Arid		■		
Geology				
Hard Rock				
Sandy Loam	■	■	■	
Porous Rock	■		■	

Demand on data
For this criterion the quantity of different parameters of the three models has been investigated. It appears that the closure relations found by Reggiani (2000) have 53 different parameters, which requires a high demand on data. The closure relations by Lee (2005a) and Zhang (2005) have, respectively, 39 and 34 different parameters. Based on this, Zhang has the lowest demand on data, because it requires less known parameters to run the model. Zhang also have the highest rate of shared parameters (18) in his set of closure relations. Reggiani and Lee have respectively 11 and 10 shared parameters in their set.

Physical basis
Reggiani, et al. (1999, 2000) presented closure relations developed on intuitive grounds and expressed as linear functions of the mean values of the velocities on both sides of the boundaries, and the differences in hydraulic potentials. However, there was no effort made to connect these to ground reality, and especially to capture these effects of sub-REW and sub-time variability. Besides, the assumption of linear dependence is highly restrictive in the light of field evidence that shows strong nonlinearities, including threshold behaviour.
The method used by Lee (2005a), has been thoroughly discussed in chapter 4, but will be briefly described. For the development of the closure relations he discussed four categories: field experiments, theoretical/analytical derivations, numerical experiments, and hybrid approaches. Empirical closure relations based on field observations may be the best candidate for the closure relations as they best represent the intrinsic natural variability occurring with actual catchments. In the theoretical approach, the emphasis is on deriving closure relations through analytical integration or up scaling of small-scale physically based equations. It has the advantage that the

closure relations, as well as the REW-scale parameters, retain some of their traditional meaning. On the other hand, numerical simulation approach seeks to derive closure relations based on simulated datasets that could be generated through application of distributed physically based models, based on small-scale physical theories. The last approach represents a combination of any of the above mentioned approaches.
Last, but not least, the closure relations defined by Zhang are in the middle of the other two. The term for this is porous conceptual model.

Climate
At this moment the REWASH model has been applied to catchments in Europe, which has a temperate climate. It is not known how the model works in other climates, so therefore the applicability of this model is set to a temperate climate.
The model by Reggiani has been tested to several cases in Europe, which among the Geer Catchment in Belgium. For WL Delft Hydraulics it has also done some modelling in Cebu and Taiwan, which have a tropical climate.
The CREW model has now been tested in Germany and Australia. The first has a temperate climate and the latter has both a semi-arid and a tropical climate, where the rain falls during summer (November-February). CREW is still under development and in the following year it will be tested on many otherdifferent climates.

Geology
Both Reggiani and Lee have executed an sensitivity analysis to explore the effects of different soil types on seepage flux and saturation areas. The soil types were sand, silty loam and sandy loam. No comments are made about the results of the models and if hard or porous rock was used.
It should be noted however that Reggiani had the same study catchment as Zhang, the Geer River Basin in Belgium. Here, the groundwater aquifer of the catchment consists of Cretaceous chalks. For schematic representation of soils, see Figure 69

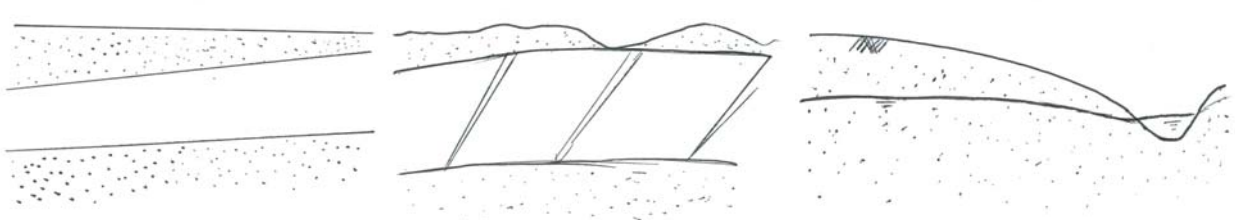

Figure 69 Three different geology structures, from left to right: hard rock, porous rock and sandy loam

11. Conclusions and Recommendations

11.1. Conclusions

11.1.1. REW approach

Ever since the REW approach has been developed, people have made modifications to improve the results. In this research two models were investigated, namely CREW and REWASH. Both models have the same theoretical background although the outcome is different. Differences have been recognised e.g. in the way hydraulic conductivities for the unsaturated and saturated zone have been defined, the definition of groundwater flow, mass exchange across mantle segment and the description of the variable source area.
It depends on the climate, soil moisture and physiography which of the closure relations are most suitable. In the near future, the developed closure relations can be used for each model in a way that for that specific climate, soil and physiography the most optimum solution can be found.
It is however, the question whether this new approach is capable to overcome some of the disadvantages of other existing models. This approach promised to overcome complexity in terms of data input requirements. As there is no experience with other models, it is difficult to dispute that. Based on my experience, a lot of input parameters are required for modelling the catchment, especially with increasing the numbers of REW's, e.g. geometry. Moreover, the accuracy of the parameters, e.g. hydraulic conductivity, is difficult to estimate. During my research I have used parameters from literature as a guide for calibrating the catchment.

11.1.2. Data analysis

By using the top down approach, a systematic approach (from annually to daily) has been found to analyse the available data. There was data available from around 1978 till 1990 for precipitation, evaporation and discharge.
The precipitation in the Collie River Basin decreases from 1200 mm in the west till 600 mm in the east. Evaporation is in the range of 1400-1600mm per year. Over the last 30 years the evaporation has been fairly constant, average 1400 mm/year. For this data analysis three sub-catchments have been chosen for the period 1979-1990, namely Collie River South, James Crossing and Harris River.
On basis of the double mass analysis and the residual mass curve the conclusion can be drawn that there is a good correlation between the gauge stations in this catchment. For the annual runoff analysis it was seen that 1989 and 1990 have a great influence on linear runoff for the Harris River. This might be caused by the preparations for building the Harris Dam. The threshold in annual time scale is 390 mm of precipitation
From the monthly analysis the formula of Kagan showed that the correlation between stations was 0.88. 1987 was a relatively wet year which also led to more runoff. With a simple multiple linear regression model the interception per month was found. For all three sub catchments this was in the order of 60 mm per month. This model also showed that the fallen precipitation has an influence for four months on the runoff. In the Collie River Basin the groundwater process is dominant. The average discharge is 0.07 mm/day.

Through daily analysis, the conclusion can be drawn that the precipitation fell in small amount of days. This results in high surface runoff. If monthly rainfall is normal, the runoff can still be high, due to the fact that during this month the precipitation fell in a short period of time.
The interception analysis has shown a strong correlation with the Budyko curve as the formulae have strong similarities.

11.1.3. Implementation of the model: CREW

The analysed data was used to test the model of its applicability to the Collie River Basin, Western Australia. This basin lies approximately 200 km south of Perth. During the implementation of the model several problems were encountered and solutions were found. For the derivation of the quantity of REW's a script has been written in PCRaster, which is a free GIS Environment software package. Secondly, the range of parameters with a physical background was specified in order to limit the possibility of equifinality, which was found during the research. Also several errors in the momentum balance for the unsaturated zone were found. The most important was that the unsaturated zone saturation degree was greater than ½ at equilibrium state, while in fact it can be either dry or fully saturated.
During the calibration the computation time varied between several minutes to hours. This depends on the amount of REW's used. Also parameters don't control the computation time, but influence the processes simulated, thus giving rise to different errors in each computation time step. Therefore, different parameter sets can lead to different computation time.
As the Collie River Basin has a large spatial variability in precipitation, it was necessary to modify the CREW model, to be able to have a heterogeneous precipitation field. The data for each REW was derived on basis of the inverse distance as interpolation technique, using PCRaster. Besides the variability in precipitation in the basin, the vegetation also shows large differences. In the Collie River Basin intensive Coal mining still takes place. Several artificial lakes have been created since the beginning of the mining. These lakes and the production of the mining have an influence on the model results.
Based on the results and the modifications made to CREW, it can be said that the model still requires some modifications, however the peaks in the Collie River are reasonably simulated. So it is concluded that CREW is applicable for the Collie River Basin.

11.1.4. Results model

When a heterogeneous precipitation field wad applied, the peaks were better captured by the model.
Besides the importance of the spatial variability of the precipitation, the temporal and spatial variability of the vegetation is also important in the runoff process. Until now this has not been investigated. Finally, routing also could play a role in the model performance since the cross-sectional areas vary strongly between upstream and downstream channelsin the catchment. In the results this can be seen from the time delay between the simulated and observed runoff.

It is observed that the first year is always poorly simulated, caused by the initial conditions. After this year the model represents measured data reasonably well, considering that several processes are not taken into account.

Up till now the results for 5 and 27 REW's are similar, but it is expected that as soon as parameters are defined for each REW the latter should give better overall results, as the variability in the catchment is better represented. Until now the interception has been manually extracted from the data, but in newer versions of the model this can be taken into account.

As was found in literature for the Collie River Basin, the saturated excess overland flow is an important streamflow generation mechanism and is predicted by the model.

In this research the top-down approach was used for analysing the available data. The REW-approach on the other hand, is a bottom-up approach. By using both it can be seen that both give more or less similar results. What is found with one analysis can be checked with the other one. By using both, better understanding about the system and occurring hydrological processes is established. Moreover, it helps to see patterns and thresholds in a system, without (too) complex modelling.

11.2. Recommendations

11.2.1. Collie River Basin

On the east side of the town Collie, there is a large flat area, which during wintertime is used as a floodplain. This has a consequence in the streamflow, more water can be stored here, so less water will flow to the outlet. Therefore the model can overestimate the discharge during certain periods. With a revised version of the script that was used to define the REW's based on Strahler order, this phenomenon can be taken into account. To achieve this, the slopes should be taken into account and this floodplain should be used as a routing component.
Also the influence of vegetation on the runoff has not been quantified in the model, in the sense of the differences that exist in the vegetation cover. Some parts of the catchment have been cleared in the past for agriculture. In those areas the runoff will be higher than in forested areas. Also the quantity of water, which the different Eucalypt species uses per day, may differ or at least the density differs. So the temporal and spatial distribution in vegetation is important to implement in the model.
During the simulations the slopes in the Collie River Basin has been assumed the same all over the catchment. In a catchment like the Collie River it is necessary to define the differences in slopes. This might have an influence on the runoff and storage capacity in the subsurface.
The influence of reforestation on transpiration, interception and Hortonian overland flow can be significant. This could lead to errors in the simulation especially in those areas where cleared land is reforested. Eucalyptus species cause an average change of 40 mm in annual flow for a 10% change in cover with respect to grassland.
In the Collie River Basin routing is an important aspect of modelling the catchment. Routing can be optimized by fine-tuning state variables such as the cross-sectional area and the depth of the river. After all, the river has a larger perimeter near the outlet and more water flows there than in the upstream part. Until now this has been manually extracted from a map and fieldtrips.
As mining still takes place in the Collie River Basin, the modelling has to take this into account. Until now it is not known how this influences the results. As the lakes have a large storage capacity, this should influence the water velocity and discharge

For the heterogeneous precipitation field, the inverse distance was used as interpolation technique. However, for this process, all the gauge stations were taken into account. For future simulations it is recommended that with using the inverse distance, only two or three gauge stations are taken into account. When all the stations were taken into account, the spatial variability in precipitation in the Collie River Basin has decreased. The peaks in the precipitation have disappeared in the case of using all the gauge stations. The range from 1200 mm in the west till 600mm east is more even. In that way the spatial variability is better represented. This might help to improve the simulated runoff, as calculated precipitation is now lower than it should be.
For the Collie River Basin there are two stations where the potential evaporation is measured. For this research only one station was available and as the evaporation varies over the catchment, it is recommended to use both stations in the future.

Seasonality, with wet periods in winter and dry in summer, can be found in Australia. It can be observed that there exists spatial variability in soil moisture during winter time. This leads to differences between the REW's. By observing this for each REW, more knowledge regarding the catchment can be gathered.

11.2.2. CREW

The physical meaning of each parameter, their ranges of variability to keep them realistic for the area, and more sophisticated methodologies for the estimation of parameter values, should all be carefully investigated through application of the model to different settings of initial and boundary conditions and different climates. It is important to realize that a perfect model can never be created and therefore knowing the limitations of a model helps to improve the understanding of the processes involved. The choice of a model should be based on the purpose for which it is intended and the results it produces.
Depending on the purpose of the model, try to learn from patterns in a catchment. Let the model help to identify the most important hydrological processes. The top-down analysis with data for identifying processes in a catchment is (a) perfect tool.
In the last decades the parameters were questioned and the input variables treated as perfect. As the input variables (precipitation, runoff etc.) drive the modelling, it is important to question them. With every measurement errors are made, e.g. observation errors, measurement techniques errors. Therefore, data must always be checked on errors and deficiencies.

The interception until now has been manually extracted from the precipitation data, as the version that was available during the research did not contain this feature. By now the model has included this feature, so it is important to review the assumptions made to the interception in this basin and see if the model is capable of taken this properly in account

Until now, only the output of the first REW has been analysed. However for each case the water balances for each REW are different. So it is important to analyse all the water balances. It is recommended to work from upstream to downstream in order to get the balances correct. More over, as the stream flow differs from one REW to another, it is recommended to check with one of the gauge stations used in this research, if the model predicts the runoff accurately.

By using hourly discharge data, the routing aspect can be improved in the model. At this moment there is a delay time in the model by several days. This can be corrected by the hourly data, as it will gain better insight in the routing process.

From this research the conclusion can be drawn that in some catchment the necessity of a heterogeneous precipitation field is evident, however the same can apply for a heterogeneous evaporation field. In this research only one station was available, but in the Collie River Basin the evaporation also varies between 1600 mm in the west till 1400mm in the east. It is recommended that in the same way as with the precipitation the heterogeneous evaporation field is calculated. The script that was made to calculate the precipitation over the catchment is, after a few changes, also applicable for this case.

Nomenclature

Latin symbols

$\mathbf{A}$	mantle surface with horizontal normal delimiting the REW externally	
A	linearization coefficient for the mass exchange terms	$[TL^{-1}]$
A	Horizontally projected surface area of a REW	$[L^2]$
B	linearization coefficient for the mass exchange terms	$[ML^{-3}]$
d	diffusivity index	$[-]$
e	water mass exchange per unit surface area divided by water mass density	$[LT^{-1}]$
e_{ca}	Interception flux taking place on C-zone	$[MT^{-1}]$
e_{ua}	Transpiration flux from U-zone	$[MT^{-1}]$
e_{oa}, e_{ra}	Evaporation fluxes from O-zone and R-zone respectively	$[MT^{-1}]$
e_p	potential evaporation	$[LT^{-1}]$
e_{cu}	Infiltration flux from C-zone to U-zone	$[MT^{-1}]$
e_{sr}	Base flow from S-zone to river channel	$[MT^{-1}]$
e_{us}	Recharge flux from U-zone to S-zone	$[MT^{-1}]$
e_{so}	Seepage flux from S-zone to O-zone	$[MT^{-1}]$
g	gravitational acceleration	$[LT^{-2}]$
h_c	Capillary pressure head	$[L]$
h_o, h_r, h_s	Total hydraulic head for O-zone, R-zone and S-zone	$[L]$
i	precipitation intensity	$[LT^{-1}]$
i_{dc}	Interception threshold for C-zone	$[LT^{-1}]$
J	rate of rainfall input or evaporation	$[LT^{-1}]$
k_v	Ratio of potential rates of transpiration and soil surface evaporation	$[-]$
$\overline{K_s}$	mean saturated hydraulic conductivity	$[LT^{-1}]$
K_{su}, K_u	Saturated and effective hydraulic conductivity for U-zone	$[LT^{-1}]$
K_{sr}, K_{ss}	Saturated hydraulic conductivity for the river bed and S-zone	$[LT^{-1}]$
l_r	the length of a channel reach	$[L]$
M	Vegetated fraction of land surface, or canopy density	$[-]$
m	pore size distribution index	$[-]$
m_r	average channel cross sectional area	$[L^2]$
n	Manning roughness coefficient	$[TL^{-1/3}]$
p	pressure	$[FL^{-2}]$
P_r	the wetted perimeter of a river cross section	$[L]$
q_s	steady flow from saturated zone to channel reach	$[LT^{-1}]$
s_u	Saturation degree of U-zone	$[-]$
v_o	Velocity of the flow on the surface of O-zone	$[LT^{-1}]$
v_r	Velocity of the flow in the river channel	$[LT^{-1}]$

w_r	top width of the channel	$[L]$
y_o	Depth of flow sheet over the overland flow zone surface	$[L]$
y_r	Water depth of the river channel	$[L]$
y_s, y_u	Average water depth of S-zone and U-zone	$[L]$
z_r, z_s, z_{surf}	average elevation for riverbed, ground surface and soil bottom from datum	$[L]$

Greek symbols

α_{sf}	Scaling factor for O-zone area computation	$[-]$
α_{si}	Lumped scaling factor for regional groundwater flow	$[L^2T^{-1}]$
α_{us}	Scaling factor for flux exchange between U-zone and S-zone	$[-]$
γ_o	Average surface slope angle of O-zone in radian	
γ_r	Average slope angle of the channel bed in radian	
η	the slope gradient of a slope unit	$[-]$
ε	soil porosity	$[-]$
λ	Soil pore disconnectedness index	$[-]$
Λ_r	Depth of transition zone of the riverbed for the base flow	$[L]$
Λ_s	Typical length scale for the seepage flux	$[L]$
Λ_{co}	Contour curve separating the two overland flow zone from each other	$[-]$
μ	Soil pore size distribution index	$[-]$
θ_f, θ_s	Field capacity and saturated soil moisture content of U-zone	$[-]$
ρ	water mass density	$[ML^{-3}]$
Σ	projection of the total REW surface area onto the horizontal plane	$[L^2]$
ξ	Darcy-Weisbach friction factor	
$\lvert\Psi\rvert$	soil matric potential head of unsaturated zone at the catchment scale	$[L]$
$\lvert\Psi_b\rvert$	bubbling pressure head	$[L]$
ϕ	the gravitational potential	$[-]$
ω_o	Variable source area fraction of O-zone	$[-]$
ω_u	Unsaturated zone area fraction	$[-]$

Subscripts

bot	subscript for the region delimiting the domain of interest at the bottom
l	subscript indicating the various REW's within the watershed
top	subscript for the atmosphere, delimiting the domain of interest at the top
u, s, c, o, r	subscripts indicating sub regions within a REW
w, g	designate the water and the gaseous phase respectively
$_{jA,ext}$	exchange from the *j*-sub region across the external watershed boundary
$_{jA,l}$	exchange from the *j*-sub region across the *l*th mantle segment

References

Abott M.B., Bathurst J.C., Cunge J.A. O'Connell P.E. and Rasmussen J., 1986a
An introduction to the European Hydrologic System Systeme Hydrologique Europeen, SHE, 1: History and philosophy of a physically based, distributed modelling system, J. Hydrol., **87**, 45-59.

Abott M.B., Bathurst J.C., Cunge J.A. O'Connell P.E. and Rasmussen J., 1986a
An introduction to the European Hydrologic System Systeme Hydrologique Europeen, SHE, 2: Structure of a physically based, distributed modelling system, J. Hydrol., **87**, 61-77.

Beven K.J., 1984
Infiltration into a class of vertically non-uniform soils, Hydrol. Sci.J., **29**, 425-434.

Beven K.J., 1989
Changing ideas in hydrology: the case of physically based models, J. Hydrol., **105**, 157-172

Beven K.J., Lamb R., Quinn P., Romanowicz R. and Freer J., 1995.
TOPMODEL, In: Computer models of Watershed hydrology, Singh V.P. (Ed.), Water Resources Publications, USA, pp. 627-668.

Beven K.J., 1993.
Prophecy, reality and uncertainty in distributed hydrological modelling. Advances in Water Resources, **16**, 41-51.

Beven K.J., 1996a
A discussion of distributed hydrological modelling. In: Distributed Hydrological modelling, Abbott M.B. and Refsgaard J.C. (Eds.), Kluwer Academic Publishers, Dordrecht, The Netherlands, pp. 255-278.

Beven K.J., 1996b
Response to comments on *"A discussion of distributed hydrological modelling"*. by J.C. Refsgaard *et al.,* In: Distributed Hydrological modelling, Abbott M.B. and Refsgaard J.C. (Eds.), Kluwer Academic Publishers, Dordrecht, The Netherlands, pp. 289-295.

Beven K.J., 2002.
Towards an alternative blueprint for physically based digitally simulated hydrologic response modelling system,. Hydrol. Process., **16**, 189-206.

Beven K.J., Calver A., and Morris E., 1987
The institute of Hydrology distributed model. Institute of Hydrology Report No. 98, UK

Bras R.L., 1990
HYDROLOGY: AN INTRODUCTION TO HYDROLOGIC SCIENCE, Reading, Mass., USA: Addison-Wesley-Longman

Brutsaert W., 1934
Evaporation in the atmosphere, D. Reidel Publishing Company, Dordrecht, The Netherlands, 224-243

Dunne T, 1978
Field studies in hillslope flow processes, In: Hillslope Hydrology, Kirkby M.J. (Ed.), John Wily & Sons, Chichester, UK, pp. 227.293.

Freeze R.A., Harlan R.L., 1969
Blueprint for a physically- based digital-simulated hydrologic response model, J. Hydrol., **9**, 237-258.

Grayson R.B., Moore I.D. and McMahon T.A. 1992
Physically based hydrologic modelling,2, Is the concept realistic? Water Resourc. Res., **28**, 2659-2666

Groen M.M de, 2002
Modelling interception and transpiration at monthly time steps; Introducing Daily Variability through Markov Chains, IHE Delft, The Netherlands.

Jothiyangkoon C., Sivapalan M., Farmer, .L.,2001.
Process controls of water balance variability in a large semi-arid catchment: downward approach to hydrological development, J. Hydrol.. **254**, 174-198.

Kirkby M.J., 1997
TOPMODEL, a personal view, Hydrol. Process., **11**, 1087-1097

Lee H., Sivapalan M. and Zehe E., 2005a
Representative Elementary Watershed (REW) approach, a new blueprint for distributed hydrologic modelling at catchment scale. In: Predictions in ungauged basins: International perspectives on state-of-the-art and pathways forward, Proceedings of the Australia-Japan workshop on PUB Working Groups, Edited by S.W. Franks, M. Sivapalan, K. Takeuchi and Y. Tachikawa, IAHS Press, Wallingford, Oxon, UK. In press

Lee H., Sivapalan M. and Zehe E., 2005a
Representative Elementary Watershed (REW) approach, a new blueprint for distributed hydrologic modelling at the catchment scale: the development of closure relations. In: Predicting ungauged streamflow in the Mackenzie Basin: Today's techniques & Tomorrow's solutions, C. Spence, J.W. Pomeroy, A. Pietroniro (Editors), Canadian Water Resources Association (CWRA), Ottawa, Canada

Lee H., Sivapalan M. and Zehe E., 2005b
Representative Elementary Watershed (REW) approach, a new blueprint for distributed hydrologic modelling at the catchment scale: Numerical implementation. In: Physically Based models of river runoff and their application to ungauged basins, Proceedings, NATO Advanced Research Workshop, P.E. O'Connell and L. Kuchment (Editors).

Mauger G.W., Bari M., Dixon R.N.M., Dogramaci C.C. and Platt, J., 2001
Salinity Situation Statement Collie River, Water and Rivers Commission, Water Resource Technical Report series, report WRT29, 36p.

Refsgaard J.C. and Storm B., 1995
MIKE SHE, In: Computer models of Watershed Hydrology, Singh V.P.(Ed.), Water Resources Publications, USA, pp. 809-846

Reggiani P., Sivapalan M., Hassanizadeh S.M., 1998.
A unifying framework for watershed thermodynamics: balance equations for mass, momentum, energy and entropy and the second law of thermodynamics. Adv. in Water Resourc., **22 (4)**, 367-398.

Reggiani P., Hassanizadeh S.M., Sivapalan M. and Gray W.G., 1999.
A unifying framework for watershed thermodynamics: constitutive relationships. Adv. in Water Resourc., **23 (1)**, 15-39.

Reggiani P, Sivapalan M. and Hassanizadeh S.M. 2000.
Conservation equations governing hillslope responses: exploring the physical basis for water balance. Water Resour. Res., **36**, 1845-1863.

Reggiani P., Sivapalan M., Hassanizadeh S.M. and Gray W.G., 2001.
Coupled equations for mass and momentum balance in a stream network: theoretical derivation and computational experiments. Proc. R. Soc. Lond., **457**, 157-189.

Reggiani P. and Schellekens J., 2003
Modelling of hydrological responses: the representative elementary watershed approach as an alternative blueprint for watershed modelling. Hydrol. Process., **17**, 3785-3789.

Reggiani P. and Rientjes T.H.M., 2005
Flux parameterization in the Representative Elementary Watershed (REW) approach: Application to a natural basin, Water Resour. Res., 41, W04013, doi:10.1029/2004WR003693.

Rutherford J.L., 2000
Hydrogeology of the COLLIE, 1:250.000 sheet, Western Australia, Water and Rivers Commission, Hydrogeological map explanatory notes series, report HM7, 36p.

Savenije H.H.G., 2000
Hydrology of catchments, rivers and deltas. Lecture notes of the course Hydrology of Catchments, Rivers and Deltas (CT5450), Delft University of Technology, Section Hydrology and Ecology.

Savenije H.H.G., 2001
Equifinality, a blessing in disguise? , Hydrol. Process., **18**, 2835-2838.

Savenije H.H.G., W.M.J. Luxemburg, 2003
Hydrological Measurements. Lecture notes of the course *Hydrological Measurements* (CT4440), Delft University of Technology, Section Hydrology and Ecology.

Savenije H.H.G., 2004
The importance of interception and why we should delete the term evapotranspiration from our vocabulary, Hydrol. Process., **18**, 1507-1511.

Sharma M.L, 1984
Evapotranspiration from a eucalyptus community, Agric. Wat. Manage., **8**, 41-56.

Sharma M.L., Barron R.J.W., and Fernie M.S., 1987
Areal distribution of infiltration parameters and some soil physical properties in lateritic catchments, J. Hydrol., **94**, 109-127.

Silberstein, R.P., Held, A., Hattion T., Viney N.R., Sivapalan M., 2001
Energy balance of a natural jarrah (Eucalyptus marginata) forest in Western Australia: measurements during the spring and summer, Agriculture and Forest Meteorology, **109**, 79-104.

Sivapalan M., Ruprecht J.K., Viney N.R., 1996
Water and salt balance modelling to predict the effects of land-use changes in forested catchments. 1. Small catchment water balance model. Hydrol. Process., **10**, 393-411.

Sivapalan M., Viney N.R. and Jeeveraj C.G., 1996b
Water and salt balance modelling to predict the effects of land use changes in forested catchments: 3. The large catchment model, Hydrol. Process., **10**, 429-446

Stokes R.A., 1985
Stream water and chloride generation in a small forested catchment in south western Australia, M. Eng. Sc Thesis, Department of Civil Engineering, University of Western Australia, 176 pp.

Van den Akker C. and Boomgaard M.E., 2001
Hydrology, Lecture notes of the course Hydrology (CT3010), Delft University of Technology, Section Hydrology and Ecology.

Williamson D.R., Stokes R.A. and Ruprecht J.K., 1987
Response of input and output of water and chloride to clearing for agriculture, J. Hydrol., **94**, 1-28

Zhang G.P., Fenicia F., Rientjes T.H.M., Reggiani P. and Savenije, H.H.G., 2005
Modelling runoff generation in the Geer River Basin with improved model parameterizations to the REW approach. Phys. Chem. Earth, **30**, 285-296.

Zhang G.P. and Savenije, H.H.G., 2005
Rainfall-runoff modelling in a catchment with a complex groundwater flow system: application of the Representative Elementary Watershed (REW) approach, Hydrol. Earth Sys. Sci. Discuss., **2**, 639–690.

Appendices

Appendix 1: Thesis Committee

- **Prof. dr. ir. H.H.G. Savenije**
  Delft University of Technology (TU Delft)
  Faculty of Civil Engineering and Geosciences
  Department of Water Management
  Section Water Resources

- **Prof. M. Sivapalan**
  University of Western Australia (UWA)
  Centre for Water Research (CWR)
  Section Surface Hydrology
  Perth, Australia

  New position:
  University of Illinois
  Department of Geography
  Watershed Hydrology
  Urbana-Champaign, USA

- **Ir. W.M.J. Luxemburg**
  Delft University of Technology (TU Delft)
  Faculty of Civil Engineering and Geosciences
  Department of Water Management
  Section Water Resources

- **Prof. ir. J.C. van Dijk**
  Delft University of Technology (TU Delft)
  Faculty of Civil Engineering and Geosciences
  Department of Water Management
  Section Sanitary Engineering

Appendix 2: Catchment Boundaries of the Collie River

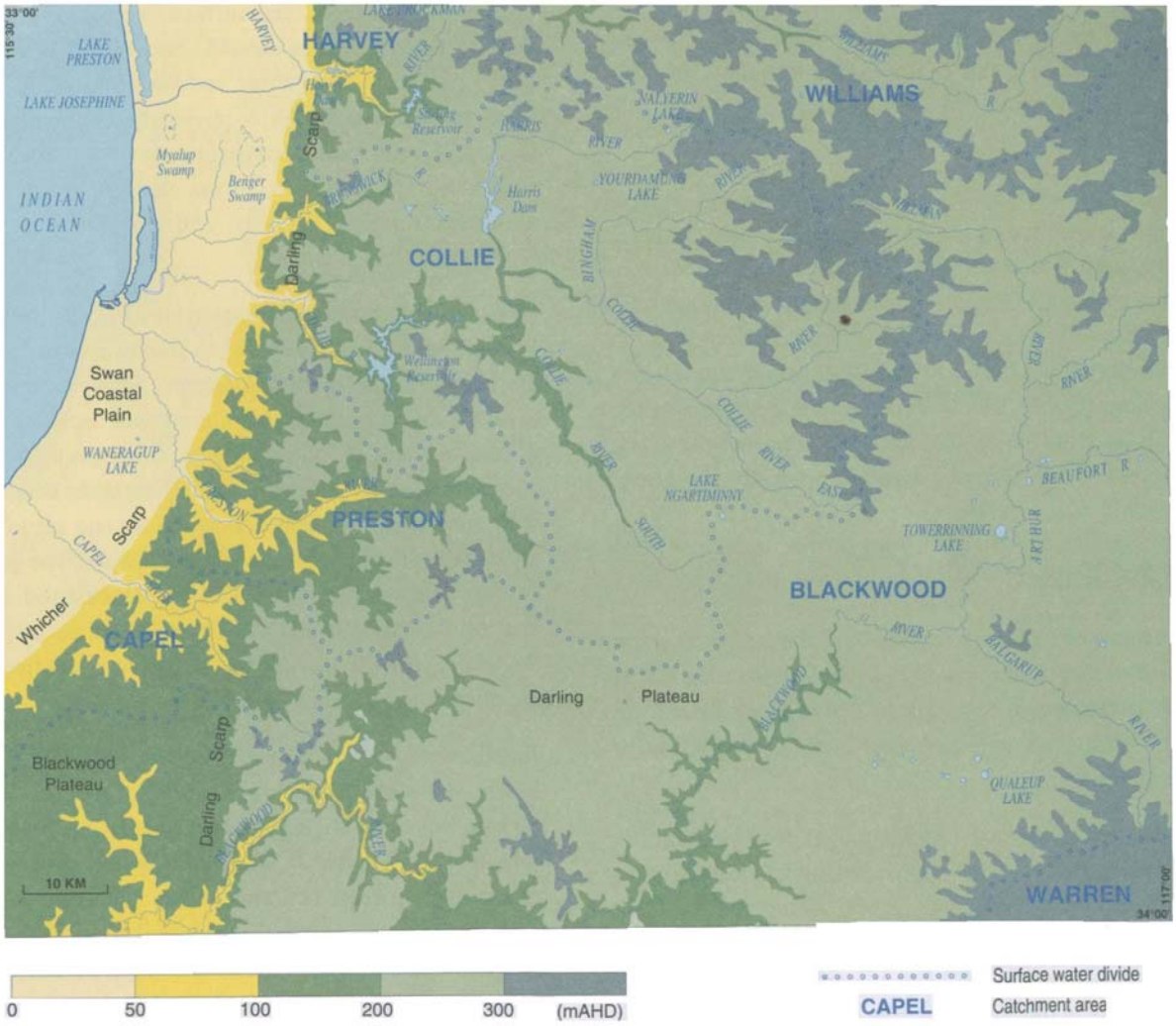

Appendix 3: Vegetation

Darling Plateau

Uplands

Cooke (Ce)
Mosaic of open forest of *Eucalyptus marginata* subsp. *marginata-Corymbia calophylla* (subhumid zone) and open forest of *Eucalyptus marginata* subsp*. thalasssica-Corymbia calophylla* (semi arid and arid zones) and on deeper soils adjacent to outcrops, closed heath of Myrtaceae-Proteaceae species and lithic complex on granite rocks and associated soils in all climate zones, with some *Eucalyptus laeliae* (semi arid), and *Allocasuarina huegeliana* and *Eucalyptus wandoo* (mainly semi arid to perarid zones)

Dwellingup (D1)
Open forest of *Eucalyptus marginata* subsp. *marginata-Corymbia calophylla* on lateritic uplands in mainly humid and subhumid zones.

Dwellingup 2 (D2)
Open forest *of Eucalyptus marginata* subsp. *marginata-Corymbia calophylla* on lateritic uplands in subhumid and semi-arid zones.

Dwellingup 4 (D4)
Open forest to woodland of *Eucalyptus marginata* subsp. *thalassica -Corymbia calophylla* on lateritic uplands in semi-arid and arid zones.

Hester (HR)
Tall open forest to open forest of *Eucalyptus marginata* subsp. *marginata-Corymbia calophylla* on lateritic uplands in perhumid and humid zones

Yalanbee (Y5)
Mixture of open forest of *Eucalyptus marginata* subsp. *thalasssica- Corymbia calophylla* and woodland of *Eucalyptus wandoo* on lateritic uplands in semi-arid to perarid zones.

Mornington (MH)
Open forest to woodland of *Eucalyptus wandoo- Eucalyptus marginata* subsp. *marginata-Corymbia calophylla* on lateritic uplands in the semi-arid zone.

Sandalwood (SD)
Woodland of *Eucalyptus marginata* subsp. *marginata* with some *Corymbia calophylla* and *Eucalyptus wandoo* over *Hakea prostrata* and *Dryandra sessilis* on uplands in semi-arid and arid zones.

Wilga (WG)
Woodland of *Eucalyptus marginata* subsp. *marginata-Corymbia calophylla* on sandy gravels on low divides in the subhumid zone.

Kulikup 2 (KU2)
Open forest of *Eucalyptus marginata* subsp. *marginata-Corymbia calophylla* with some *Eucalyptus wandoo* and occasional *Eucalyptus astringens* fs 24 (near breakaways) over *Acacia microbotrya* on undulating uplands in the semi-arid zone.

Depressions and Swamps on Uplands

Goonaping (G)
Mosaic of open forest of *Eucalyptus marginata* subsp. *marginata* (humid zones) and *Eucalyptus marginata* subsp. *thalassica* (semi-arid to perarid zones) on the sandy-gravels, low woodland of *Banksia attenuata* on the drier sandier sites (humid to perarid zones) with some *Banksia menziesii* (northern arid and perarid zones) and low open woodland of *Melaleuca preissiana-Banksiaa littoralis* on the moister sandy soils (humid to perarid zones).

Swamp (S)
Mosaic of low open woodland of *Melaleuca preissiana-Banksia littoralis*, closed scrub of Myrtaceae spp., closed heath of Myrtaceae spp. and sedgelands of *Baumea* and *Leptocarpus* spp. On seasonally wet or moist sand, peat and clay soils on valley floors in all climatic zones.

Qualeup (QUw)
Woodland of *Eucalyptus marginata* subsp. *marginata-Corymbia calophylla* on drier soils ranging to woodland of *Eucalyptus rudis-5Melaleuca* rhaphiophylla and low woodland of *Melaleuca preissiana-Banksia littoralis* on lower slopes in the semi-arid zone.

Stockton (SK)
Woodland of *Eucalyptus marginata* subsp. *marginata Nuytsia floribunda-Banksia* spp. With tall shrublands of Melaleuca spp. and occasional *Eucalyptus rudis* on upland depressions.

Valleys

Balingup (BL)
Woodland of *Eucalyptus marginata* subsp. *marginata-Corymbia calophylla* on slopes and woodland of Eucalyptus rudis on the valley floor in the humid zone.

Murray 1 (My1)
Open forest of *Eucalyptus marginata* subsp. *marginata-Corymbia calophylla-Eucalyptus patens* on valley slopes to woodland of fs24 *Eucalyptus rudis-Melaleuca rhaphiophylla* on the valley floors in humid and subhumid zones.

Murray 2 (My2)
Open forest of *Eucalyptus marginata* subsp. *thalassica-Corymbia calophylla*-Eucalyptus *patens* and woodland of *Eucalyptus wandoo* with some *Eucalyptus accedens* on valley slopes to woodland of *Eucalyptus rudis-Melaleuca rhaphiophylla* on the valley floors in semi-arid and arid zones.

Catterick (CC1)
Open forest of *Eucalyptus marginata* subsp. *marginata-Corymbia calophylla* mixed with *Eucalyptus patens* on slopes, *Eucalyptus rudis* and *Banksia littoralis* on valley floors in the humid zone.

Yarragil (Yg1)
Open forest of *Eucalyptus marginata* subsp. *marginata-Corymbia calophylla* on slopes with mixtures of *Eucalyptus patens* and *Eucalyptus megacarpa* on the valley floors in humid and subhumid zones.

Yarragil 2 (Yg2)
Open forest of Eucalyptus *marginata* subsp. -*thalaissica Corymbia calophylla* on slopes, woodland of *Eucalyptus patens-Eucalyptus rudis* with *Hakea prostrata* and *Melaleuca viminea*.

Pindalup (Pn)
Open forest of *Eucalyptus marginata* subsp. *marginata-Corymbia calophylla* on slopes and open woodland of *Eucalyptus wandoo* with some *Eucalyptus patens* on the lower slopes in semi-arid and arid zones.

Lukin 2 (LK2)
Woodland of *Eucalyptus wandoo* with some mixtures of *Eucalyptus marginata* subsp. *thalassica* and -*Corymbia calophylla* on the valley slopes with occasional *Eucalyptus rudis* on valley floors on semi-arid and arid zones.

Darkin 2 (Dk2)
Mixture of open woodland of *Eucalyptus marginata* subsp. *Marginata-Banksia attenuata* and low open woodland of *Eucalyptus wandoo* and stand of *Eucalyptus drummondii* (northern) and *Eucalyptus decipiens* (southern) on lower slopes in the arid zone.

Darkin 3 (Dk3)
Open woodland of *Allocasuarina huegeliana-Acacia* acuminata with occasional *Eucalyptus rudis* and *Eucalyptus wandoo* on variable slopes near granite outcrops and woodland of *Eucalyptus astringens-Eucalyptus wandoo* on breakaways in the arid zone.

Valley floors and swamps

Collie plain

Uplands

Collie (CI)
Open forest of Eucalyptus marginata subsp. Marginata-Corymbia calophylla-Allocasuarina fraseriana on gravely-sandy upland soils in the subhumid zone.

Cardiff (CF)
Open woodland of *Allocasuarina fraseriana-Banksia* spp. *Xylomelum occidentale-Nuytsia floribunda* on sandy soils on valley slopes in the subhumid zone.

Depressions and swamps

Muja (MJ)
Open woodland of *Melaleuca preissiana-Banksia littoralis-Banksia ilicifolia* with some *Eucalyptus patens* on moister sites, *s24 Banksia* spp. On drier sites of valley floors in the subhumid zone

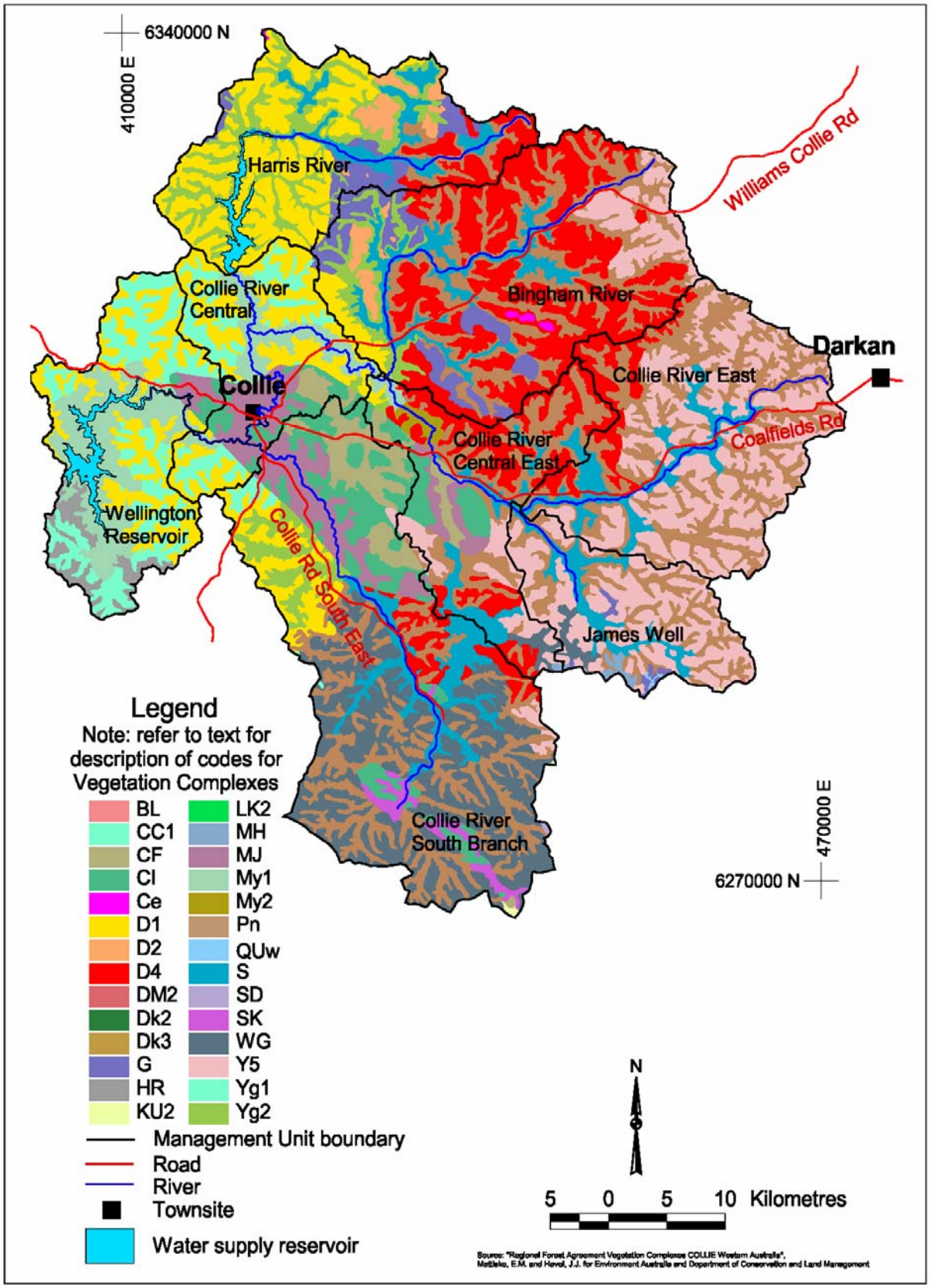
6340000 N
410000 E
Harris River
Williams Collie Rd
Collie River Central
Bingham River
Darkan
Collie
Collie River East
Coalfields Rd
Collie River Central East
Wellington Reservoir
Collie Rd South East
James Well
Collie River South Branch
470000 E
6270000 N
Legend
Note: refer to text for description of codes for Vegetation Complexes
BL
CC1
CF
CI
Ce
D1
D2
D4
DM2
Dk2
Dk3
G
HR
KU2
LK2
MH
MJ
My1
My2
Pn
QUw
S
SD
SK
WG
Y5
Yg1
Yg2
Management Unit boundary
Road
River
Townsite
Water supply reservoir
N
5 0 5 10 Kilometres
Source: "Regional Forest Agreement Vegetation Complexes COLLIE Western Australia", Mattiske, E.M. and Havel, J.J. for Environment Australia and Department of Conservation and Land Management

Appendix 4: Geological map of the Collie river Basin

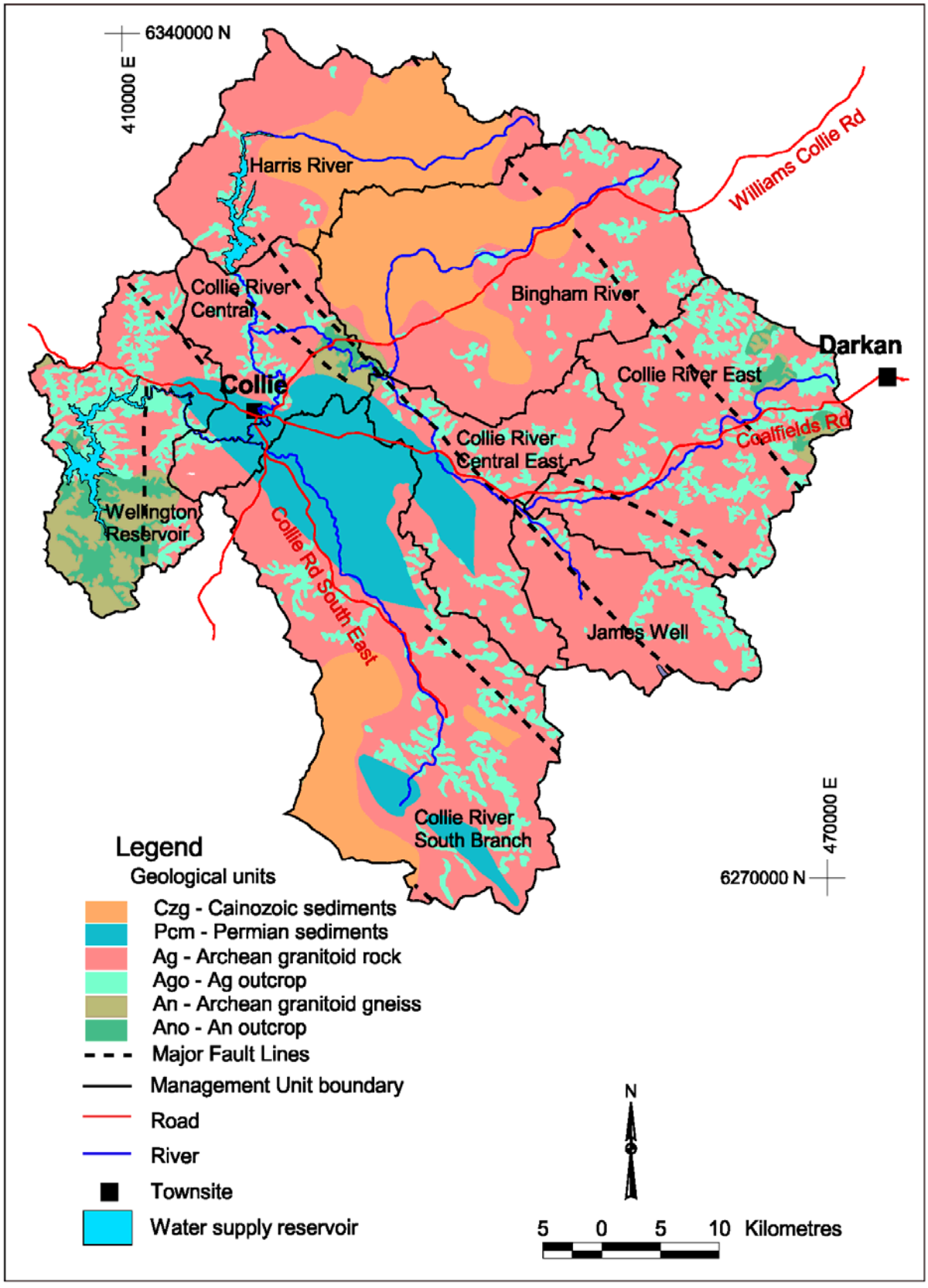

Appendix 5: Soil-Landscape systems

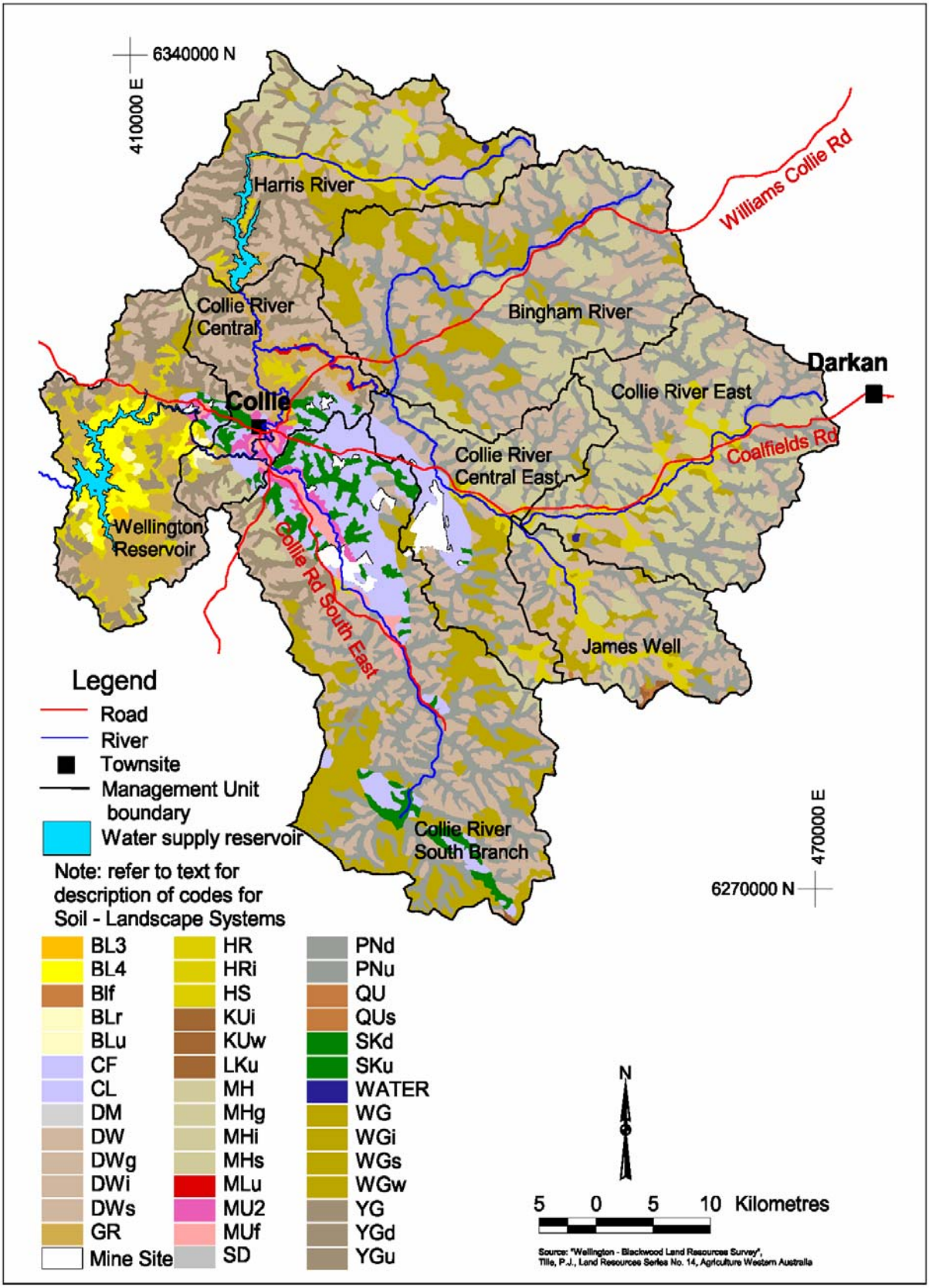
6340000 N
410000 E
Harris River
Williams Collie Rd
Collie River Central
Bingham River
Darkan
Collie
Collie River East
Coalfields Rd
Collie River Central East
Wellington Reservoir
Collie Rd South East
James Well
Collie River South Branch
470000 E
6270000 N
Legend
Road
River
Townsite
Management Unit boundary
Water supply reservoir
Note: refer to text for description of codes for Soil - Landscape Systems
BL3
BL4
Blf
BLr
BLu
CF
CL
DM
DW
DWg
DWi
DWs
GR
Mine Site
HR
HRi
HS
KUi
KUw
LKu
MH
MHg
MHi
MHs
MLu
MU2
MUf
SD
PNd
PNu
QU
QUs
SKd
SKu
WATER
WG
WGi
WGs
WGw
YG
YGd
YGu
N
5 0 5 10 Kilometres
Source: "Wellington - Blackwood Land Resources Survey", Tille, P.J., Land Resources Series No. 14, Agriculture Western Australia

Appendix 6: Location and details of the gauge stations

Streamflow

station #	stn type	river	official station name	lat (°S)	long (°E)	catch. area	opened	closed	owner	division	basin	district
612001	Rv	Collieeast Trib	Coolangatta Farm	33.332	116.262	1340	1968		WRC (WA)	6	612	9A
612002	Rv	Collie	Mungalup Tower	33.372	116.097	2550	1969		WRC (WA)	6	612	9A
612007	Rv	Binghamtrib	Dons Catchment	33.28	116.472	4	1973		WRC (WA)	6	612	9A
612008	Rv	Binghamtrib	Ernies Catchment	33.295	116.443	3	1973		WRC (WA)	6	612	9A
612009	Rv	Pollard Brook Tr	Lemon Catchment	33.297	116.405	3	1972		WRC (WA)	6	612	9A
612014	Rv	Bingham	Palmer	33.278	116.273	392	1975		WRC (WA)	6	612	9A
612016	Rv	Batalling Ck	Maxon Farm	33.317	116.573	17	1976		WRC (WA)	6	612	9A
612017	Rv	Harris	Tallanalla Rd	33.29	116.155	382	1976	1993	WRC (WA)	6	612	9A
612021	Rv	Bingham	Stenwood	33.197	116.468	50	1978		WRC (WA)	6	612	9A
612025	Rv	Camballan Ck	James Well	33.457	116.425	175	1982		WRC (WA)	6	612	9A
612026	Rv	Mairdebing Ck	Maringee	33.518	116.535	13	1982		WRC (WA)	6	612	9A
612027	Rv	Hansons Brook	Riverbend	33.283	116.158	8	1983	1987	WRC (WA)	6	612	9A
612028	Rv	Harristrib	Scar Rd	33.258	116.135	15	1983	1987	WRC (WA)	6	612	9A
612029	Rv	Harristrib	Norm Rd	33.263	116.148	21	1983	1987	WRC (WA)	6	612	9A
612034	Rv	Collie	South Branch	33.388	116.162	668	1952		WRC (WA)	6	612	9A
612230	Rv	Collieeast Trib	James Crossing	33.383	116.58	169	1966		WRC (WA)	6	612	9A

Rainfall

station #	stn type	official station name	lat (°S)	long (°E)	obs interval	opened	closed	owner	division	basin	district
509079	Rn	Harris R @ Nalyerin Lake	33.157	116.344	Continuous	01-Jul-65	06-Apr-00	WRC (WA)	6	612	9A
509081	Rn	Harris R @ Balinghalls Farm	33.226	116.155	Continuous	01-Jul-65		WRC (WA)	6	612	9A
509082	Rn	Harris R @ Sandy Rd	33.103	116.184	Continuous	01-Jul-65		WRC (WA)	6	612	9A
509108	Rn	Collie R East Branch @ James Crossing	33.379	116.576	Continuous	01-Jun-72		WRC (WA)	6	612	9A
509109	Rn	Hamilton R @ Worsley	33.309	116.048	Continuous	01-May-72		WRC (WA)	6	612	9A
509247	Rn	Salmon Brook @ Salmon Catchment	33.416	115.984	Continuous	18-Oct-73	17-Mar-99	WRC (WA)	6	612	9A
509248	Rn	Bingham R Trib @ Dons Catchment	33.279	116.471	Continuous	16-Oct-73		WRC (WA)	6	612	9A
509249	Rn	Bingham R Trib @ Ernies Catchment	33.292	116.445	Continuous	01-May-74		WRC (WA)	6	612	9A
509309	Rn	Bingham R @ Palmer	33.276	116.275	Continuous	01-Apr-75		WRC (WA)	6	612	9A
509321	Rn	Batalling Ck @ Maxon Farm	33.315	116.574	Continuous	01-Feb-76		WRC (WA)	6	612	9A
509374	Rn	Bingham R @ Stenwood Transect	33.187	116.494	Continuous	04-May-79	03-Feb-99	WRC (WA)	6	612	9A
509376	Rn	Collie South Catch. @ Argo Farm	33.661	116.381	Continuous	17-Feb-78	01-Feb-99	WRC (WA)	6	612	9A
509392	Rn	Harris R @ Tallanalla Rd	33.288	116.152	Continuous	12-Jul-79	13-Jan-93	WRC (WA)	6	612	9A
509407	Rn	Mairdebing Ck @ Mardi	33.503	116.565	Continuous	23-Dec-82	01-Feb-99	WRC (WA)	6	612	9A
509408	Rn	Camballin Ck @ James Well	33.456	116.426	Continuous	11-Jun-82		WRC (WA)	6	612	9A
509409	Rn	Mairdebing Ck @ Maringee	33.517	116.536	Continuous	19-May-82	25-Mar-99	WRC (WA)	6	612	9A

Collie Catchment

NRM & SALINITY DIVISION

LOCALITY MAP

LEGEND

- Collie_cat_ll.shp
- Collie_mask.shp

Towns

- S Major Town/City (>5000)
- s Town (>500)
- s Minor Town (<500)
- % WIN Meteorological Sites (DEWCP)
- & WIN Surface Water Sites - Stream Gauging (non DEWCP)
- % Bom met site.shp
- # WIN Surface Water Sites - Stream Gauging (DEWCP)
- Rivers 250K, GA
- Hydrographic Catchments - Subcatchments
- Topo 250K, Lakes

N

4 0 4 8 Kilometres

Projection information

Vertical Datum: Australian Height Datum (AHD)
Horizontal Datum: Geodetic Datum of Australia (GDA 94)

Requestee: Ellen Tromp
Map Author: Artemis Kitsios
Date: 22/04/05

SOURCES

WRC acknowledges the following datasets and their Custodians in the production of this map:

Dataset Name - CUSTODIAN ACRONYM - Metadata Date

509082
509079
509374
612021
509081
612028
612029
509309
612014
612027
612017
509248
612007
509249
612009
612008
509109
612001
ALLANSON
COLLIE
612002
612034
509247
612025
509408
612026
509376

Appendix 7: Precipitation

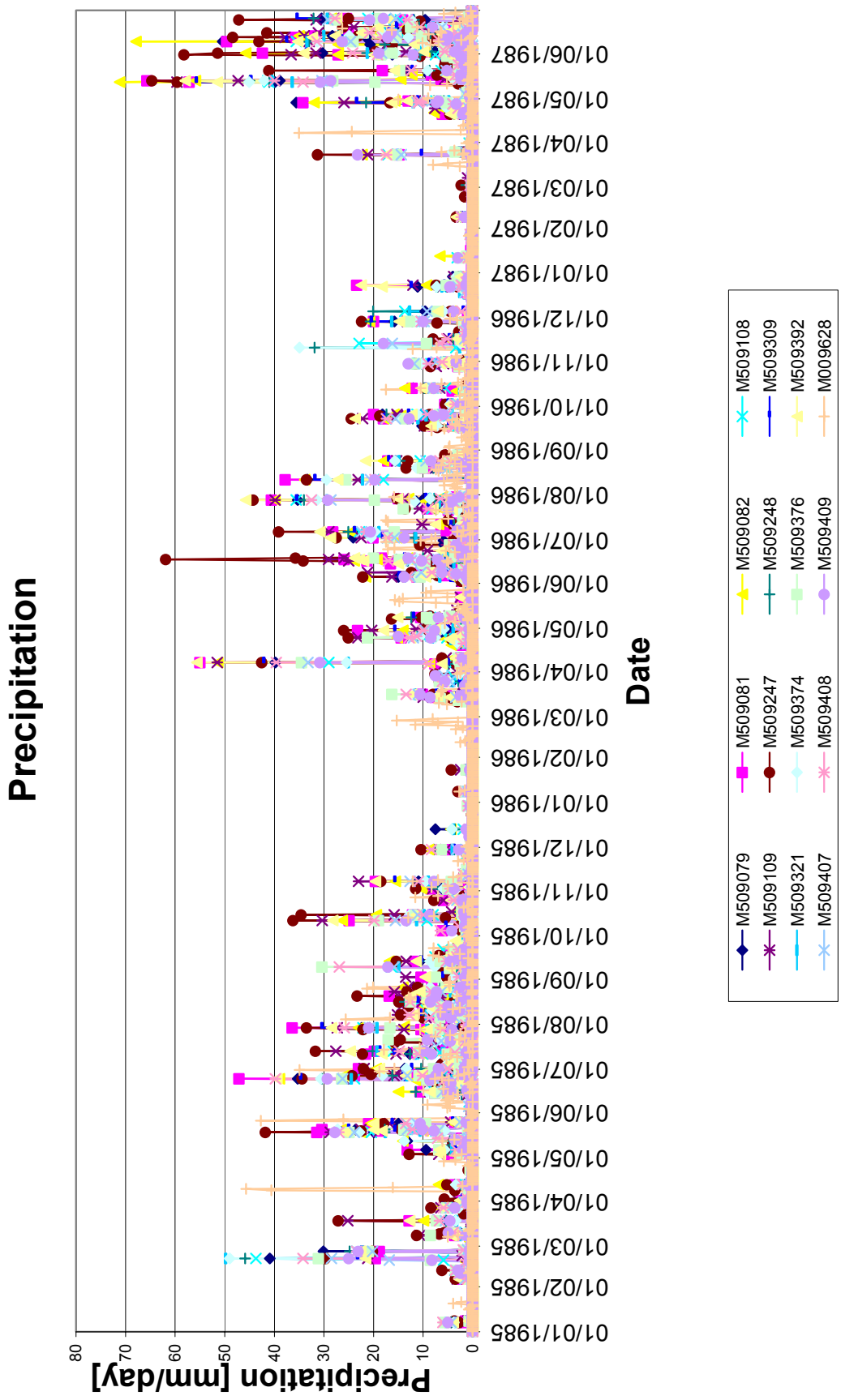

Appendix 8: Cumulative Precipitation

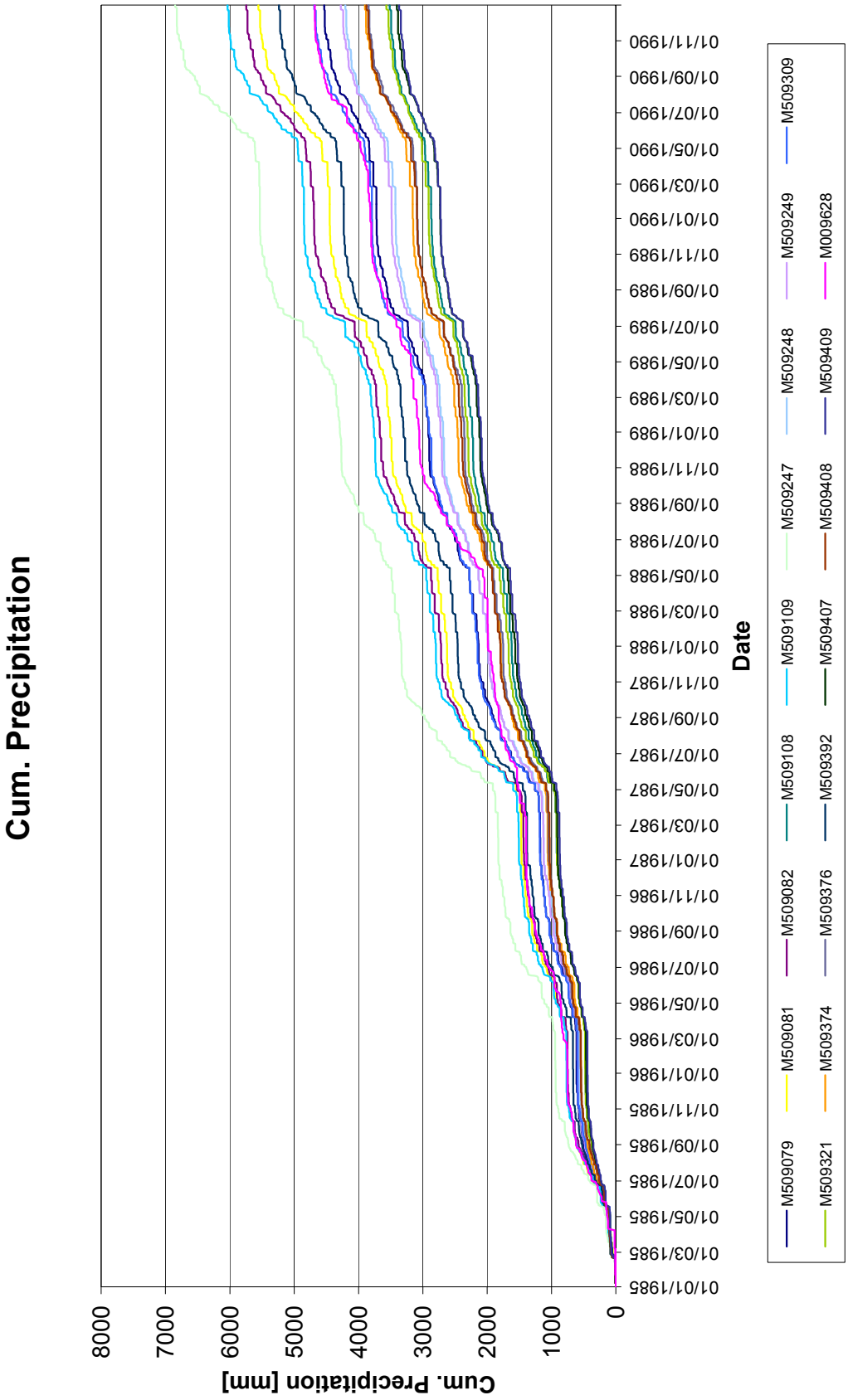

Appendix 9: Runoff in years between 3 stations

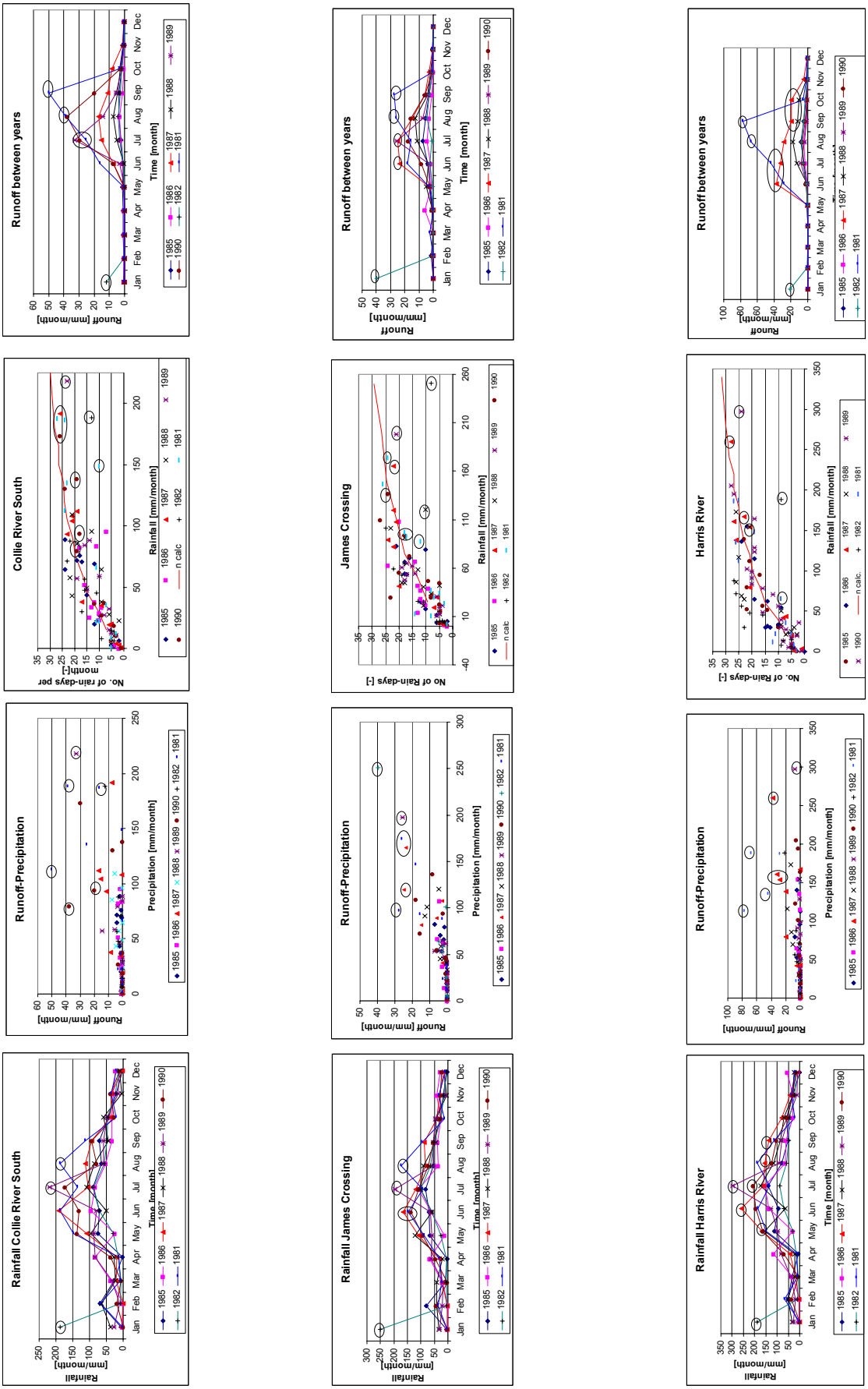

Appendix 10: Input data REW modelling

GENERAL_INFO.inp

1000.0d0	!slfactor : scaling factor for length unit conversion, if input info. is based on [mm], then slfactor=1000.0 as the code uses [m] as length scale.
1.0d0	!x1 : 1.0<=x1<x2, indicative value as simulation starting point calculated from 1.0 as that of the first data in data sequence
730.0d0	!x2 : x1<x2<=ndata, x2=the end of simulation we are planning + 1 ; indicative value of simulation ending point
0.000001d0	!eps : desired accuracy=eps*yscal(i)(16.2.8) p.711 at Numerical Recipes in Fortran, W.H.Press.
1.00E-13	!hmin [sec] : 0<=hmin<=h1<=hmax<=datah; minimum allowed step size, if the next step size is less than hmin, then program will inform the modeller of this. hmin can be zero p.714, we suggest hmin <0.001 [sec]
86400.0d0 10.0d0 86400.0d0	!hmax [sec] : 0<=hmin<=h1<=hmax<=datah; hmax is related to the frequency of output, water balance calculation; we suggest hmax=1.0d0 [sec] or hmax=datah [sec] !h1 [sec] : 0<=hmin<=h1<=hmax<=datah; initial step size !datah [sec] : 0<=hmin<=h1<=hmax<=datah; data time scale; for example, hourly or 10 min measured data has 3600.0 or 600.0 as datah value respectively
2	!ipopt : Print out option; 0 for simplified output; 1 for detailed output; 2 for fastest mode (for manual calibration), when ipopt=2, we only get SV1.OUT & WB1.OUT and other SV*.OUT & WB*.OUT file will not be printed out but all other output file will be updated; otherwise, no print results out
1	!ipop2 : ipop2>0; Print out time interval, for example, if ipop=1 (or 2) then simulation results at each time step (=data time scale) (every 2nd step like 0,2,4,6,...) is printed out; only if ipopt=0 or 2 then ipop2 works.; First(=initial conditions) and last step results are always printed out.
1	!ipop3 : ID of REW whose water balance calculation & derivatives are printed out for examination purpose ; Print out option; if ipopt=0, 1, or 2 then this print option works. otherwise this has no effect to anything
1	!nvopt : 1 for simplified (kinematic for overland flow & diffusion wave for channel flow) momentum balance equations; others for dynamic momentum balance equations
0	!ihopt : 1 for constant step size; others for adaptive stepsize control
60.0d0	!hcon [sec] : constant step size; if ihopt is 1, hcon is activated, if not, useless; dmod(datah,hcon)=0.0d0
1	!iropt : 1 for adopting heterogeneous rainfall field from "REpQ.INP" file; if iropt=1, "REpQ.INP" should define separate rainfall input for each REW in order of REW ID. Data sequence will be: rainfall input for 1st REW, 2nd REW, ..., Ep(Potential evaporation), Qobs(Observed streamflow); if iropt.ne.1, then data sequence will be: one rainfall input for all REWs, Ep(Potential evaporation), Qobs(Observed streamflow)
11	!iglobe : 1 for adopting GLOBE parameter optimization routine; this works only when you have GLOBE program in your computer;if you don't have GLOBE in your computer, do not set 1 as iglobe value;To install GLOBE, use any portal website and search GLOBE by keywords, GLOBE & Solomatine ; others for manual calibration
0	!maxMC : the number of Monte Carlo run; this works only if iglobe=2; Seeding value for random number generator(IDUM) can be found in CREW_MCS.INP file; IDUM is seeding value for random number generator; this works only if iglobe=2 in "GENERAL_INFO.INP" file; see p.271-272 in Numerical Recipes in Fortran 2nd Ed. for the details

GEOINFO5.inp

1	!nsame : 1 for using same values across REWs, others for using different valued at each REW; if nsame is not 1, then you should specify each value of deg_c in order of REW number you specified.
5.0d0	!deg_c(nREWs) : C-zone slope in degree
1	!nsame : for deg_o
5.0d0	!deg_o(nREWs) : O-zone slope in degree
1	!nsame : for deg_r
10.0d0	!deg_r(nREWs) : R-zone slope in degree
0	!nsame : for rlength, 1 for using artificial catchment.
8000.0d0	!rlength(1)[m] : Channel length
50000.0d0	!rlength(2)[m] : Channel length
45000.0d0	!rlength(3)[m] : Channel length
45000.0d0	!rlength(4)[m] : Channel length
55000.0d0	!rlength(5)[m] : Channel length
0	!nsame : for sigma
30830000.0d0	!sigma(1) [m**2]: Projected catchment area to horizontal plane
673180000.0d0	!sigma(2) [m**2]: Projected catchment area to horizontal plane
513350000.0d0	!sigma(3) [m**2]: Projected catchment area to horizontal plane
499180000.0d0	!sigma(4) [m**2]: Projected catchment area to horizontal plane
811460000.0d0	!sigma(5) [m**2]: Projected catchment area to horizontal plane
1	!nsame
225.0d0	!zr(nREWs) [m] : Elevation of channel bed from datum
1	!nsame
221.5d0	!zs(nREWs) [m] : Elevation of S-zone bed from datum; zs<zr
0	!nsame
6.0d0	!Ztotal(1) [m] : Total soil depth; Ztotal>zr-zs; Ztotal=ys+yu*wu
5.0d0	!Ztotal(2) [m] : Total soil depth; Ztotal>zr-zs; Ztotal=ys+yu*wu
5.0d0	!Ztotal(3) [m] : Total soil depth; Ztotal>zr-zs; Ztotal=ys+yu*wu
5.5d0	!Ztotal(4) [m] : Total soil depth; Ztotal>zr-zs; Ztotal=ys+yu*wu
5.5d0	!Ztotal(5) [m] : Total soil depth; Ztotal>zr-zs; Ztotal=ys+yu*wu

Continuation of *GEOINFO5.inp*

```
**********************************************************************************************************************
ir    iso(nREWs)iur(nREWs,1)iur(nREWs,2)idr(nREWs)   cosdel(nREWs,1)   cosdel(nREWs,2) cosdel(nREWs,3)     ca(nREWs)
**********************************************************************************************************************
1     -2        3        2        0        40.0d0          35.0d0         0.0d0        2528000000.0d0
 2     1        0        0        1         0.0d0          0.0d0         35.0d0        673180000.0d0
 3     2        4        5        1        15.0d0          5.0d0         40.0d0        1823990000.0d0
4      1        0        0        3         0.0d0          0.0d0         10.0d0        499180000.0d0
5      1        0        0        3         0.0d0          0.0d0          5.0d0        811460000.0d0
**********************************************************************************************************************
explanation on the variables:
ir              : integer, ID of REW user specified, The order of REW ID is affected from e_rinlet calculation
iso(nREWs)      : integer, Horton stream order to each REW, (-) sign is assigned to the REW located at the watershed outlet
iur(nREWs,1)    : integer, ID of upstream REW connected through channel reach exchanging mass and momentum.     0 if iso()=1
iur(nREWs,2)    : integer, ID of the other connected upstream REW though channel reach.    0 if iso()=1
idr(nREWs)      : integer, ID of the REW connected to current REW though downstream of current one. 0 if iso()<0
cosdel(nREWs,1) : doubleprecision, the angle between channel reach of current REW and the REW has ID of iur(nREWs,1) at the channel joint
                  Unit is degree, 0 if iso()=1
cosdel(nREWs,2) : doubleprecision, the angle between channel reach of current REW and the REW has ID of iur(nREWs,2) at the channel joint
                  Unit is degree, 0 if iso()=2
cosdel(nREWs,3) : doubleprecision, the angle between channel reach of current REW and the REW has ID of idr(nREWs) at the channel joint
                   Unit is degree, 0 if iso()<0
ca(nREWs)       : doubleprecision, Upper located part of the catchment area based on the outlet of the REW under consideration.
                  Unit is [m**2], sigma(1)=ca(1)
```

INITIAL_STATES.inp

1 0.0d0	!nsame ! yc(nREWs) [m] ; average thickness of C-zone
1 0.0d0	!nsame ! vc(nREWs) [m/sec] ; flow velocity at C-zone
1 2.0d0	!nsame ! yo(nREWs) [m] ; average thickness of O-zone
1 0.00001d0	!nsame ! vo(nREWs) [m/sec] ; flow velocity at O-zone
1 5.79E-12	!nsame !0.005[mm/day]= 5.7870E-12 [m/sec]! qbsteady(nREWs) [m/sec] ; steady outflow from S-zone to R-zone
1 2.32E-02	!nsame !zmr(nREWs) [m**2] ; flow cross sectional area in R-zone
1 3.70E+00	!nsame ! vr(nREWs) [m/sec] ; flow velocity at R-zone
1 0.11d0	!nsame ! su(nREWs) [-] ; saturation degree at U-zone
1 3.5d0	!nsame ! ys(nREWs) [m] ; average thickness of S-zone; ys<Ztotal; suggested value of ys(nREWs,t=0)=zr(nREWs)-zs(nREWs)+small value

PARAMETERS.inp

1 1.0216d0	!nsame ; 1 for using same values across REWs, others for using different values at each REW; if nsame is not 1, then you should specify each value of alpha_su in order of REW number you specified. ! [1]alpha_su(nREWs) ; Recharge & Capillary rise process; 1.0 for Darcy type flux
1 0.009d0	!nsame ! [2]alpha1_os(nREWs) ; Seepage flow; related to recession scaling
1 1.0d0	!nsame ! [3]alpha2_os(nREWs) ; Seepage flow; related to recession scaling; bigger alpha2_os value induces generally smaller seepage flow as satk<1.0; very sensitive parameter
1 6.0d0	!nsame ! [4]alpha3_os(nREWs) ; Seepage flow; related to total hydrograph shape ; bigger alpha3_os value induces generally bigger seepage flow
1 0.0006d0	!nsame ! [5]alpha_uc(nREWs) ; Infiltration; bigger alpha_uc value induces higher infiltrtion rate, which in turn decreases peak discharge
1 50.0d0	!nsame ! [6]alpha_uwg(nREWs) ; Evapotranspiration; bigger alpha_uwg value induces higher exfiltration at inter-storm period and higher infiltration at the following storm period followed by lower peak discharge

Continuation of *PARAMETERS.inp*

1 2.0d0	!nsame ! [7]alpha_oc(nREWs) ; Concentrated overland flow; bigger alpha_oc value induces higher peak discharge and steeper recession hydrograph
1 1.0d0	!nsame ! [8]alpha_ro(nREWs) ; Saturated overland flow; bigger alpha_ro value induces higher peak discharge and steeper recession hydrograph
1 0.05d0	!nsame ! [9]beta1_wo(nREWs) ; Saturated surface area; wo=f[ys]
1 0.3d0	!nsame ! [10]beta2_wo(nREWs) ; Saturated surface area; wo=f[ys]
1 0.4d0	!nsame ! [11]beta3_wo(nREWs) ; Saturated surface area; wo=f[ys]
1 0.0000347d0 1 0.0000347d0	!nsame ! [12]beta1_K_U(nREWs) ; U-zone sat. hyd. conductivity [m/sec] !nsame ! [13]beta1_K_S(nREWs) ; S-zone sat. hyd. conductivity [m/sec]
1 3.6d0	!nsame ! [14]beta2_K_U(nREWs) ; U-zone pore disconnectedness index
1 1.2d0	!nsame ! [15]beta1_euwg(nREWs) ; =kv=E[epv]/E[ep]; Vegetation effect cf)LAI
1 3.3d0	!nsame ! [16]beta3_euwg(nREWs); Pore size distribution index; bigger beta3_euwg value induces higher recharge rate; 1.2, 3.3 and 5.4 for SiltyLoam, SandyLoam and Sand respectively
1 0.35d0	!nsame ! [17]beta1_PSI(nREWs) ; Bubbling pressure head [m]; small value of beta1_PSI induces higher recharge rate
1 0.7d0	!nsame ! [18]VegeDensity(nREWs); Canopy density
1 0.4d0	!nsame ! [19]porosity_U(nREWs) ; U-zone porosity; porosity_U is equal to or greater than porosity_S
1 0.4d0	!nsame ! [20]porosity_S(nREWs) ; S-zone porosity
1 0.030d0	!nsame ! [21]czn(nREWs) ; Manning roughness coefficient at C-zone [sec*m**(-1/3)]
1 0.015d0	!nsame ! [22]ozn(nREWs) ; Manning roughness coefficient at O-zone [sec*m**(-1/3)]
1 0.015d0	!nsame ! [23]rzn(nREWs) ; Manning roughness coefficient at R-zone [sec*m**(-1/3)]

Geometric Information REW's

1 REW

# REW	Surface area [km^2]	Strahler order	Length Channel [km]	Cum surface area [km^2]
1	2528	1	213	2528

5 REWs

# REW	Surface area [km^2]	Strahler order	Length Channel [km]	Cum surface area [km^2]
1	30.83	3	8	2528
2	673.18	2	50	673.18
3	513.35	1	45	1823.99
4	499.18	1	45	499.18
5	811.46	1	55	811.46

27 REW's

# REW	Surface area [km^2]	Strahler order	Length Channel [km]	Cum surface area [km^2]
1	30.82	3	3	2528
2	76.32	3	7	1704.07
3	379.27	1	34	379.27
4	44.58	3	12	1324.8
5	11.04	2	3	513.35
6	2.31	2	3	407.24
7	33.55	1	6	33.55
8	95.07	1	7	95.07
9	249.20	2	20	371.38
10	34.85	1	5	34.85
11	87.33	1	5	87.33
12	52.11	2	11	811.45
13	100.46	1	12	100.46
14	26.73	2	5	658.88
15	63.60	1	8	63.60
16	5.04	2	1.5	568.55
17	163.74	1	8	163.74
18	41.50	2	4	399.77
19	60.83	1	8	60.83
20	133.12	2	7	297.44
21	86.23	1	4	86.23
22	78.09	1	4	78.09
23	37.22	2	3	673.19
24	60.73	1	5	60.73
25	324.12	2	21	575.24
26	64.57	1	5	64.57
27	186.55	1	8	186.55

Appendix 11: Users Manual PCRaster/Matlab for developing heterogeneous precipitation field

Simulating environmental processes with computer models is expanding rapidly in scientific and applied research in fields such as hydrology, ecology, process geomorphology, land degradation and crop yield studies. Computer models help us to understand better the characteristics of environmental processes and the impact of any changes made to them. Building environmental computer models is difficult because these models must describe both the space and time variation of natural phenomena and must be able to handle huge amounts of environmental data. PCRaster is a system that combines environmental modelling and GIS. It offers a powerful Dynamic Modelling language for building iterative spatio-temporal environmental models, which is fully integrated in the GIS.

PCRaster; general info

The PCRaster Environmental Modelling language is a computer language for construction of iterative spatio-temporal environmental models. It runs in the PCRaster interactive raster GIS environment that supports immediate pre- or post-modelling visualisation of spatio-temporal data.
The PCRaster Environmental Modelling language is a high level computer language: it uses spatio-temporal operators with intrinsic functionality especially meant for construction of spatio-temporal models. Compared with low level computer languages (e.g. C, Pascal) this has the advantage that models are programmed and structured according to the way of thinking applied in spatial-temporal sciences such as Geography or Geology. It allows researchers in these fields to construct models by themselves in a relatively short period of time, even when they do not have experience in programming.

Nutshell; general info

NutShell is a shell for the free GIS PCRaster environmental software package. Its function is to facilitate the running of PCRaster commands and edit and run PCRaster models (scripts). It uses the executables and help files in the PCRaster directory on your hard disk (or network). NutShell is made in the first place to facilitate teaching, but it may also come in handy on networks that do not allow writing to the windows registry database.
(Manual: *ftp://ftp.geog.uu.nl/pub/lisem/nutshell.pdf*)

Downloads

Both programs can be downloaded of the following website:
http://www.geog.uu.nl/lisem/body_download.html

User's Manual

1. Convert DEM to a map suitable for PCRaster

If a DEM is available of the selected basin, you should convert this into a *ASCII formatted Arc view met header* (e.g. in Arc view). Once this is done, it is fairly simple to convert it to a map that is suitable for PCRaster.

To convert the .asc from arc view to .map (suitable for PCRaster) use the following commands in NutShell:

1. First you have to make a clone.map in order to be able to make a .map file. You can create such a map by typing
   Mapatrr <name>.map
   Then you have to fill in information about your DEM, this information can be obtained by opening your DEM file in Notepad.

   Number of rows
   Number of columns
   Data type
   Cell presentation
   Projection
   X upperleftcorner
   Y upperleftcorner
   Cell length
   Angle
   File ID

   Hereafter you have to define the clone map, by stating the following command:
   pcroptions= --clone <name clone map>

2. After the making of the clone map has been completed, the DEM map can be transformed from a ASCII file to a file which is suitable for PCRaster, with the command:
   asc2map -a <name file DEM>.asc <new name of file>.map

2. Computing subcatchments REW

For computing the subcatchments (REW's) in a basin, a script (subcatch.mod) has been written which is based on Strahler order. (see Scripts) Make sure that the names of the maps are correct.(Ldd.map is the converted ASCII map to a PCRaster format) After checking this, the model can be run. PCRaster will make three maps, namely

Points.map This contains all the points that are used to make the subcatchments
Order.map Indicates the streams which are equal or larger as the chosen threshold value for Strahler.
Catch.map Indicates the defined REW's. (see Figure 1)

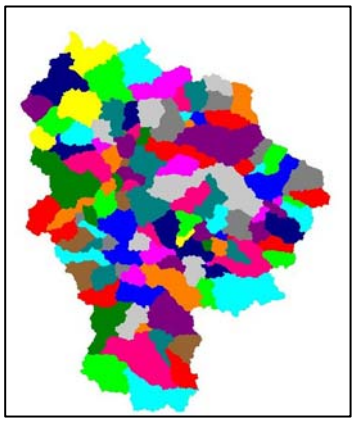

Figure 1 Example of catch.map

3. Calculation of the area of the REW's

In order to calculate the area of the in the previous step defined REW's, the following command can be given:

Pcrcalc result.map = areaarea(catch.map)

By opening the result.map the area of the REW's can be found.

4. Derivation of separate rainfall input files for each REW

For this derivation 2 programs have to be used, namely PCRaster and Matlab. We start by using PCRaster. Here the script named raininvdis.mod will be used (see Scripts). The interpolation technique that is used with this script is the inverse distance.

Before the script can be used, several files have to be made, namely:
mask = catdem1.map;
in the script for mask is used a map called Catdem1.map, this is a simple clone map with the precise no of rows, columns etcetera for the basin. It can of course have any name desired.

RainTimeSeries = rain197919801.tss
The rain timeseries is a file which contains the precipitation data for each station used. Column 1 gives the time steps, column 2 the data for station 1, column 3 the data for station 2 etcetera.
This file can be made with any text editor. However it is important that the type of file is a tss file. When saving the file, save it as a .tss and then PCRaster will have no problem reading the file.

stats = coordnom.map
This file contains the location of the various gauge stations. Nom stands for nominal, which means that the stations all have a number. With the following steps this file can be made.

1. Make a clone map, e.g. *Mapattr <name clone map>* (give the right number of rows, columns etc.
2. Define a clone map, by using the command: *pcroptions= -- clone <name clone map>*
3. Make a text file which contains location of the gauge stations, you can make for instance column 1: x-coordinate; column 2 y-coordinate. column 3: stationID (1 till n stations), (e.g. colfile.txt)
4. In order to make the coordnom.map the function col2map has been used.
   Col2map – clone <name clone map> -N –x 1 – y 2 colfile.txt Coordnom.map

Once the previous steps have been conducted, the script can be run. However, do check if the right end time is used. For each time step PCRaster will make a map with the areal rainfall. In order to get a table which will give the rainfall for each defined REW, we are now switching to Matlab. Note however that PCRaster should have finished calculating the maps for each time step.(see figure 2)

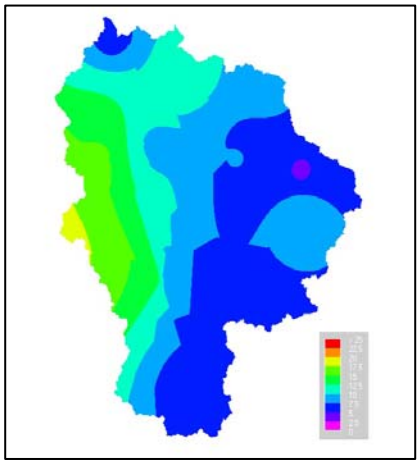

Figure 2 Example of the maps PCRaster makes for each time step, this one is for the Collie River Basin 26th of June 1980

With Matlab 2 scripts will be used, namely, Read_PCR.m and CreateTss.m (see Scripts))
Special attention should be paid to CreateTss.m because here the references to several files should be correct stated, as well as defining the right end time.
After running CreateTss.m, the rainfall for each REW can be found by opening RainTss, which is found under the workspace area in Matlab

Scripts

Subcatch.mod

```
#! --unitcell
# Compute subcatchments REW
# H.C.W. 01 - 1995
# Modified by E. Tromp april 2005

binding

# Ldd map
LddIn=ldd.map;


Catchments=catch.map;

# Order threshold. Every substream above this Strahler order will be assigned a REW
OrderThreshold= 8;

areamap

LddIn;

timer

1 1 1;

initial


Order=streamorder(LddIn);

        # Compute stream order

Temp1=if(Order ge OrderThreshold, Order);
LdTemp=lddmask(LddIn,boolean(Temp1));
Temp2=if(upstream(LdTemp,scalar(Temp1)) gt scalar(Temp1),boolean(1));
Temp2=if(downstream(LdTemp,scalar(Temp1)) gt scalar(Temp1),boolean(1), Temp2);
Points=nominal(uniqueid(Temp2));
basin1=subcatchment(LddIn,Points);


report points.map = Points;
report order.map  = Temp1;
report Catchments = subcatchment(LddIn,Points);
```

Raininvdis.mod

```
# model for simulation of rainfall
# model for calculation rainfall over Collie Catchment
# spatial differentiation for rainfall
# timestep of 1 day => modelling time two years
# H.C.W 1- 1995
# Modified by E. Tromp april 2005

binding
 mask          = catdem1.map;
 RainTimeSeries = rain197919801.tss;  # timeseries with rain at rainstations
 stats         = coordnom.map;          # reported stack of maps with rain
 prec          = rainfall;            # reported maps with rain (mm/24hours)
 precsum       = rainsums;


timer
 1 366 1;       #begintime endtime timestep

initial

 prectemp = 0;
 Rainsum = 0;
dynamic
 # calculate and report maps with rainfall at each timestep (mm/24 hours)

 Rainpoints = timeinputscalar(RainTimeSeries,stats);

 Interpolateresidue    = inversedistance(mask, Rainpoints, 2, 3500000, 6);
 report tss\Rainfall   = max(Interpolateresidue, 0);
```

Read_PCR.m

```
% Read_PCR.m V. 2, by H.C. Winsemius, M.Sc Civil Engineering
%
% Function for reading PCRaster .map files, including relevant information from the header.
% Information about the .map file format was taken from the CSF api document, which can be
% downloaded from http://www.pcraster.nl/
%
% Input is required from a higher order function or procedure in the form of a string, which denotes the
% file location. Output is given in the form of a matrix, representing the raw map, x axis and y axis,
% which start in the upper-left corner.
%
% Note: some header lines were skipped, because they usually do not contain relevant information.
%
% The function is tested for the following formats:
% - Scalar
% - Ldd
% - Nominal
% - Boolean
%
% Images can easily be plotted by typing the command 'imagesc(x, y, map)'
%
% Thanks to the PCRaster forum group for helping me out defining the relevant parts of the maps!! :-)
%
% Copyright TU Delft, January 2005
% More info: contact H.C. Winsemius +31(0)15-2784845 or
% h.c.winsemius@citg.tudelft.nl

% modified by E. Tromp, TU Delft, April 2005

function [x, y, map] = Read_PCR(input);
fid = fopen(input);
fread(fid,66);
maptype = fread(fid,1,'int16');
minval  = fread(fid,1,'int64');
maxval  = fread(fid,1,'int64');
xul = fread(fid,1,'real*8');
yul = fread(fid,1,'real*8');
nrrows = fread(fid,1,'uint');
nrcols = fread(fid,1,'uint');
cellx = fread(fid,1,'real*8');
celly = fread(fid,1,'real*8');
fread(fid,132);
if maptype == 0
   data   = fread(fid,nrrows*nrcols,'uint8');
   i = find(data == 255);
   data(i) = NaN;
elseif maptype == 38
   tmp   = fread(fid,nrrows*nrcols,'uint32=>uint8');
   data = double(tmp);
   i = find(data == 255);
   data(i) = NaN;
elseif maptype == 90
   data   = fread(fid,nrrows*nrcols,'real*4');
end

map    = reshape(data,nrcols,nrrows);
x      = xul + [0:nrcols]' * cellx;
y      = yul - [0:nrrows]' * celly;
fclose(fid);
```

CreateTss.m

```
% CreateTss.m
% Copyright TU Delft, January 2005
% More info: contact H.C. Winsemius +31(0)15-2784845 or
% h.c.winsemius@citg.tudelft.nl

% Modified by E.Tromp, TU Delft, MSc.student

% Procedure to make timeseries for specified sub-catchments.
%
% - Read delineated catchments from REW map. Every area is assigned a ID number
% - mask and lump for every time step rainfall and potential evaporation.
% - mask and lump GWSmax and Sumax
% - mask and lump initial conditions Su0 and GWS0

% filelocations input
clear all;

% cellpars  = 'd:\lukulu\input\cellpars\';
hydropars = 'C:\My documents\threshold 10\tss\';          % where the file is placed

timeseries = 'C:My documents\threshold 10\tss\';
rainfall = 'rainfall.';

input = sprintf('%s%s',hydropars,'catch.map');
[x, y, REW] = read_PCR(input);
count = max(max(REW));

for t = 1:366
   disp(t);

   if t < 10
      step = sprintf('%s%g','00',t);
   elseif t < 100
      step = sprintf('%s%g','0',t);
   else
      step = sprintf('%g',t);
   end
   input = sprintf('%s%s%s',timeseries,rainfall,step);
   [x, y, rain] = read_PCR(input);
   for nr = 1:count
      id = find(REW == nr);
      RainTss(t,nr) = mean(rain(id));
   end
end
```

Appendix 12: User guidance

Distributed Hydrologic Modelling at the Catchment Scale with Representative Elementary Watershed approach

User guidance for CREW Model ver.0.0

Supplement of User's Guide for _____Model ver.0.0

Ellen Tromp

MSc. Student
University of Technology Delft
Faculty of Civil Engineering and Geosciences,
Department of Water Management, Section Water Resources
Stevinweg 1, 2628 CN Delft, The Netherlands
e.tromp-ct@student.tudelft.nl

Preface

This user guidance is made on the experience of working with the CREW model for 6 months. This guidance should be used with the user's manual made by Mr. H. Lee, who developed the code and model. This is a supplement of the previously mentioned user's manual. An attempt has been made to clarify any indistinctness in the user's manual which might lead to incorrect results.
For more details regarding the REW theory, model parameters, please refer to the user's manual.

For my MSc. Research I have applied the model to the Collie River Basin. This CREW model had never been applied in a situation like the Collie River Basin. First, it is a very large catchment (2500 km^2). Secondly, the rainfall varies between 600 mm in the east till 1200 mm in the west. This has great influences on the runoff. In order to capture the hydrological processes it was necessary to implement a heterogeneous precipitation field in the CREW model.

Ellen Tromp
Perth, July 2005

1. Preparation of inputfiles

For each input file, if necessary, a few comments are made to which attention should be paid while preparing the input files for the CREW model.

GENERAL_INFO.inp
Make sure that the length scale and time scale conversion factor are correct, because the model uses the SI unit system, which means that the model uses [m] and [sec] as units

GEOINFO*.inp
1. If the number of REW's is derived, with for instance Strahler order, all the REW's should get an integer. The REW at the outlet should get number 1. While moving upstream the REW's should get increasing values. The reason for this is the way that the code calculates the inflow and outflow for each REW. If the numbering fails the previous mentioned method, the model will have less accuracy.

2. In case several REW's are defined, the following parameters should be defined for each REW
   - *Rlength*, channel length [m]
   - *Sigma*, the projected catchment area to horizontal plane [m^2]

   And if the soil depth differs strongly within the catchment, the same applies for *Ztotal*, total soil depth. [m]

3. Finally make sure that the parameter *ca* has the correct catchment area. So the catchment area is the total area, located upstream of the outlet of the REW under consideration.

PARAMETERS.inp
There are several parameters which have a physical basis, while others have to be estimated.
Here below an overview of the parameters with a physical basis will be given:

- **alpha_su**; Recharge & Capillary rise process
  if 1.0 is used for this parameter, then Darcy's law has been used. If preferential flow pathway or macropore in unsaturated zone is considered, water flow in unsaturated zone may be faster than the flow following Darcy's law. That case, alpha_su can be larger greater than 1.0 but till what value this can be extended is still unknown.
  Suggested range is 1.0 - 2.0
- **beta1_K_U**: U-zone sat. hyd. conductivity [m/sec]
  range: 3.40E-06 - 8.60E-05
- **beta1_K_S** ; S-zone sat. hyd. Conductivity
  range: 3.40E-06 - 8.60E-05
- **beta2_K_U**: U-zone pore disconnectedness index
  range: 3.4 - 4.7 (*Reggiani, 2000*)
- **beta3_euwg**; Pore size distribution index
  range: 1.2 - 5.4 (*Reggiani, 2000*)
- **beta1_PSI**: Bubbling pressure head
  range: 0.15d0 - 0.45d0 (*Reggiani, 2000*)
- **porosity_U**:U-zone porosity; porosity
  range: 0.20d0 0.40d0 (*Reggiani, 2000*)
- **porosity_S**: S-zone porosity
  range: 0.20d0 - 0.40d0 (*Reggiani, 2000*)
- **czn, ozn, rzn**: Manning roughness coefficients for C-,O-,R-zone
  look for literature for these parameters, depends on the catchment

- As for the other parameters there is no literature showing the range of the parameters. These should be estimated during the calibration. Try to find parameter values which can produce reasonable results, in terms of e.g. saturated area fraction, hydrograph, annual water balance.

2. Choice of Parameters

The choice for the parameters, where no literature is available, has a direct influence on the computation time. During this research it has been found that the computation time could be between 4 minutes and more than 4 hour. It is not known until now, which parameters cause long computation time. It is a matter of running the model lots of times, until the model produces reasonable results and a short computation time. During the calibration, pay attention to the derivatives and the parameter values, because this give better insight in how the parameters are correlated to each other and might show parameter ranges so the quantity of adaptive step sizes in order to reach the required accuracy remains low.

3. Heterogeneous Precipitation Field

Depending on the catchment the precipitation might vary strongly within the boundaries. In that case it might be necessary to implement a heterogeneous precipitation field within the CREW model. For each defined REW the precipitation over that area, can be imported. With the use of the inverse distance as interpolation technique the rainfall data from several stations was used to come to rainfall data for each REW. In the research, another program, called PCRaster, was used to automate this process. With the same program also the REW's were defined on basis of Strahler order. This program is a free GIS PCRaster environmental software package. More info can be found in the users manual PCRaster/ Matlab for deriving a heterogeneous precipitation field.

Appendix 13: Model results

5 REW's

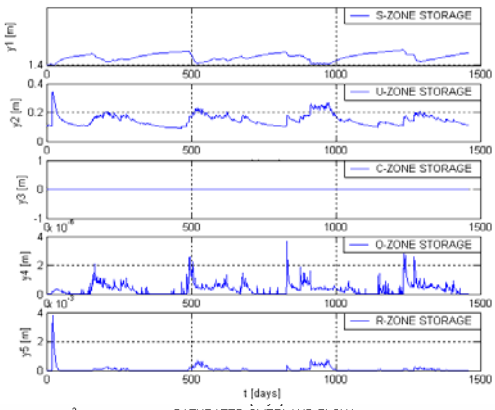

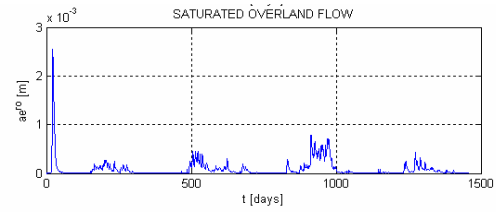

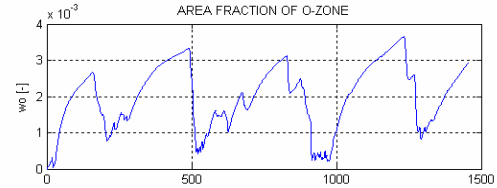

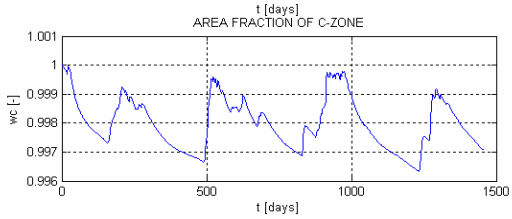

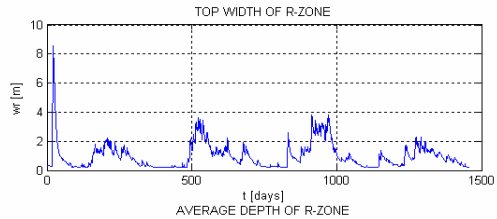

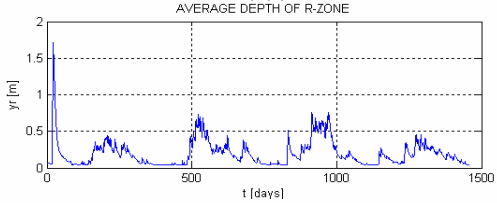

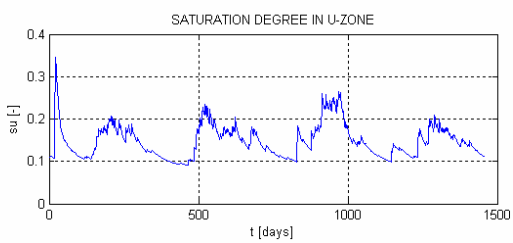

27 REW's